RESEARCH DEPARTMENT

TECHNICAL REPORT No. 58

AN EVALUATION OF THE PERFORMANCE OF THE ECMWF OPERATIONAL FORECASTING SYSTEM IN ANALYSING AND FORECASTING TROPICAL EASTERLY WAVE DISTURBANCES PART 1: SYNOPTIC INVESTIGATION

by

R.J. Reed*, A. Hollingsworth, W.A. Heckley, F. Delsol

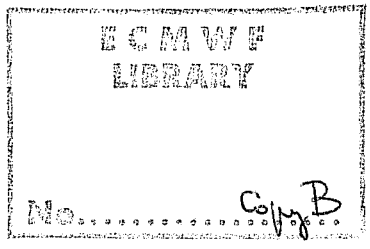

* Permanent Affiliation:
Department of Atmospheric Sciences
University of Washington
Seattle, Washington, U.S.A.

September 1986

ABSTRACT

Substantial changes were made to the ECMWF model in May 1985. The extensive revisions to the physical parameterisations were designed to improve the treatment of the large scale flow in the tropics. In addition, the resolution was increased substantially to a triangular truncation at T106. The purpose of this paper is to evaluate the performance of the new forecasting system on the analysis and forecasting of easterly waves and their associated tropical storms over Africa and the tropical Atlantic.

A wave history generated for the months of August and September 1985 with use of operational analyses and Meteosat imagery provides the framework for evaluating the performance of the analysis system. The difficulties caused by lack of data are discussed. Shortcomings of the analysis system are illustrated using examples of short-scale and markedly divergent systems. On the other hand examples are also presented demonstrating the ability of the analysis system to make sense of widely scattered observations.

The maxima in the vorticity field provide a set of useful markers to track the easterly waves, both in the analyses and in the forecasts. The 48hr forecasts of the positions and intensities of the vorticity maxima are verified in those cases for which there is sufficient observational data to have confidence in the low-level wind analysis. The verification results are quite encouraging.

A particular feature of the paper is the series of synoptic studies of the four waves which gave rise to named storms (Danny, Elena, Fabian, Gloria) during the period.

CONTENTS

1. INTRODUCTION

Numerical weather prediction in the tropics has been the subject of a number of recent review papers (Gilchrist et al. 1982, Rowntree and Cattle 1983, Krishnamurti 1985). Much of the research discussed in these reviews concerns experimental analyses and forecasts with special data sets collected during the GARP Atlantic Tropical Experiment (GATE) in 1974, or during the Global Weather Experiment (FGGE) in 1978-79. One of the ultimate goals of the field programs and the ensuing research work has been to provide a basis for routine numerical weather prediction in the tropics. In this paper we discuss the analysis and forecasting of easterly waves in August and September 1985, using an operational analysis and forecast system.

In an earlier report Kanamitsu (1985) studied the predictability of the operational ECMWF forecast model in the tropics using archived data for 1983 and 1984. He considered separately the forecasts for the quasi-stationary and the transient components of the flow. Serious errors were found in the treatment of the quasi-stationary component of the flow, in agreement with the findings of other workers (Heckley 1985; Tiedtke et al., 1987). In the non-stationary component of the flow he found that transient disturbances having the character of easterly waves (Riehl, 1954; Burpee and Reed, 1982) were successfully predicted in the Atlantic for periods as long as three to four days in advance. However, no inspection of the waves was made on a day-by-day basis nor were comparisons made with actual data or with satellite cloud patterns. Thus, it is possible that some of the apparent success stemmed from the fact that in a data sparse region, such as the tropical Atlantic, the verifying analyses may be dominated by the first-guess or forecast fields.

Substantial changes were made to the operational forecast model in May 1985. The physical parameterisations were extensively revised (Tiedtke et al., 1987), the resolution was increased from triangular 63 truncation to triangular 106, and there were associated changes in the representation of orography (Jarraud, Simmons and Kanamitsu 1985). The revised parameterisation schemes included a representation of shallow convection, a more effective representation of deep convection, and a new cloud representation. These changes were designed to improve the representation of the quasi-stationary flow in the Tropics, and substantial improvements have in fact been achieved, although there is still scope for improvement (Tiedtke et al., 1987).

The introduction of this new model, coupled with the need for more extensive verification of the forecasts, made it desirable to conduct further studies regarding the predictability of the easterly waves. Moreover, the improved treatment of the time-mean flow together with the higher resolution of the new model raised the possibility that this model may be more successful than previous models in predicting the development of tropical storms. Many of the tropical storms and hurricanes that develop in the Atlantic and Caribbean have their origins in the easterly waves. Bengtsson et al. (1982) gave evidence of some success in tropical storm prediction with an earlier version of the ECMWF operational model. Their study highlighted the need for increased horizontal resolution.

The purpose of this report is to evaluate the success of the T106 model in analysing and forecasting easterly waves, and their related tropical storms, during a two month period in the summer of 1985. Over Africa the easterly waves are often termed African waves, and we will use the term to include these as well. The evaluation was carried out by looking at the waves (and

storms) on an individual basis. In the process a large number of plotted maps and satellite pictures were examined, only a sample of which can be presented here.

Section 2 contains wave histories and statistics derived from the histories. Section 3 is concerned with the analysis of the waves, namely with the data coverage and the characteristics of the analysis system. Illustrative examples are given. The forecast performance is evaluated in Section 4 on the basis of error statistics compiled for a large number of cases in which the observational data are deemed sufficiently numerous to define the waves. In addition, examples of forecasts are given for five selected cases. Four of these cases are concerned with waves that transformed into tropical storms or hurricanes.

2. WAVE HISTORIES AND CHARACTERISTICS

Identification and tracking of individual waves is a prerequisite for carrying out the objectives of this study. Initial attempts at constructing wave histories made use of operationally-produced, once-daily 850 mb streamline/isotach analyses. However, considerable difficulty was experienced in obtaining smooth and consistent tracks from the trough axes and circulation centres appearing on these charts. Moreover circulation centres were often lacking so that it was not possible to assign a latitudinal position to the wave disturbance. To overcome these difficulties we prepared next from the data archives a series of 6 hourly 850 mb charts with vorticity isopleths superimposed. The vorticity maxima allowed both latitudinal and longitudinal positions to be assigned and generally proved easier to track. Nevertheless, in some cases a problem still persisted in determining consistent and unambiguous positions. The problem was particularly acute over data-sparse ocean regions and stemmed from a tendency of the analyses to develop multiple vorticity centres (but often within a common synoptic-scale wave trough) or to lack a well defined centre in the typical case where the vorticity weakened in mid-ocean.

To help overcome the problem two additional sources of information were used: Firstly, 700 mb streamline analyses prepared on a 6 hourly basis from analysed wind data and, secondly, once daily satellite images appearing in the Meteosat Image Bulletins for August and September (European Space Agency, 1985). Since wave axes proved simpler to locate at 700 mb than at 850 mb, greater weight was given to the 700 mb analyses in determining longitudinal positions of the wave disturbances. However, it was still necessary to use 850 mb vorticity maxima in determining latitudinal positions.

Satellite visible images for the Atlantic often reveal distinctive inverted "V" and vortical cloud patterns characteristic of easterly waves (Anderson et al., 1973). In cases where there was disagreement between the position indicated by the cloud pattern and that given by the analysis, or where the analysed position was obscure, the satellite derived position was chosen. The final wave history obtained from the combined use of the 850 mb and 700 mb maps and the satellite imagery appears in Table A1 of the Appendix. Smoothed tracks of the individual disturbances, based on the data in Table A1, are shown by half-monthly periods in Figs. 1a-d. Heavy dots indicate the points of origin of the disturbances, considered in each case to be the point at which the vorticity maximum first behaved as a travelling centre (westward propagation speed $\geq 3°$ long d^{-1}). A dot is lacking for the first disturbance (A) which was already in existence at the beginning of the period of study. Terminating positions of the disturbances, i.e. positions beyond which they no longer could be identified, are denoted by arrowheads. The arrowheads are omitted for disturbances that moved beyond the area of interest while still identifiable. For the most part the tracks are in good agreement with wave histories prepared by G. Clark of the U.S. National Hurricane Centre and made available to us by R. Burpee.

A composite view of the regions of origin and of the disturbance tracks, based on Figs. 1a-d, is provided in Fig. 1e. This figure gives some evidence of two preferred regions of development, one in the area bounded by 8°-15°N, 0°-10°E, which lies within or near the climatological rain belt (Thompson, 1965), and a second and more prominent one to the north and west (18°-25°N, 10°W-5°E) that is located over the Sahara downwind of the Hoggar. The tracks from these regions tend to merge in the eastern Atlantic, and very little dispersion of

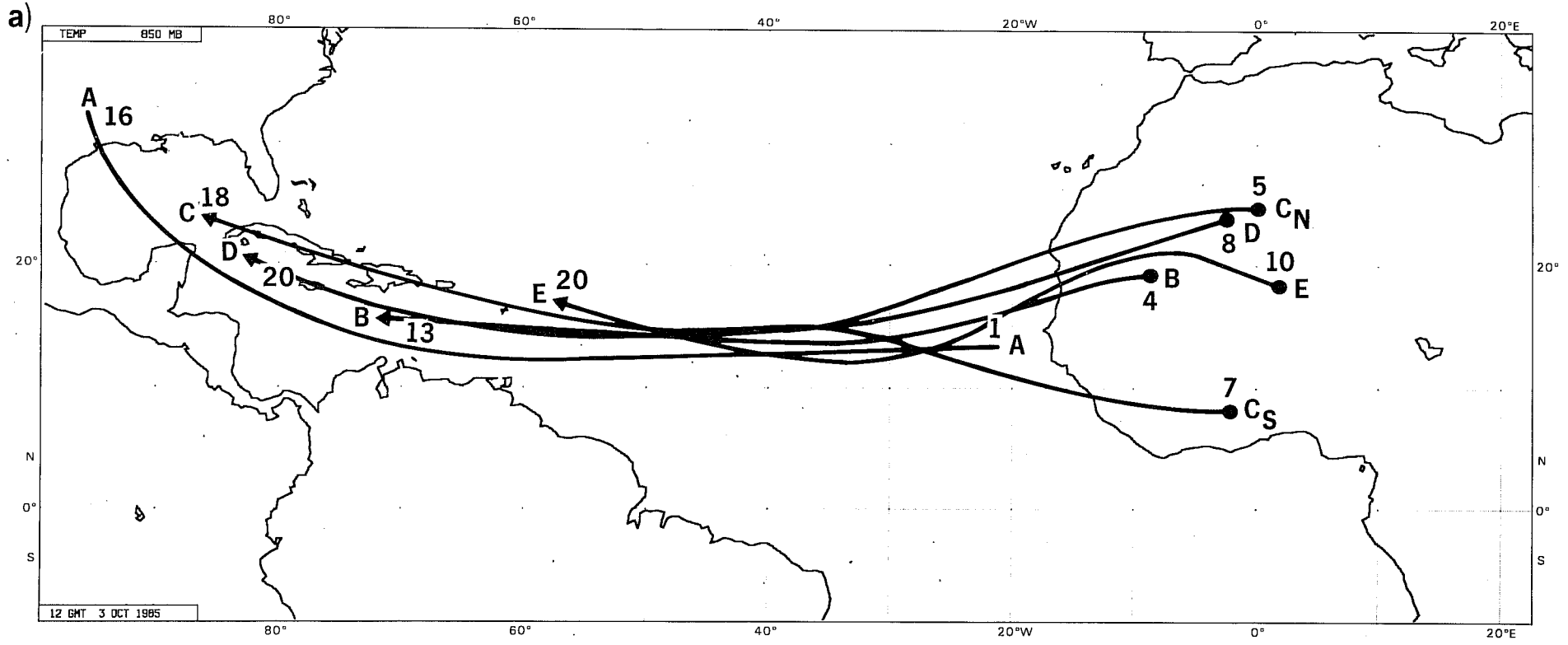

Fig. 1 Half-monthly storm tracks. (a) Aug 1-15, 1985.
The plotted numbers indicate beginning and ending dates of tracks. Subscripts "N" and "S" denote northerly and southerly components of the same system.

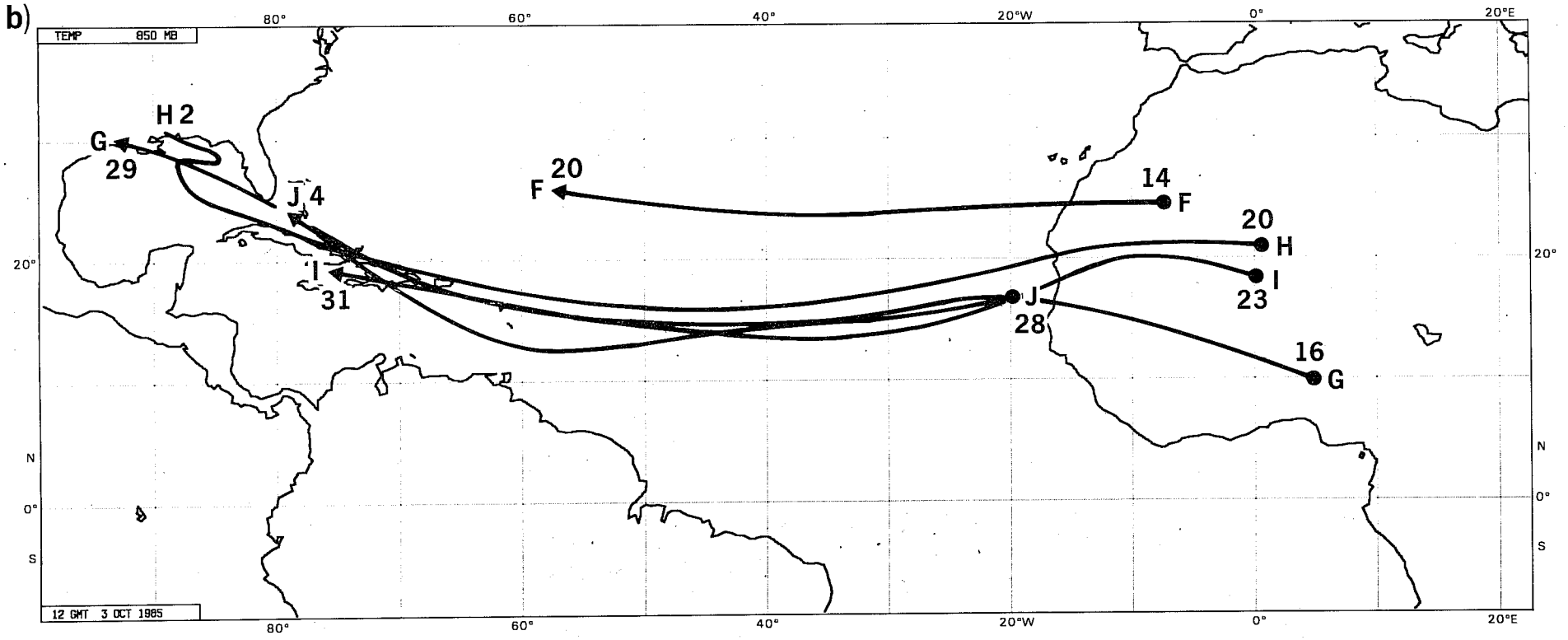

Fig. 1 Half-monthly storm tracks. (b) Aug 16-31.

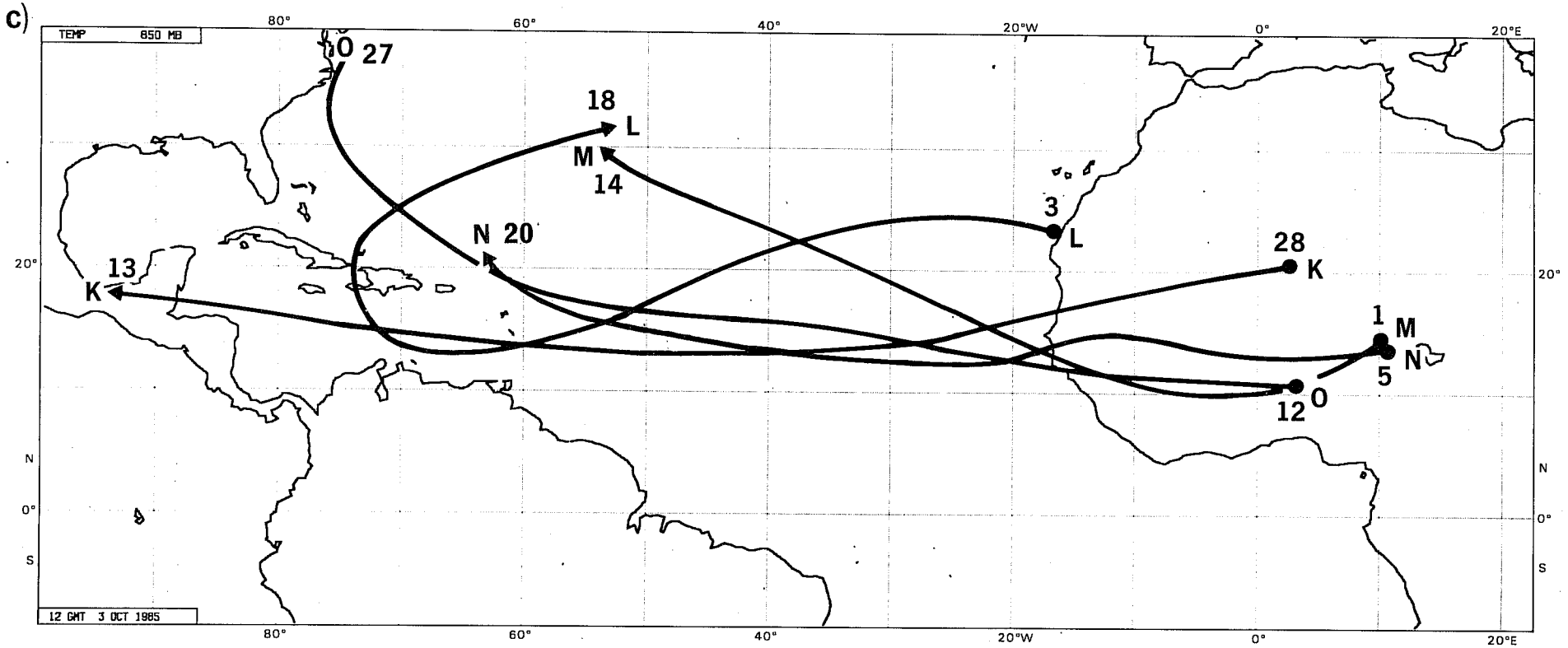

Fig. 1 Half-monthly storm tracks. (c) Sept 1-15.

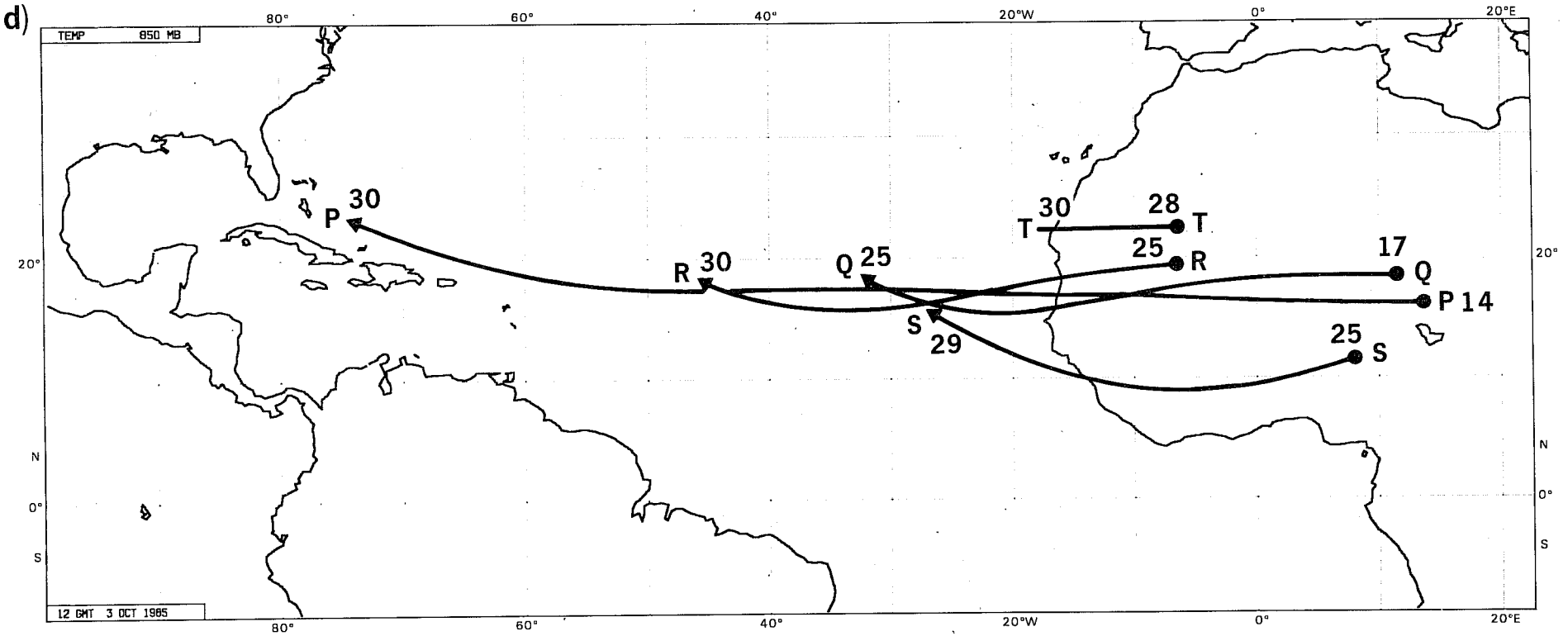

Fig. 1 Half-monthly storm tracks (d) Sept 16-30.

e)

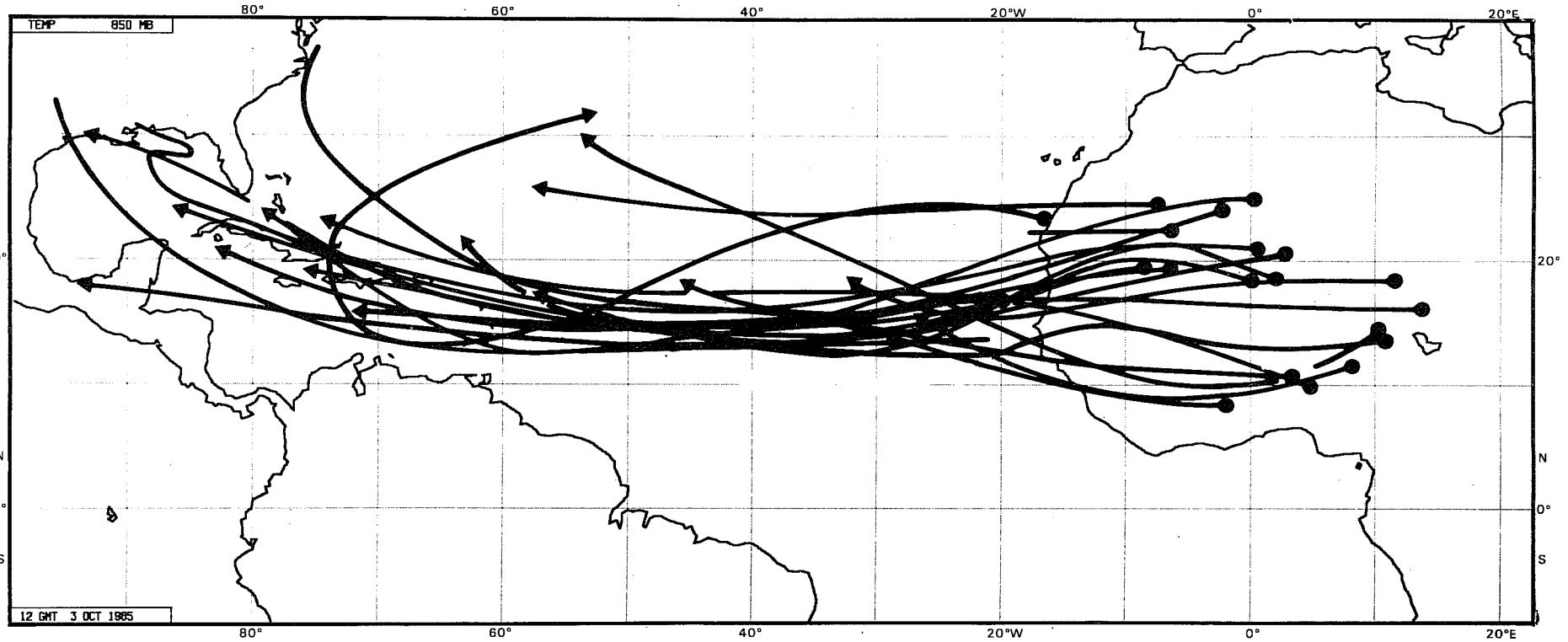

Fig. 1 (e) Composite storm tracks, Aug-Sept 1985.

the paths is noted in the central Atlantic where the systems are generally quite weak. Further west the disturbances take a variety of paths and, as will be shown later, often slow down and occasionally intensify.

These results agree in most respects with those found by Nitta and Takayabu (1985) from FGGE data for the summer of 1979. They also tracked 850 mb vorticity centres and found two storm tracks originating from approximately the same regions as shown in Fig. 1e. However, their northerly track proceeded due westward from the coast along 22°N rather than west-southwestward to merge with the southerly track as in this study. Only one of the 20 waves followed in this study took the northerly track found in 1979. Whether the difference is due to differences in the large-scale circulation in the two years or to differences in interpretation is not known. Experience from the GATE year (1974) and from many years of viewing satellite cloud fields suggests that the west-southwestward course is the normal one. A possible source of confusion are the low-level vorticity centres that form off North Africa in association with developments in the upper-tropospheric trough (Simpson et al., 1968). Without the 6 h time continuity it would have been difficult at times to decide whether these were disturbances that formed over Africa or over the ocean, as in fact they did.

From the information in Table A1 it is possible to determine wave lengths, phase speeds and periods within different parts of the domain. These are shown in Table 1. The periods were determined by counting the number of wave passages at the central longitudes of the subregions during the two month period rather than by taking the ratio of wave length to speed.

Table 1 - Wave Characteristics

Longitude Belt	Wave Length[1] (km)	Phase Speed (° long d^{-1})	Period[2] d
≤20°W	1930	6.0	-
21°-40°W	2320	6.5	3.5
41°-60°W	2790	6.8	3.6
61°-80°W	2870	7.4	4.7
>80°W	2330	3.8	-

1. From wave trough in given band to next trough upstream.
2. Based on number of wave crossings at mid-longitude of belt.

In mid-ocean the average wavelength is roughly 25° long or 2800 km, a figure in good agreement with estimates made in other studies. The lengths are somewhat shorter to the east and west where wave speeds are slower. The 6-7° long d^{-1} propagation speed in the central and eastern regions is also in close agreement with other estimates, as is the 3-4 day periods observed in these regions.

3. QUALITY OF THE ANALYSES

Maps were prepared at 6 h intervals for the two month period with all data from the operational archives plotted on them. The area covered was 10°S to 30°N, 75°E to 100°W, and the levels and variables examined were

- Surface maps with isobaric analyses, grid-point wind vectors and isotachs,
- 850 mb charts (two sets) with streamline, isotach, temperature and vorticity (ζ) analyses,
- 700 mb charts with streamline, isotach and temperature analyses,
- 200 mb charts with isotherms, grid-point wind vectors and isotachs,
- 1000 - 850 mb thickness charts.

The plotted data included

- Surface: standard ship and land station synoptic reports,
- 850 mb: radiosonde, pilot balloon and, over the oceans, cloud-track wind reports,
- 700 mb: radiosonde, pilot balloon and cloud-track wind reports,
- 200 mb: radiosonde, aircraft and cloud-track wind reports,
- 1000-850 mb thickness charts: satellite-derived, layer-mean temperatures.

In order to keep the study within tractable limits the decision was made not to examine vertical velocity, moisture and precipitation patterns. As some of the later results suggest, examination of these is an important future objective.

The principal aim of this part of the study is to determine what data were available for defining and tracking the waves and how the analysis system responded to the data (or the lack of data). Since the waves are best defined at the 850 mb and 700 mb levels and since there were more pilot balloon observations at the lower level than at the higher, it was decided to focus attention mainly on the 850 mb charts. These were examined thoroughly. Less detailed attention was given to the 700 mb charts. In general the waves were difficult to detect at the surface so that this level was almost completely ignored. Likewise the 1000-850 mb thickness charts were ignored, since it was apparent that the satellite soundings gave no useful information regarding the waves. Some attention was given to the 200 mb analyses, particularly in the central and western oceans where the familiar upper tropospheric trough had an observable effect on some waves and in addition induced a different type of low-level disturbance, an example of which will be presented in Section 4.

3.1 Data availability

An extensive statistical summary of the data availability appears in Figs. A1-A6 of the Appendix. The reader can also acquire a good idea of typical data amounts and distributions by examining the plotted maps presented in this section and the next. They show that at 850 mb an adequate network of data exists for defining the waves over most of West Africa (west of 10°E), especially when it is considered that a 6 h analysis cycle is employed and a

large number of pilot wind observations are taken at 0600 and 1800 GMT as well as at 0000 and 1200 GMT. Still, important data gaps exist over the Sahara. Of particular concern is the gap near 25°N, 5°W where the model generates a great deal of unverifiable transient vorticity at the 850 mb level. Results of Burpee (1974), based on surface wind data, suggest however that the enhanced vorticity may well be a real feature.

Over central Africa and parts of eastern Africa, an enormous data gap existed for most types of observation throughout the period of study. The area affected extends from 10°S to 20°N and 10°E to 30-40°E. Within this area no reliable identification of easterly waves was possible. However, it is our belief from the limited data available on the periphery that wave activity was essentially lacking in this region during the period of study, as it was during the GATE period (Albignat and Reed, 1980; Sadler and Oda, 1978, 1979 and 1980) when sufficient observations existed in the region to detect the waves had they been present. It should be noted, though, that easterly waves have occasionally been observed east of 10°E (e.g. Carlson, 1969).

Over the Atlantic data are sparse at 850 mb, consisting only of sporadic satellite cloud-tracks winds. These are relatively plentiful in the vicinity of the equator but not at the latitude of the storm track. West of 60°W, observations from the Caribbean Islands and from coastal South America allow the waves to be easily identified and tracked. Due to a variety of operational reasons, low-level aircraft reconnaissance reports in the vicinity of hurricanes were not available to the analyses. These would have been extremely useful.

Because of the large number of cloud-track winds and the numerous reports from aircraft, considerably more data are available at 200 mb than at lower levels.

But these data are of little help in analysing the waves over Africa and the eastern Atlantic, since the waves are best defined in the middle and lower troposphere.

3.2 Analysis Problems

The problems of analysis in the tropics have been discussed in a number of recent papers (Shaw et al., 1984; Krishnamurti, 1985; Hollingsworth et al., 1986). The series of analyses discussed in this paper contain examples of the problems involved in analysing tropical data. The questions that we shall discuss are the resolution of the analysis system, the constraints used in the analysis and the relative weight of observation and first guess.

The operational system during 1985 was tuned so that the mass and wind structure functions in the horizontal had a length scale of 480 km at 30°N, increasing to 1000 km at the equator, and decreasing to 600 km at 30°S. The functions used are Bessel function expansions as described in Shaw et al. (1984). The wind structure functions were non-divergent and the mass-stream function coupling was exactly as in Lorenc (1981), being -0.95 poleward of 30°N, 0.95 poleward of 30°S, and varying linearly with the sine of latitude between these latitudes.

The resolution of the analysis system is lowest at the equator, and is considerably higher in the mid-latitudes of both hemispheres. The parameters controlling the resolution were chosen in 1984 in accordance with operational experience up to that point. The forecast model in 1984 had substantial forecast errors on the largest scales in the Tropics. To correct these errors in the analysed fields it was essential to use broad correlation functions.

The important model change in May 1985 considerably reduced forecast errors on the largest scales (Tiedtke et al., 1987). The setting of the analysis parameters can therefore be improved over what was actually used in 1985. Improvements in the initialisation procedure to take better account of the tides (Wergen, 1986) will also increase the possibilities for increased analysis resolution in the Tropics.

The response of the analysis algorithm to observational data is affected by other factors besides the length scale of the correlation functions. The constraints used in the analysis, and the relative weighting of first-guess error and observational error are also of importance. The analysis calculation is based on the differences between the observations and the six-hour forecast. The constraint of local non-divergence is only applied to the changes, or increments, made by the analysis to the six-hour forecast. The final analysed field may contain divergence stemming from the forecast field.

If the forecast for a small scale divergent feature is poor then the analysis will also be poor, because of the constraint. An example appears in Fig 2a where sharp, small-scale features are evident in the region to the northeast of wave disturbance "S" (centre at 10°N, 13°W). Particularly prominent is the confluence line extending along 16°N between 3°W and 13°W, as shown in a manual streamline analysis (Fig 2b). This presumably convergent feature is poorly analysed, as is the very short trough-ridge system immediately upstream. The poor analysis of the wind field is partly attributable to the constraint of non-divergence, partly to the small scale of the disturbance, and partly to a poor forecast of the wind field.

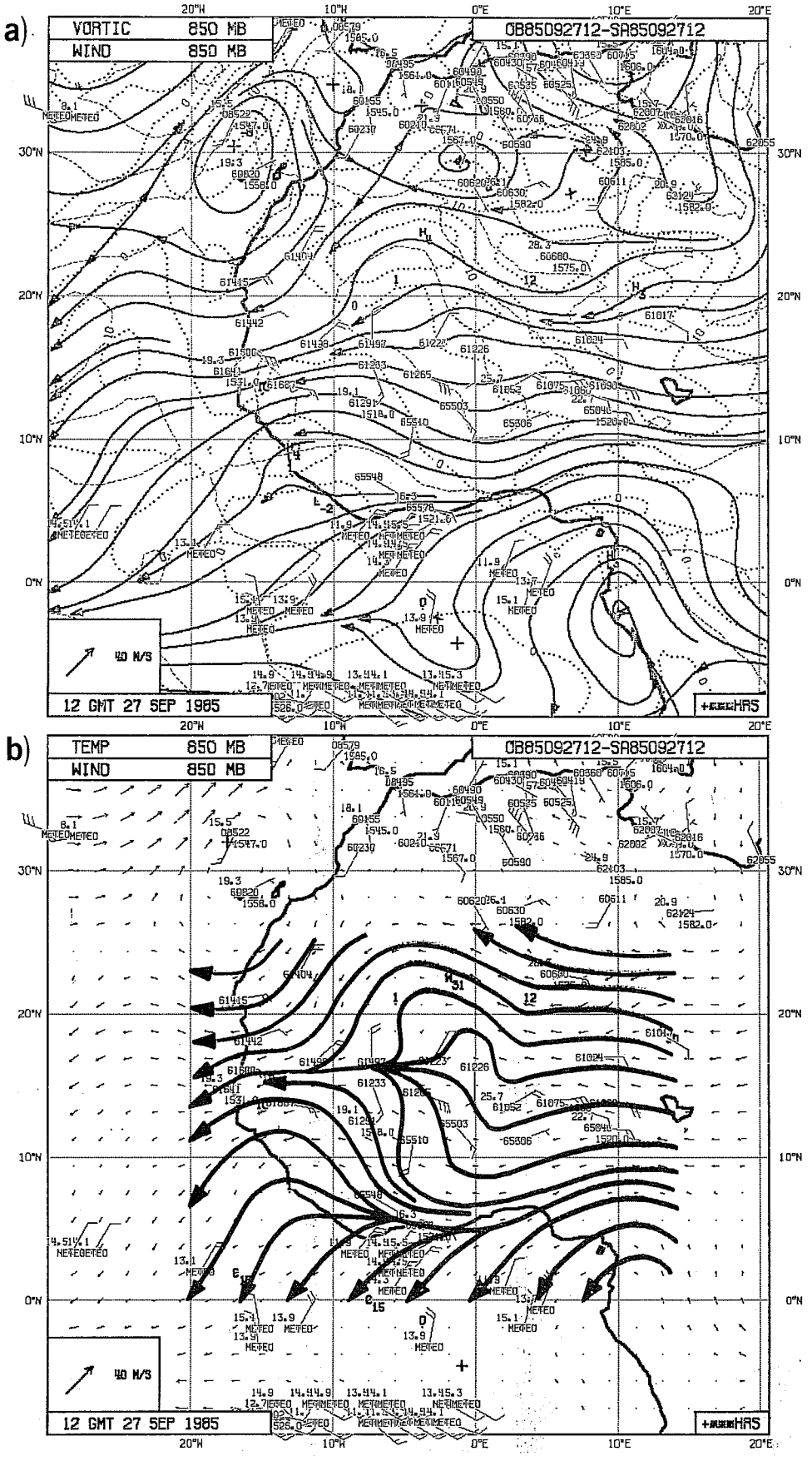

Fig. 2 (a) 850 mb ECMWF analysis, 1200 GMT 27 September 1985. Solid lines, streamlines. Dotted lines, vorticity isopleths (10^{-5} s^{-1}), dashed lines isotachs (m s^{-1}). H's indicate positions of vorticity maxima and L's positions of vorticity minima. Winds are plotted according to the usual convention: full barb = 5m s^{-1} (b) Manual streamline analysis.

Daley (1985) has recently shown that the optimum interpolation formalism can be extended to analyse the divergent wind component. His examples of one-level analyses of the upper tropospheric wind field included cases where the relaxation of the non-divergence constraint led to improved synoptic scale analyses. The present example suggests that such a modification may also lead to improved lower tropospheric wind analyses.

For contrast we next show an example of the treatment of a sharp but largely rotational feature in Fig. 3, the 850 mb streamline chart for 1200 GMT on 22 Aug. 1985. The African wave that later gave rise to hurricane Elena was at that hour just approaching the coast. The analysis shows the wave as a sharp feature with a short east-west wave length, in good agreement with the data. Incidentally, this case provides an example of the ability of the analysis system to ignore an unrepresentative local wind. Note the nearly 90° difference between the wind direction at station 60620 (Adrar, Algeria; 28°N, 0°E) and the direction given by the streamlines. Nearly every 850 mb wind reported from this station during the two month period was from a southerly direction, often in sharp disagreement with the direction reported at nearby stations.

It is important to ensure that the relative errors of observation and first guess are correctly specified. This has been achieved fairly satisfactorily in mid-latitudes in situations where data receipt is reliable. An assimilation system needs to be able to cope with data unavailability by correctly increasing the first-guess error. During the period of study there was an outage of conventional data over much of West Africa for about a week (August 24-30). The assimilation performed rather well in describing the development and movement of a well-marked dry Saharan disturbance (see section

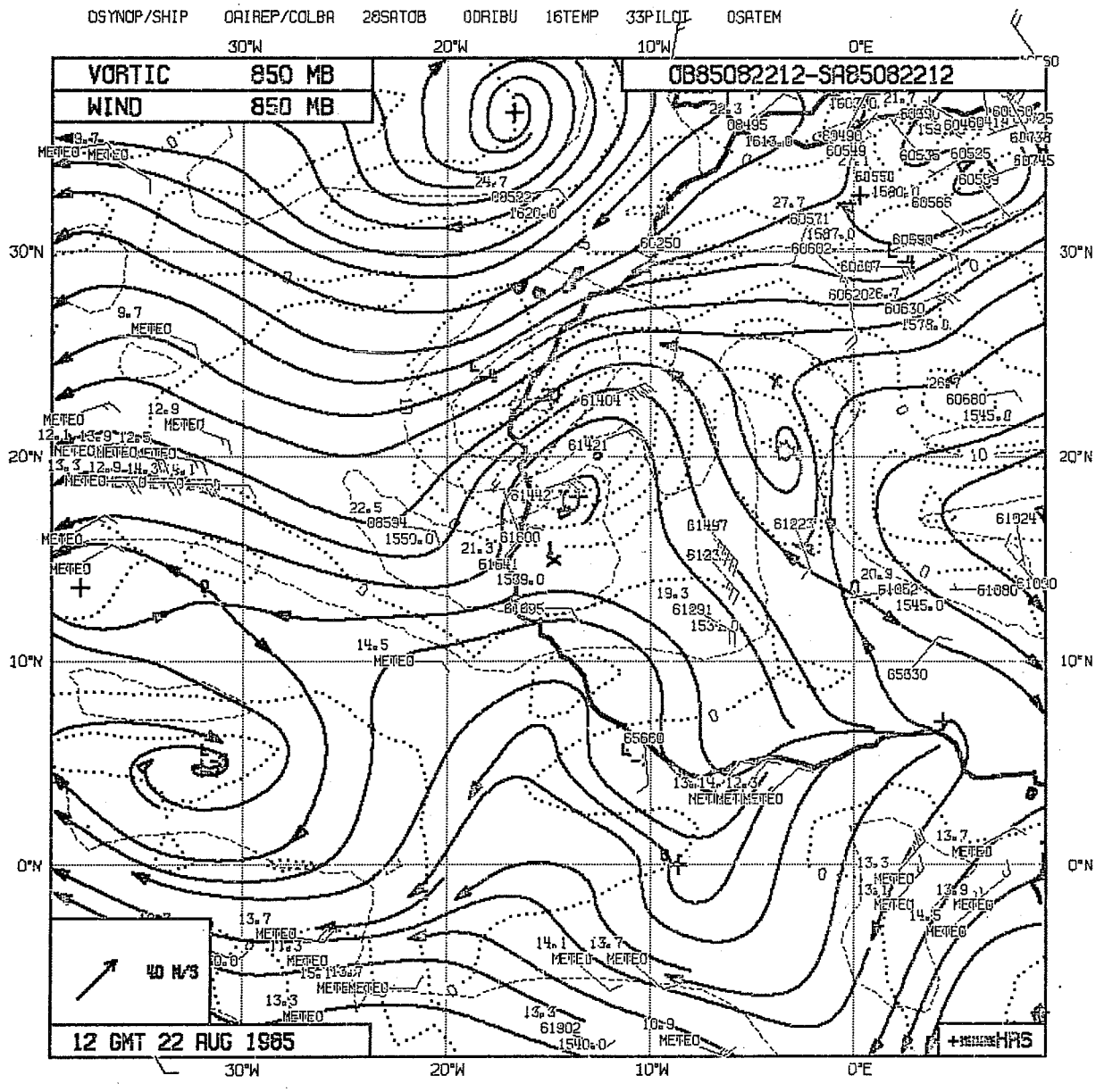

Fig. 3 850 mb analysis, 1200 GMT 22 August, 1985. For further explanation see Fig. 2a.

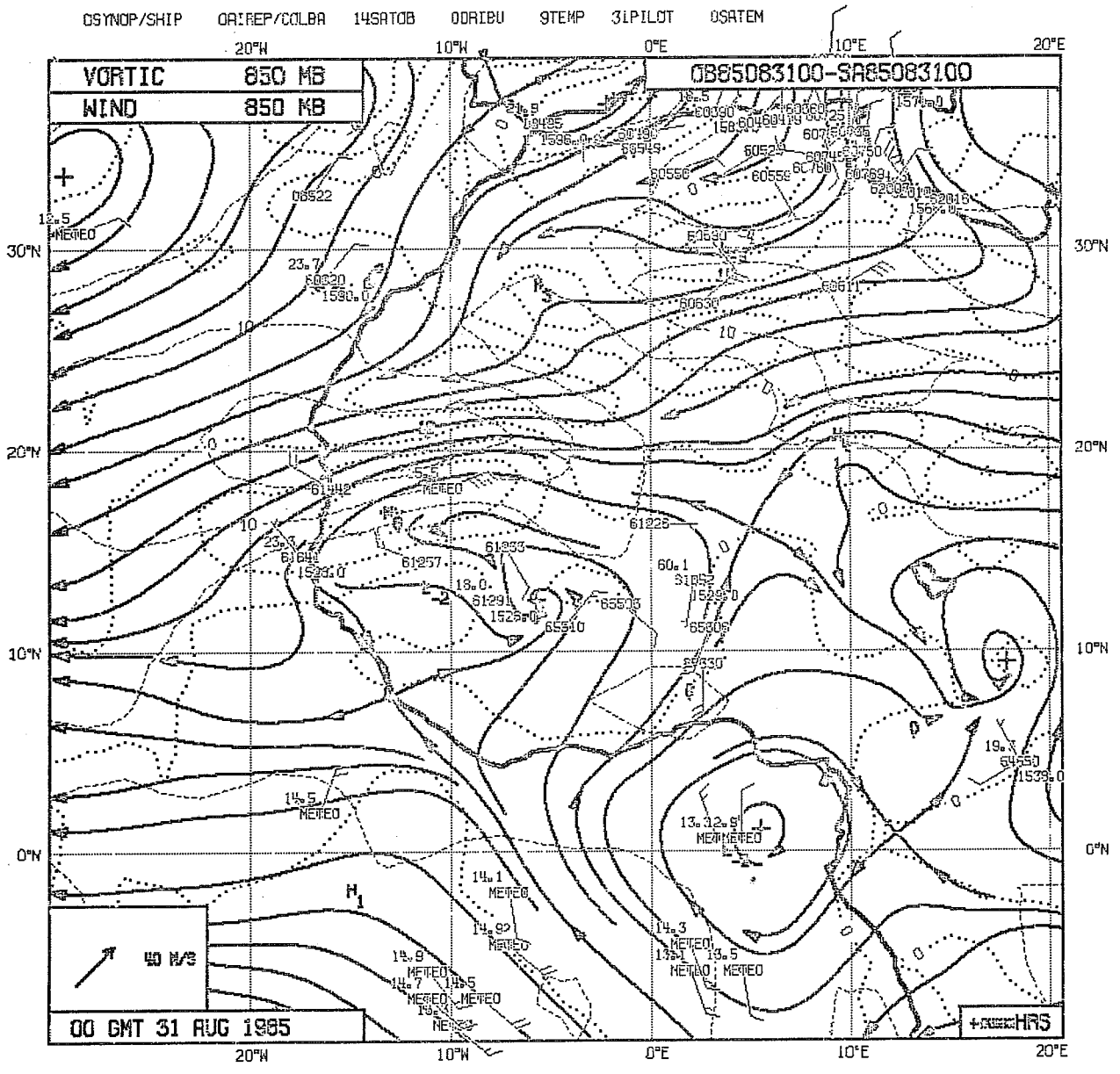

Fig. 4 850 mb analysis, 0000 GMT 31 August, 1985. For further explanation see Fig. 2a.

3.3.1. Fig. 4 shows the first analysis for which conventional data were again available (0000 GMT, Aug 31). The position of the disturbance in the interior of West Africa agrees reasonably well with the available observations. However there are places on the chart where the data have been unjustifiably ignored, for example at Dakar (station 61641), and at the station further north (Nouakchott, 61642). Both of these stations show onshore winds which are ignored by the analysis. It is likely that too much weight has been given to the first-guess. The first-guess error is estimated in a simple manner (Shaw et al. 1984), and has not been previously tested on such a prolonged outage. The algorithm to calculate the first guess error could benefit from further work.

3.3 Examples of analyses in data-sparse regions

Two examples have been chosen to demonstrate the performance of the analysis system in locating easterly waves or vortices when data were lacking, or nearly lacking, over a broad area. These examples also, of course, furnish a test of the forecast system, since the analyses in data-sparse regions are largely determined by the first-guess fields. The examples have been chosen because the analyses can be at least partly verified by independent observations, in one case by satellite observation of cloud patterns and in the other case by satellite observation of a dust pattern.

3.3.1 The mid-Atlantic passage of Gloria

The first example appears in Figs. 5-10. These depict at 48h intervals the progression of disturbance "O" and its offspring, Hurricane Gloria, across the Atlantic. Also shown, for later reference, are the 48h forecasts verifying at the analysis times. The sequence begins with the analysed 850 mb chart for 12

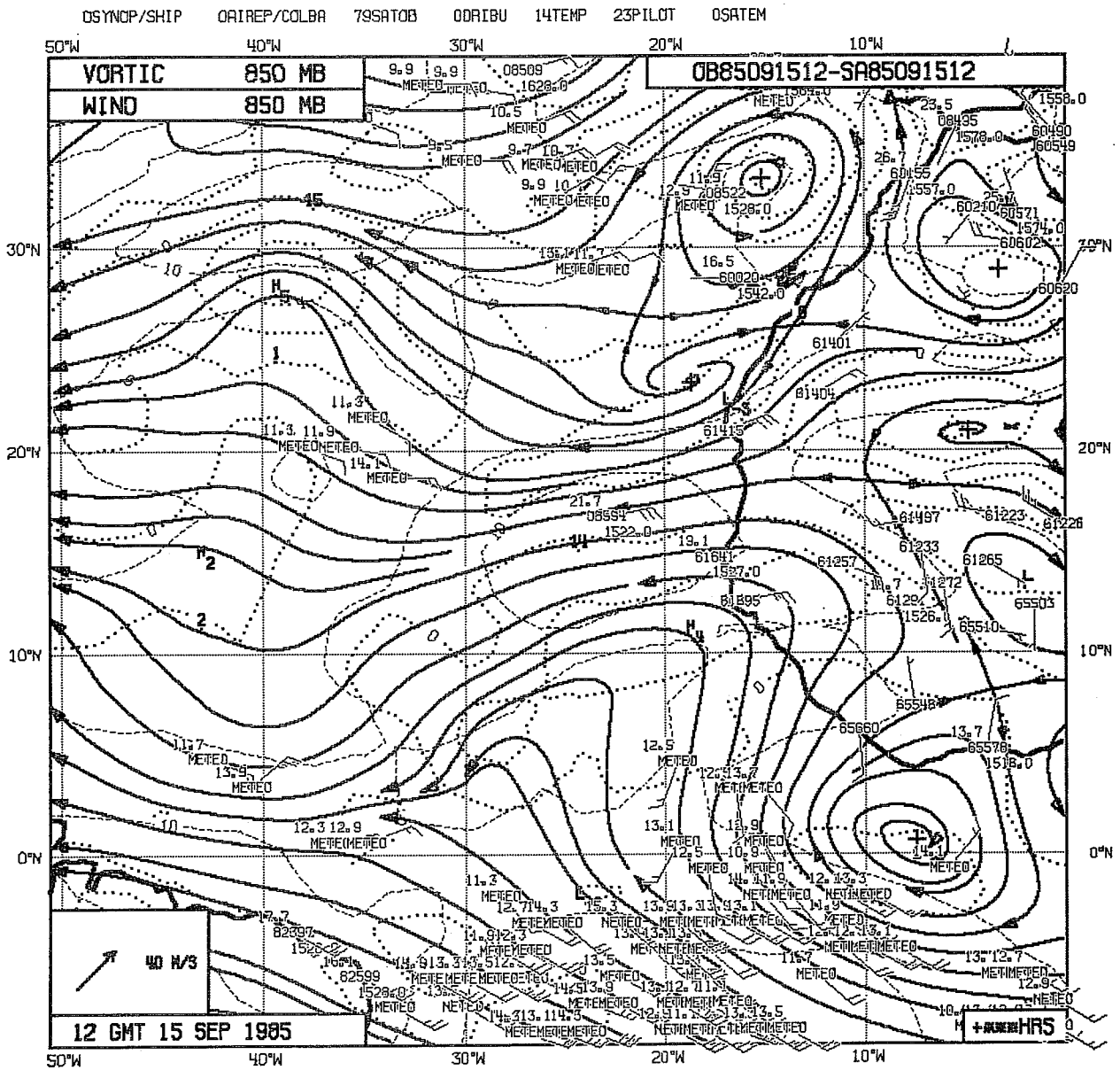

Fig. 5 850 mb analysis, 1200 GMT 15 September, 1985. For further explanation see Fig. 2a.

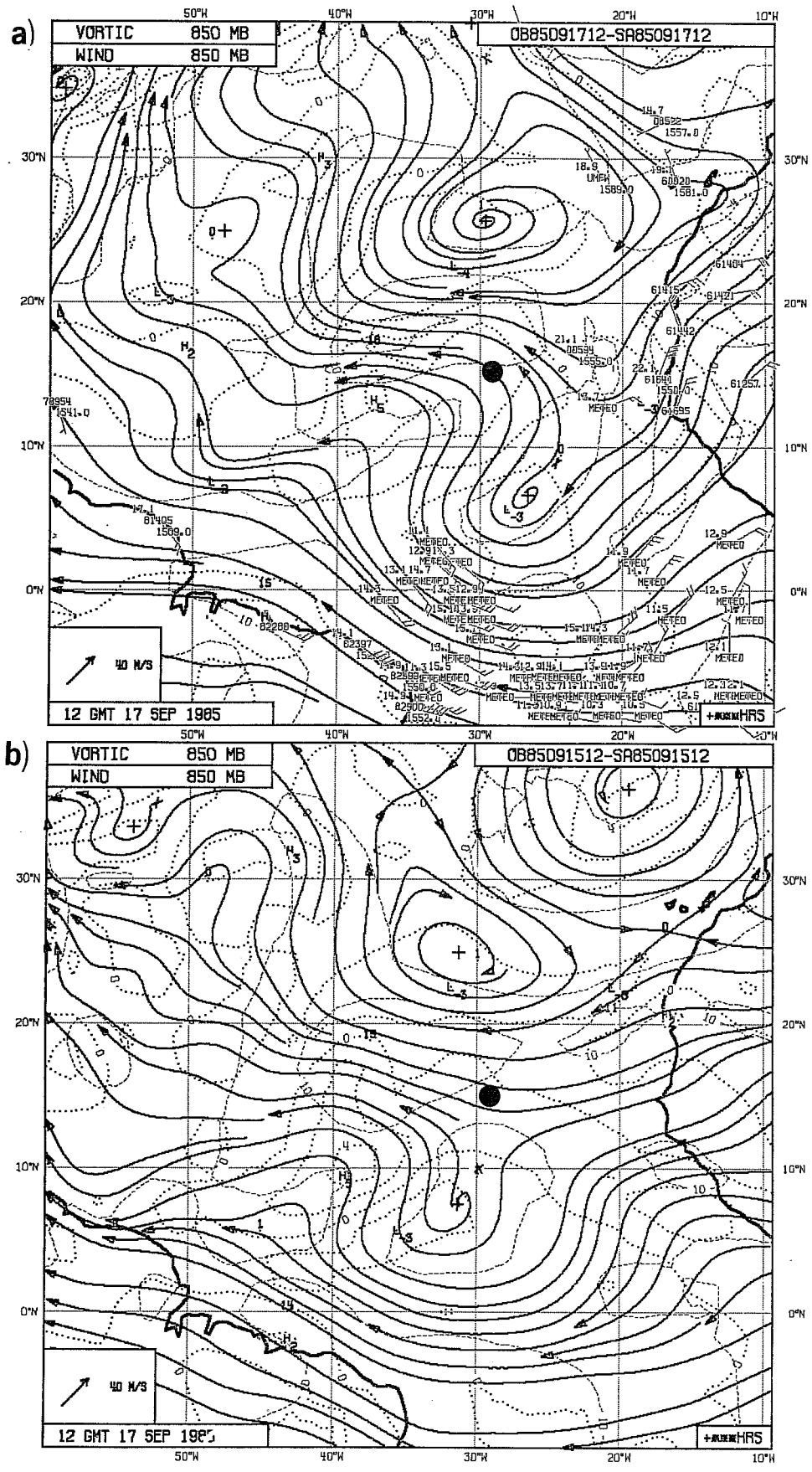

Fig. 6 (a) 850 mb analysis, 1200 GMT 17 September, 1985. (b) 48 h forecast verifying at that hour. For further explanation see Fig. 2a. Large dot indicates position of wave "O" (later Hurricane Gloria), as determined from meteorological satellite observation.

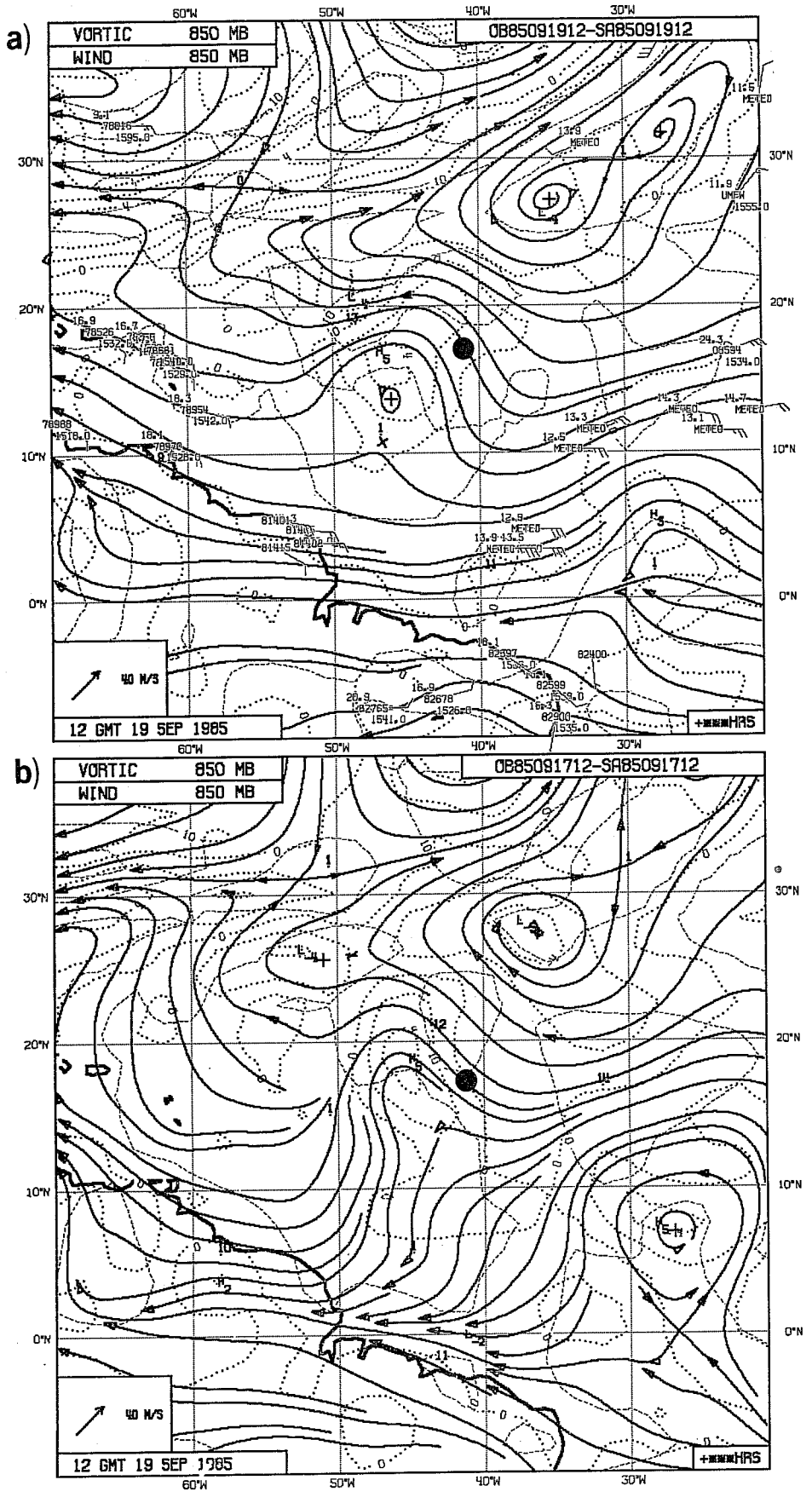

Fig. 7 Same as Fig. 6 for 19 September, 1985.

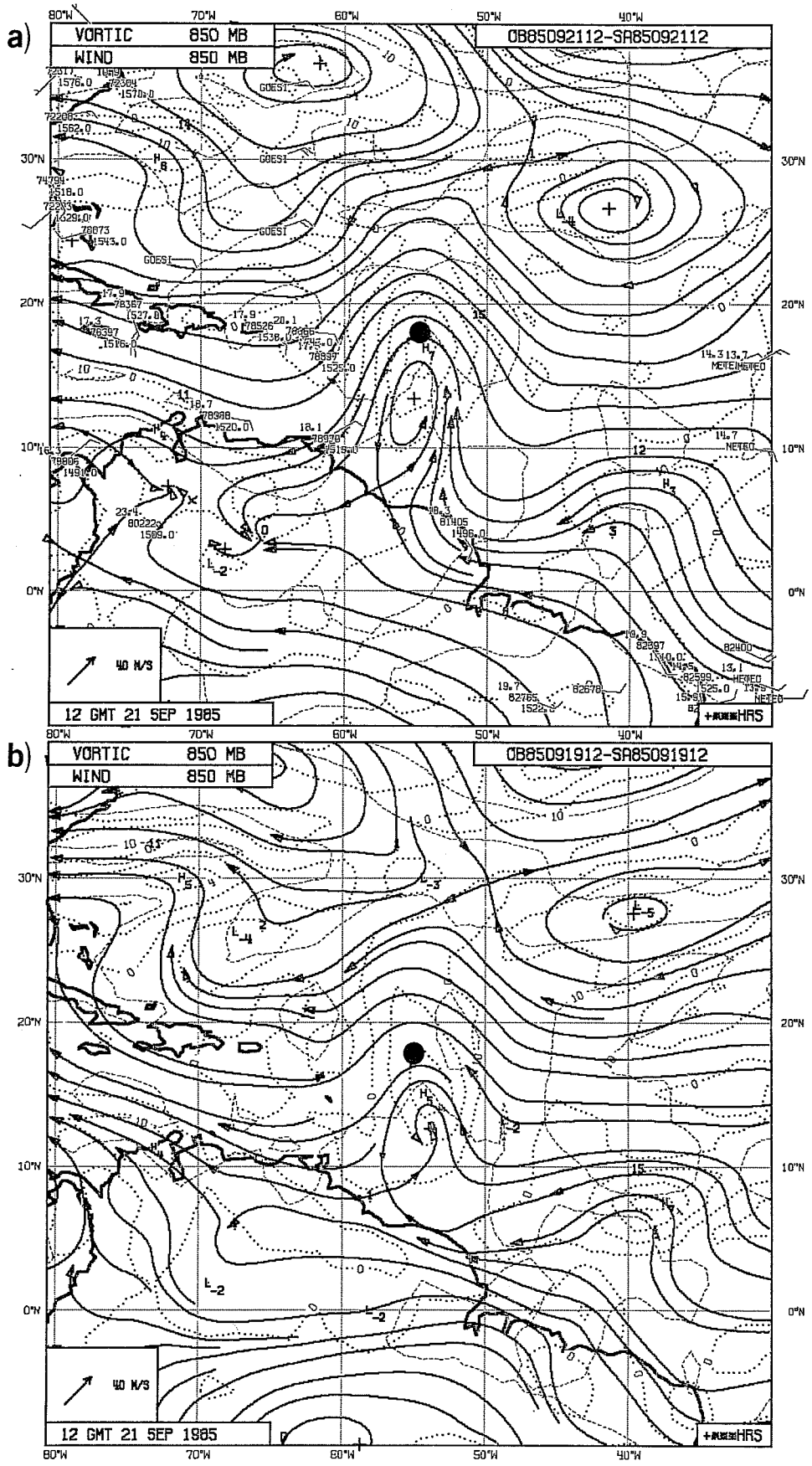

Fig. 8 Same as Fig. 6 for 21 September, 1985.

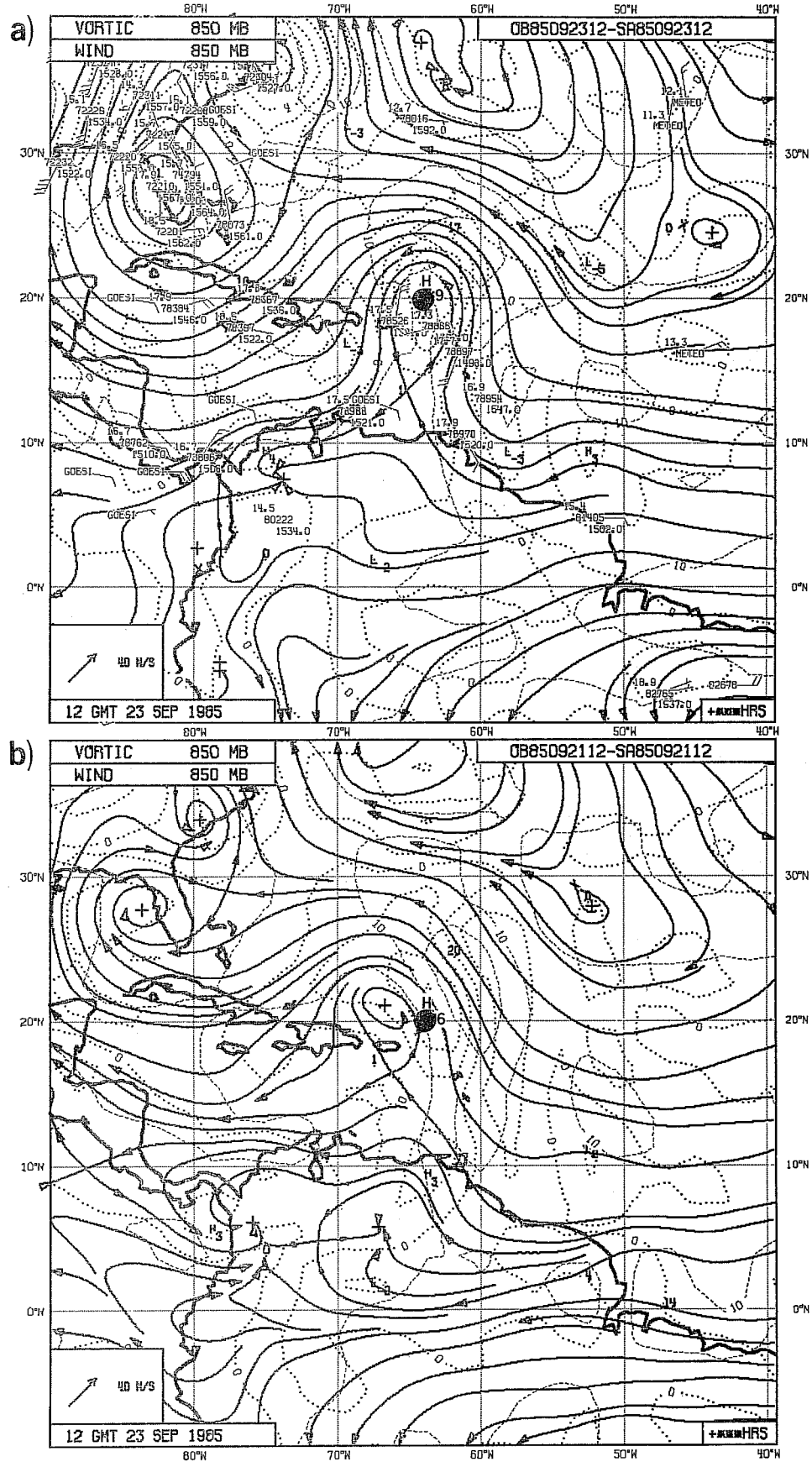

Fig. 9 Same as Fig. 6 for 23 September, 1985. Gloria is now a full hurricane and tracking is by aircraft reconnaissance.

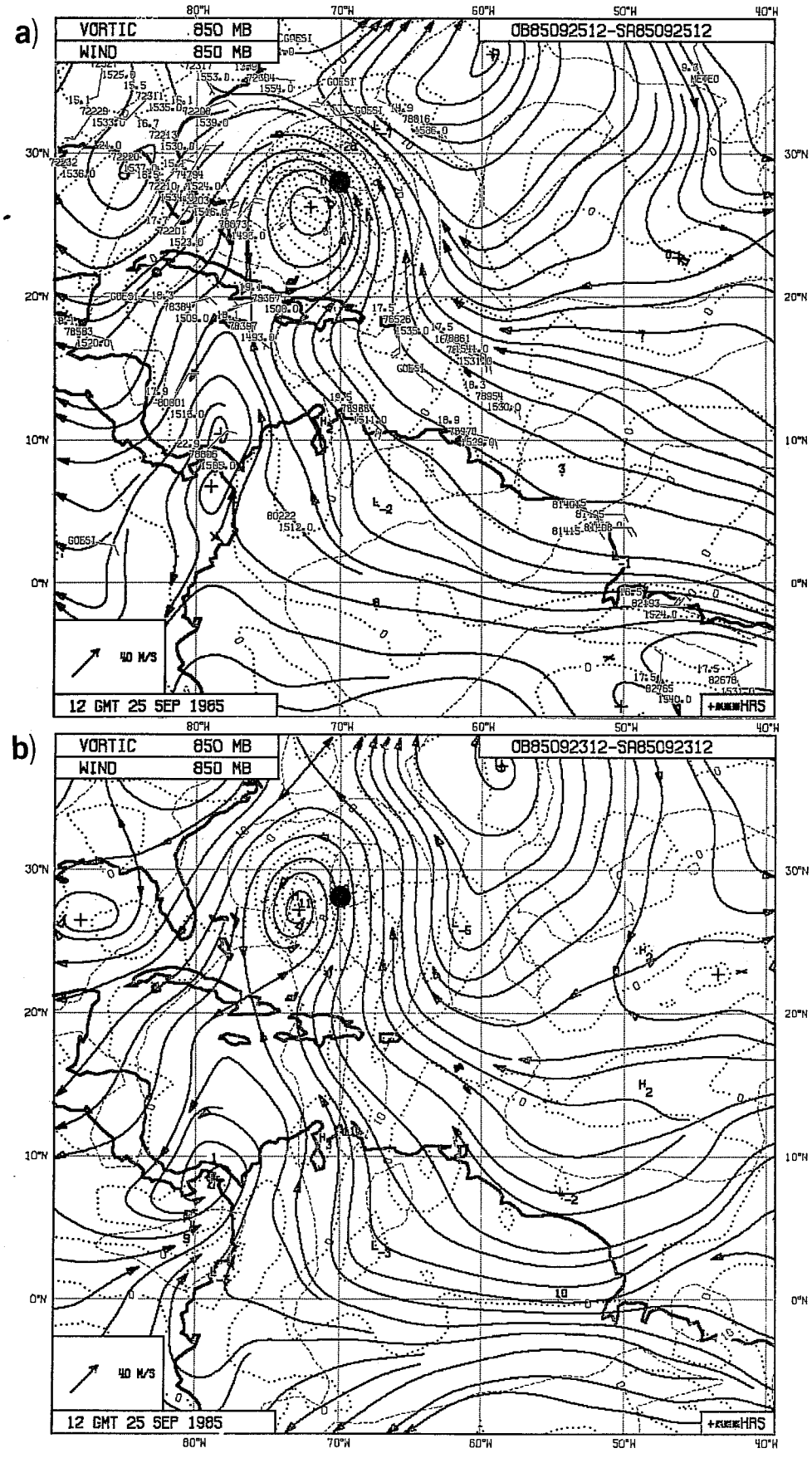

Fig. 10 Same as Fig. 6 for 25 September, 1985.

GMT 15 September, when the disturbance was located at 11°N, 19°W, a short distance off the African coast, and ends with the chart for 12 GMT 25 September, when the storm was located east of Florida and had attained hurricane strength. From the charts for 12 GMT 17, 19 and 21 September (Figs. 6a-8a) it is apparent that the analysis system maintained and even strengthened the wave during its passage across the Atlantic despite the virtual absence of data. Intermediate charts (not shown) were marked by a similar deficiency of data. Surface ship reports gave some hint of the disturbance but could hardly have been responsible for the sharply defined system at 850 mb. Cloud track winds were absent at 700 mb and scanty at 200 mb. No airplane observations were received from the area.

Satellite images(e.g. Figs. 11-12) clearly reveal the presence of an unusually well organised disturbance in the general vicinity of the analysed wave. However, from close inspection of the images it is apparent that quite sizeable errors exist in the analysed positions for 17 and 19 September, if the 850 mb vorticity maximum (denoted by the letter H) is chosen to define the analysed position. The main maximum is located roughly 1000 km west-southwest of the satellite-inferred position on the 17th and over 500 km to the west of the observed position on the 19th. On the 17th a secondary maximum is evident within the same trough at a position closer to the satellite position.

The evolution of these analysis errors can be traced with the help of the available 6 h time continuity. This reveals that the primary vorticity maximum near 13°N, 38°W on the chart for the 17th developed suddenly between 00 and 12 GMT 17 September, as an offshoot of the somewhat larger but weaker region of vorticity to the east. The latter region, in turn, represented a

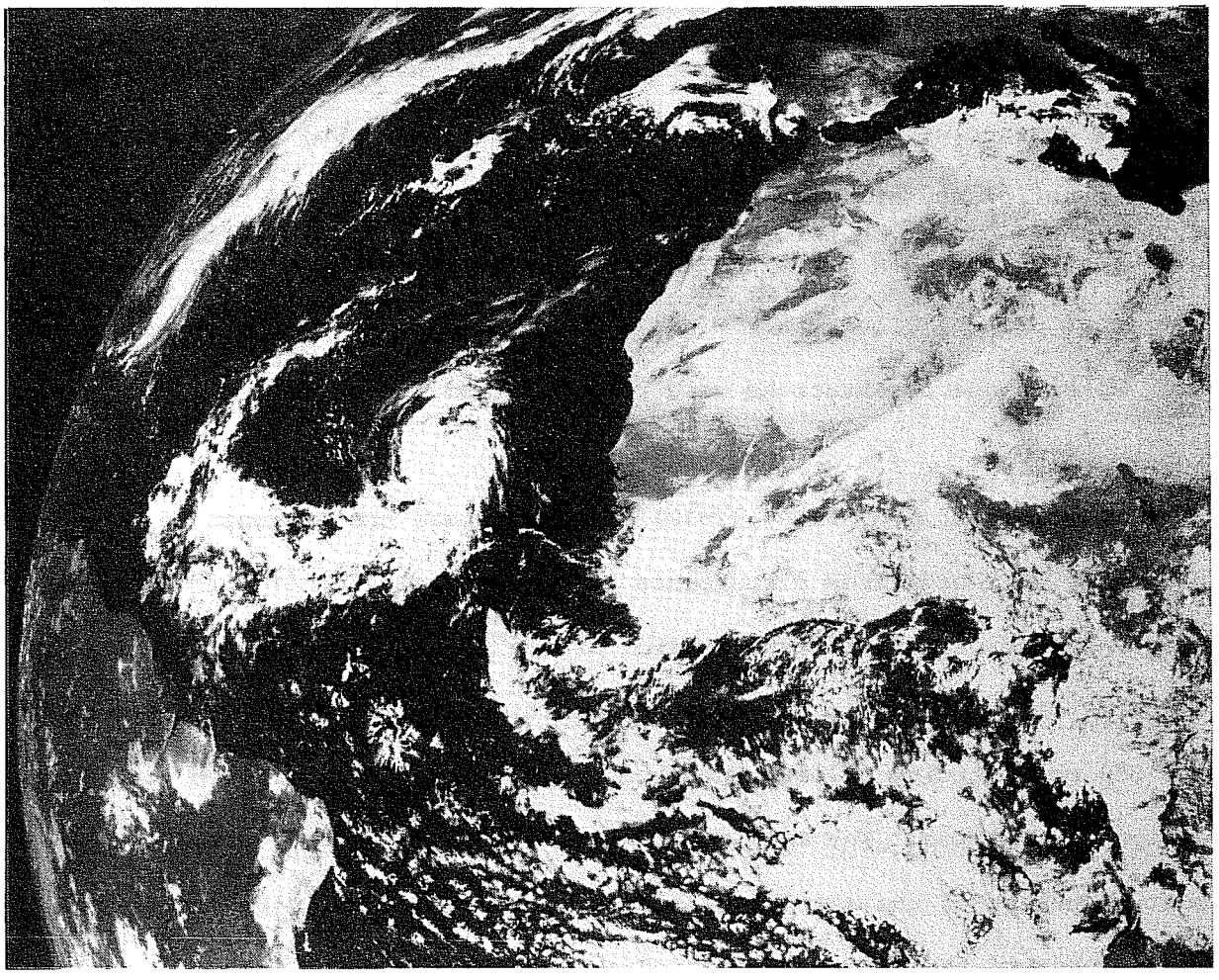

Fig. 11 Meteosat visible image of Gloria at 1155 GMT 17 September.

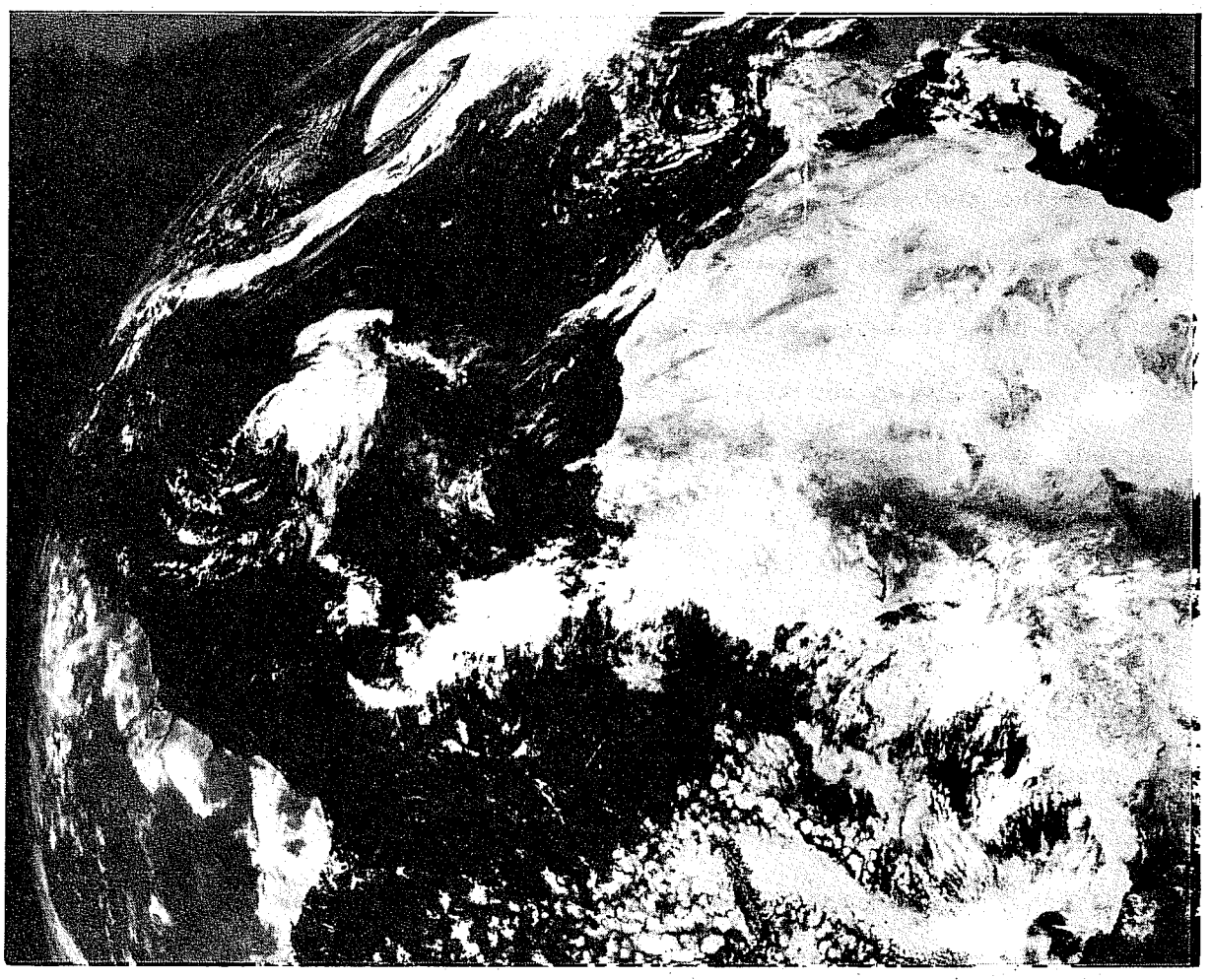

Fig. 12 Same as Fig. 11 for 1155 GMT 19 September.

new development that occurred to the rear or upstream of the maximum seen on the beginning chart (12 GMT 15 September). The original maximum moved rapidly west-southwestward and disappeared between 00 and 12 GMT on 16 September.

From this description it is evident that during the period 15-19 September the analyses of Gloria were more successful in depicting a synoptic-scale wave trough than the position of the disturbance itself. However, by 12 GMT 21 September the analysed position and the position obtained from reconnaissance aircraft were in close agreement, though the disturbance, now a tropical storm, had not yet emerged from the data-sparse region. The correction occurred gradually as the analysed storm moved systematically slower than the observed. Once in agreement the two positions remained more or less in agreement.

The seemingly complex and erratic behaviour of the vorticity maximum as the wave entered the data-sparse region is a matter requiring further study. The fact that new maxima developed rapidly in what appeared to be a random pattern suggests that their development was associated with a widely dispersed, rapidly growing phenomenon of smaller scale. Mesoscale cumulus convection is a likely candidate. In this respect it should be noted that Gloria possessed far more convective activity throughout its history than did Elena for which the analyses maintained a much simpler and more correct vorticity pattern. However, the data coverage for Elena was definitely better so this too could have contributed to the better prediction of its movement.

3.3.2 The Sahara dust storm

The second data-sparse case to be discussed occurred during a 7 day period of data outage over western and central Africa south of 22°N. Figs. 13a-f show how the assimilation system produced a wave at the border of the data network

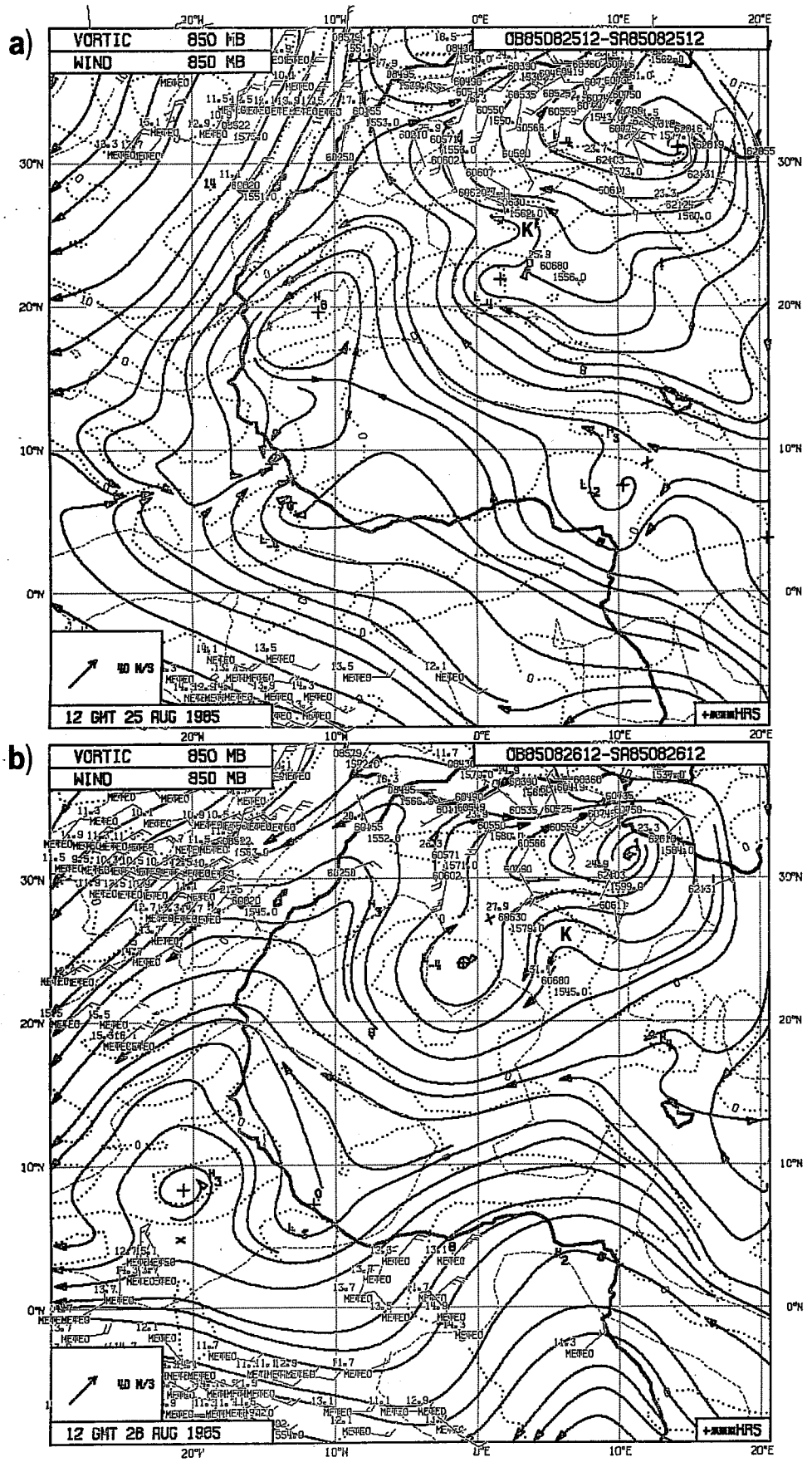

Fig. 13 850 mb analyses for 1200 GMT (a) 25 August, (b) 26 August, (c) 27 August, (d) 28 August, (e) 29 August and (f) 30 August, 1985. See Fig. 2a for further explanation.

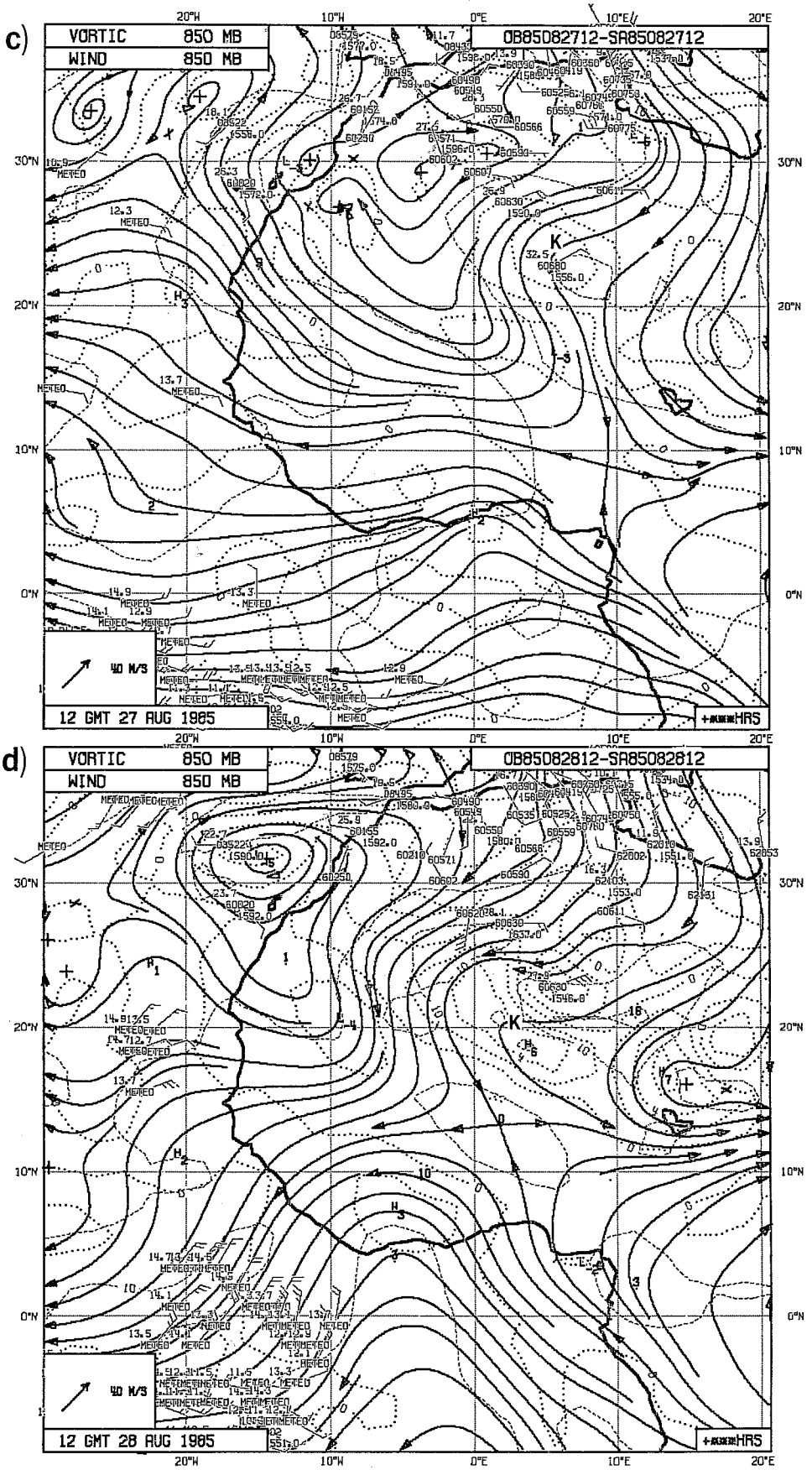

Fig. 13 (c) 27 August, (d) 28 August.

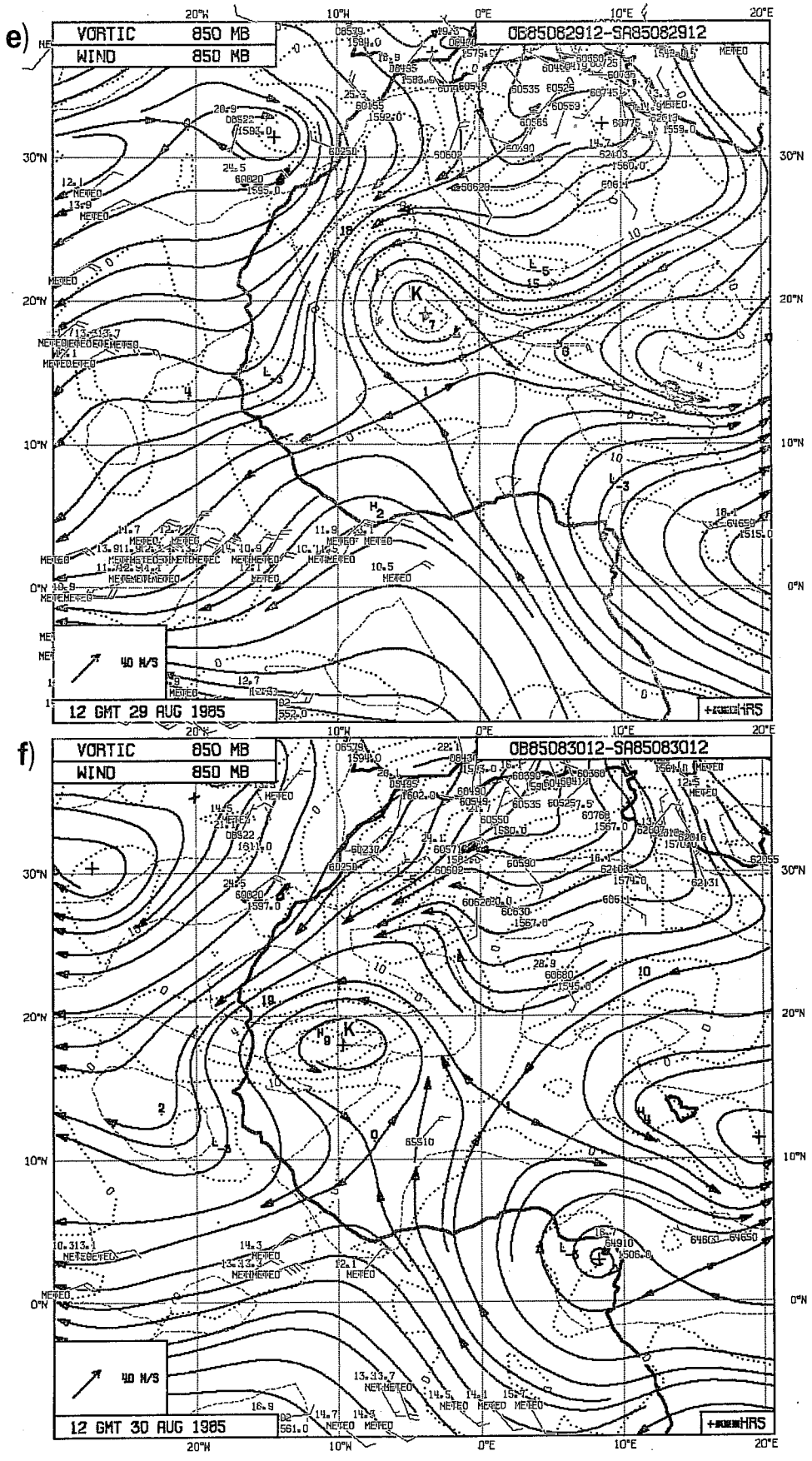

Fig. 13 (e) 29 August, (f) 30 August, 1985.

and developed it into a strong vortex ($\zeta = 9 \times 10^{-5}\ s^{-1}$) during its west-southwestward travel across the data void region. The letter "K" (cf. Table A1) denotes the vorticity maximum in question. The reality of the strong vortex is attested to by the dust signature seen in the Meteosat IR image for 1145 GMT 29 August (Fig. 14). The analysis of the vortex following resumption of the data was discussed briefly in subsection b.

The ability of the assimilation system to maintain a reasonable wave history during the 7-day period of missing data deserves comment. As this study and others have shown, African waves are a highly periodic phenomenon. They are believed to arise from the instability of the sub-Saharan, mid-trospheric jet (Burpee, 1972). Consequently, a properly functioning forecast model should - even in the absence of data - produce waves of the observed 2-3000 km length and 3-4 day period. The appearance of wave "K", in the same region as wave "I" but at a delay of 6 days, or approximately 2 wave periods, may therefore be taken as a sign that the wave instability was captured by the model. The surprising precision of the placement was almost certainly due to the fact that "K" developed along the margin of the data void region and therefore was at least weakly observed by stations in the marginal zone. It should also be noted that "K", like many of the waves examined, formed in proximity to the Hoggar mountains (see Fig. 1e) so that orography may also have been a factor in its development and in the accuracy of the prediction.

Wave "J", the antecedent wave in the sequence, is shown in the wave history, Table A1, to form downstream of "K" at the same time. Conceivably it developed earlier over the data void region but not in sufficient proximity to peripheral observations to be well analysed.

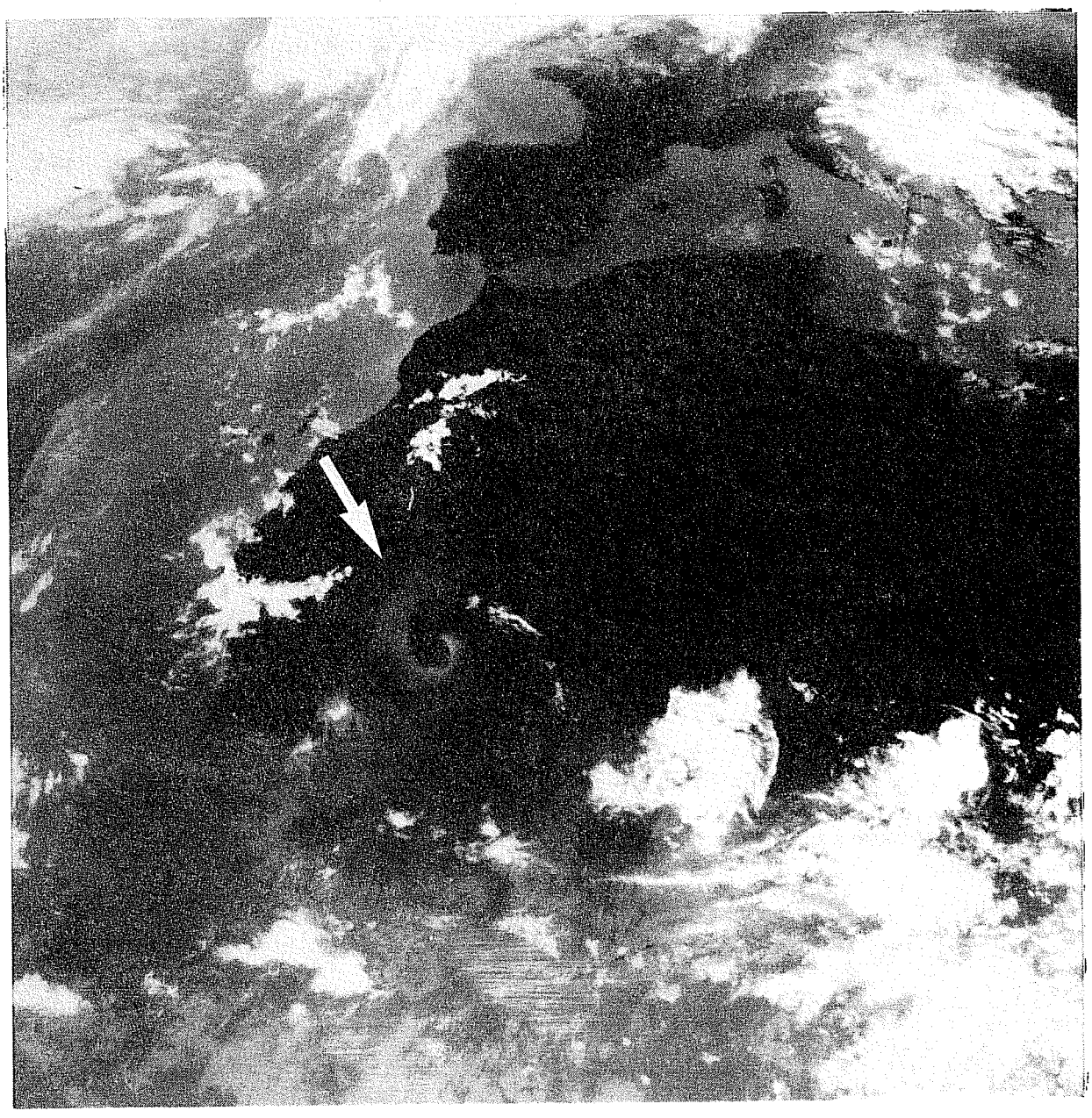

Fig. 14 Meteosat IR image of dust vortex (arrow) at 1155 GMT 29 August 1985.

4. FORECAST PERFORMANCE

Two different methods have been chosen to illustrate the performance of the forecasts: first, statistics are presented on the errors of the 48 h 850 mb forecasts in predicting the positions and intensities of vorticity maxima; second, 48 h 850 mb prognoses and the corresponding verification charts are shown for a number of selected cases. The statistical results employ only those forecasts for which adequate data exist at the verifying time to establish, with at least a moderate degree of confidence, that a wave trough and associated vorticity maximum were present within the area of verification. The selected cases were chosen mainly for their interest. They are believed to be representative of the general level of performance. Four of the cases deal with wave disturbances that developed into named storms: Danny (wave "A"), Elena (wave "H"), Fabian (wave "L") and Gloria (wave "O"). The fifth case concerns a type of development that is somewhat outside the scope of the present study. It is included in order to show the ability of the model to forecast the development of disturbances that are different in character from easterly waves - in this case a subtropical system that formed underneath the upper-tropospheric, mid-ocean trough (Simpson et al., 1968).

4.1 Statistical Results

The error statistics regarding the 48 h forecasts of 850 mb vorticity maxima appear in Table 2. The statistics have been compiled for five subregions termed: Central/West Africa (east of 0°), West Africa (0°-14°W), Eastern Atlantic (15°-29°W), Central Atlantic (30-54°W) and Western Atlantic (west of 54°W). The sample size was small in the easternmost region, in part because of data deficiencies and in part because of the limited wave activity in the region. The sample size was also small in the Central Atlantic where low-level, cloud track winds rarely existed in sufficient number to define the

Table 2 - Forecast Performance : Statistical Summary

Area	Number of cases	Latitude Error (degrees) mean	S.D.	Longitude Error (degrees) mean	S.D.	Intensity Error ($10^{-5}s^{-1}$) mean	S.D.
Central/West Africa (0° →)	3	2.3	2.1	2.7	5.0	0	2.6
West Africa (0°-14°W)	20	0.7	2.3	-0.8	2.8	-1.4	2.6
Eastern Atlantic (15°-29°W)	16	1.8	1.6	-0.6	1.8	-0.1	1.9
Central Atlantic (30°-54°W)	6	1.5	2.4	-1.5	2.8	0.5	1.9
Western Atlantic (← 54°W)	34	0.5	1.7	0.4	2.3	-2.1	3.0

waves. The data from which the statistics were compiled are shown in full in Tables A2-6 of the Appendix. The latter tables identify each wave alphabetically, give the verification dates and list for those dates the observed (O) and forecast (F) positions and intensities of the vorticity centres. Errors are forecast minus observed values. East longitudes are considered negative.

4.1.1 Africa

A modest ability to forecast the waves is evident in the area to the east of the Greenwich meridian. However, the sample size is too small to provide truly meaningful statistics. Many more verifiable cases existed for the African region west of the Greenwich meridian where there is clear evidence of forecast skill. On the average, 48 hr forecast displacements of the vorticity maxima were in error by less than one degree in both latitude and longitude. The 48 hr forecast intensities were too weak by slightly more than $1 \times 10^{-5} s^{-1}$. Average 48h longitudinal displacements were about 12° (see Table 1), and the average observed strength of the relative vorticity centres was $5.8 \times 10^{-5} s^{-1}$. Forecast positions were on the average too far to the north and too far to the east (westward propagation too slow). The position errors, though small, are all statistically significant at the 10% level according to the t-test. The intensity error is significant at the 1% level.

4.1.2 Atlantic

In the Eastern Atlantic region forecast positions are again somewhat too far to the north and east. The longitudinal position error of -0.6° is statistically significant at the 10% level. The 1.8° error in latitudinal position is significant at the 1% level. On average the observed and forecast intensities are the same. The sign of the position error remains the same in the central Atlantic. Here the forecast vorticity is slightly larger in the

mean than the observed but not significantly so. The position errors are significant at about the 10% level. In the westernmost region, where the sample size is largest, position errors are small but in the case of the latitudinal position is significant at the 5% level. As in the areas further east, the forecast position is in the mean displaced too far to the north. Forecast vorticity is weaker than observed vorticity (5.4×10^{-5} s^{-1} vs 7.5×10^{-5} s^{-1}) at the 1% significance level.

In summary, the statistical results indicate that the T106 model possesses considerable skill in predicting the behaviour of easterly waves over West Africa, in the extreme eastern Atlantic and in the far western Atlantic and Caribbean. Some skill probably exists for prediction in the western part of the central African region, though forecasts there are hampered by the lack of upstream data. Since the main wave growth occurs to the west of 10°E, the data lack, though regrettable, does not appear in most cases to be crucial to early identification of the waves.

There is evidence of forecast skill in the central Atlantic, but firm verification is rarely possible there because of the general lack of low- and mid-level winds. In some instances, satellite images can be employed to identify and locate the mid-ocean waves with considerable confidence. This was the case for waves "H"(Elena), "M" and "O"(Gloria). The satellite verification also gave evidence of some skill in mid-ocean forecasting, at least for the stronger disturbances, as will be shown in the next section for two of the systems ("H" and "O").

4.2 Selected examples

Example 1) Hurricane Danny, (11-15 August, 1985)

Between 7 and 8 August an enhanced pattern of deep cloudiness developed over and to the east of the Windward Islands (55°-60°W) as wave "A" approached the Caribbean. Intensification of the wave followed, and at 12 GMT on 11 August (Fig. 15) a well formed disturbance was clearly discernible in the central Caribbean. During the next 48 h the 850 mb vorticity maximum was forecast to move to the eastern Gulf of Mexico, off the western tip of Cuba, and maintain its intensity (Fig. 16b). The verifying map for 13 August (Fig. 16a) reveals that both position and intensity were well forecast. The subsequent 48 h forecast (Fig. 17b) called for the centre to move ashore near the Texas-Louisiana border and to maintain its intensity. The actual movement (Fig. 17a) was somewhat slower than predicted and the intensity (as analysed) was twice that predicted. At this time (12 GMT 15 Aug) the storm was a minor hurricane. In view of the limited resolution of the T106 system (lowest resolvable wave of 380 km), it cannot be expected to resolve the core of a hurricane. At most it can be expected to predict the outer circulation of the storm and to provide some measure of its intensity. In this respect the model enjoyed limited success.

Example 2) Hurricane Elena (22-28 August, 1985)

This case illustrates the ability of the model to make a highly accurate prediction of the movement of a well formed wave ("H") as it crossed the Atlantic despite the availability of only a small amount of ocean data. The system is tracked from the time it left the African coast until it achieved hurricane force over Cuba. The initial chart for the series (Fig. 3) shows Elena approaching the African coast at 1200 GMT, 22 Aug 1985. The 48 h forecasts and verifying charts for 24, 26, 28 August are shown in Figs. 18-20. The wave crossed the ocean at the unusual speed of 11° long d^{-1}, yet it can be

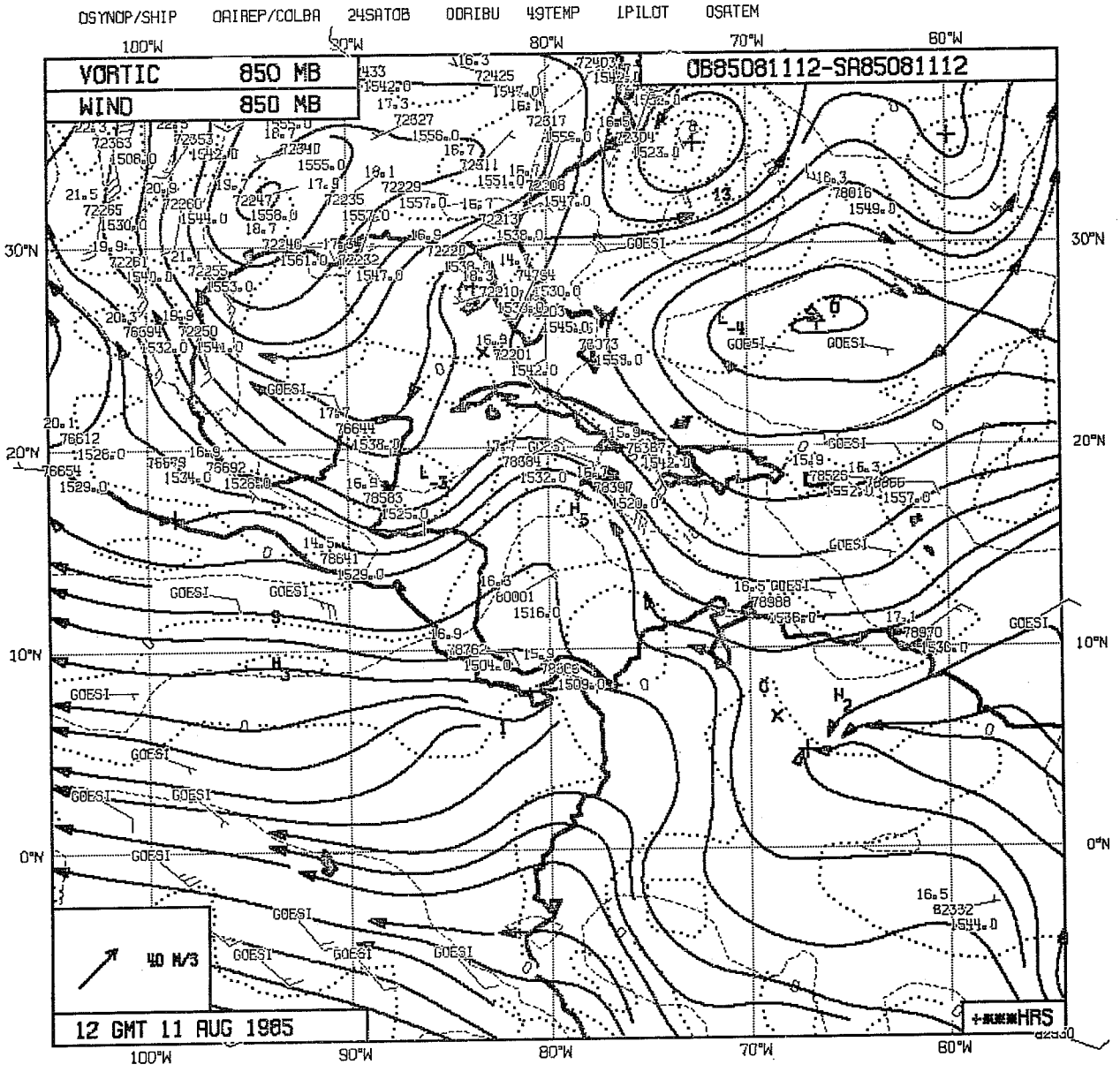

Fig. 15 850 mb analysis for 11 August, 1985. See Fig. 2a for further explanation.

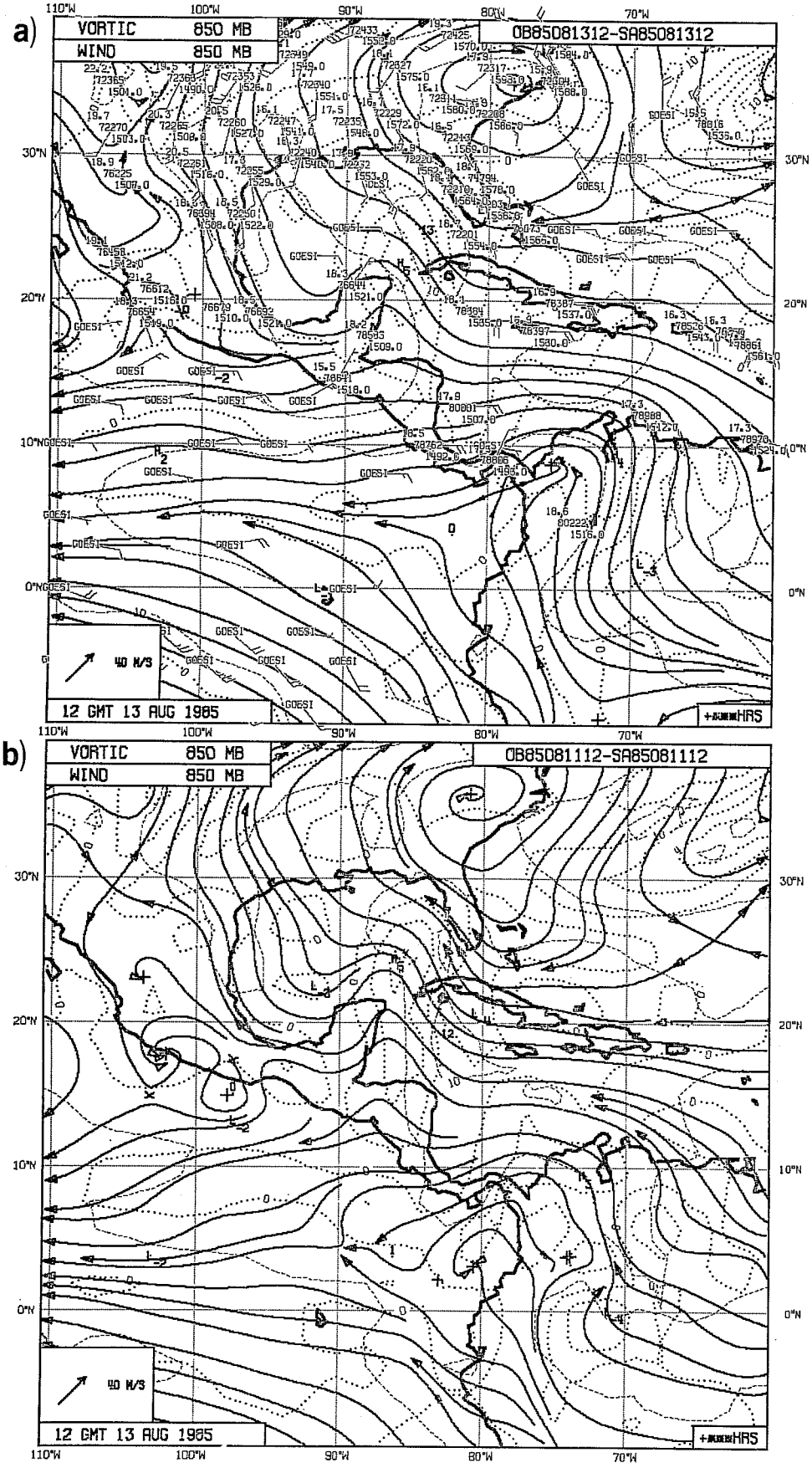

Fig. 16 (a) 850 mb analysis for 13 August, 1985. (b) 48 h forecast verifying at that hour. See Fig. 2a for further explanation.

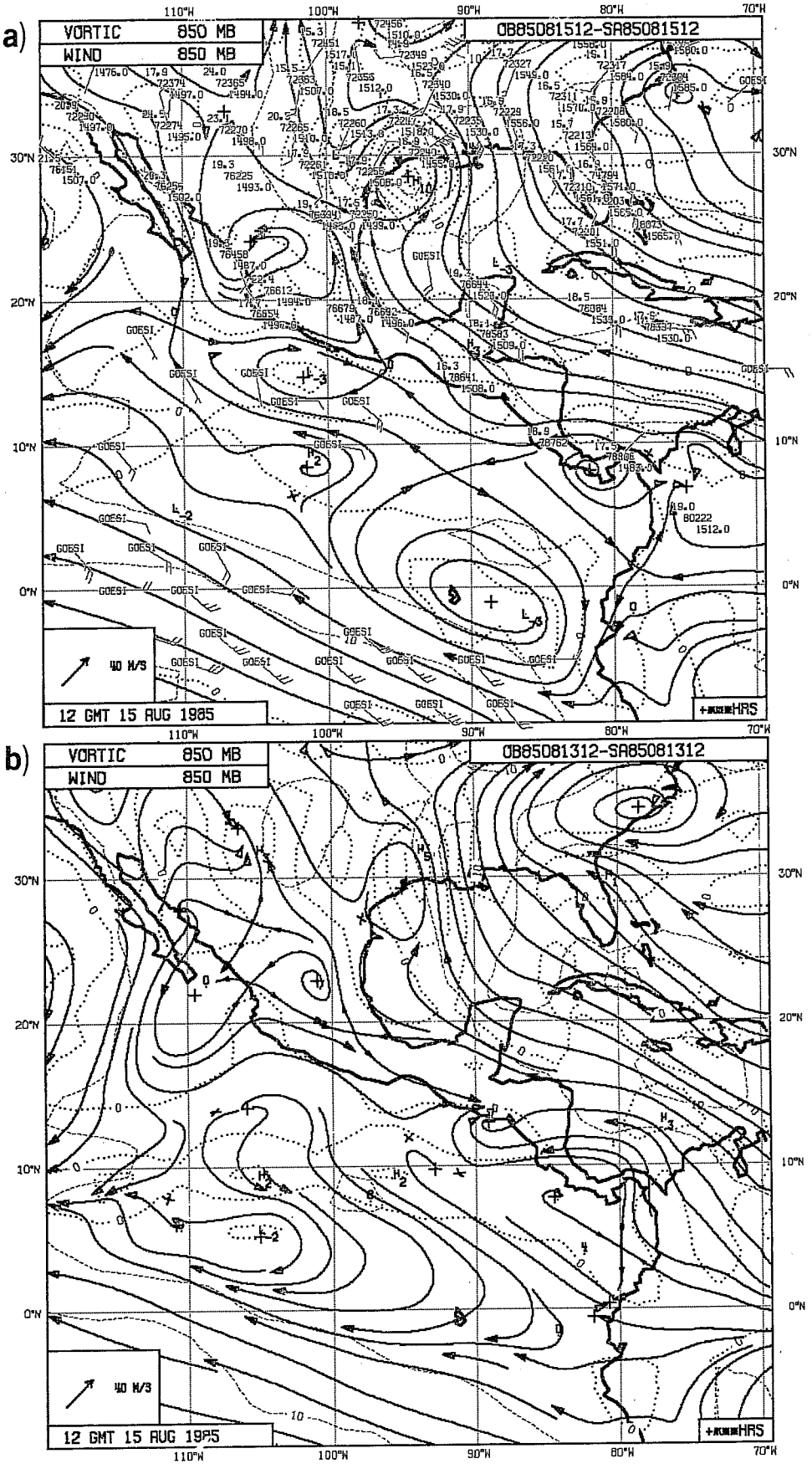

Fig. 17 Same as Fig. 16 for 15 August 1985.

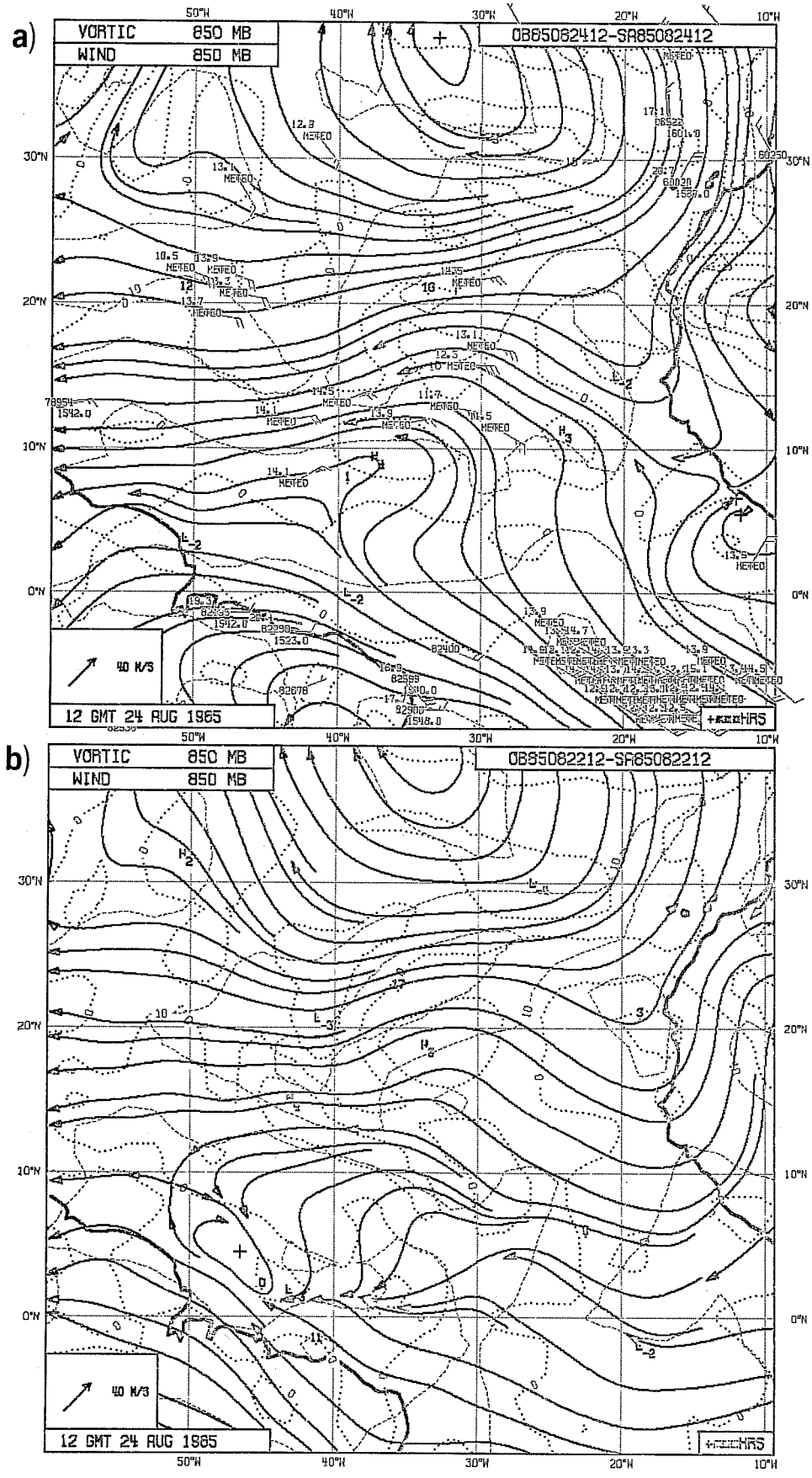

Fig. 18 (a) 850 mb analysis for 24 August, 1985. (b) 48 h forecast verifying at that hour. See Fig. 2a for further explanation.

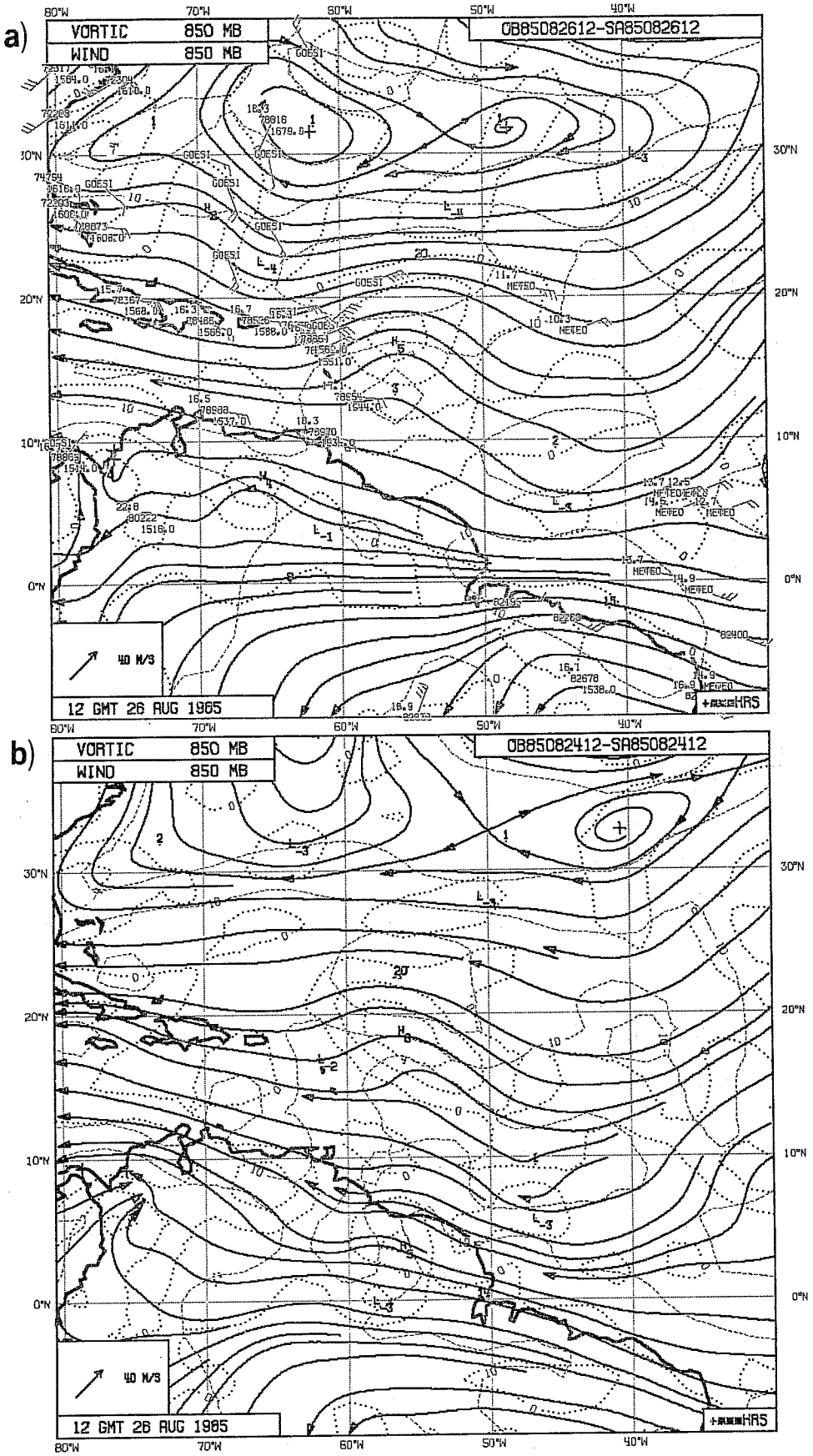

Fig. 19 Same as Fig. 18 for 26 August, 1985.
See Fig. 2a for further explanation.

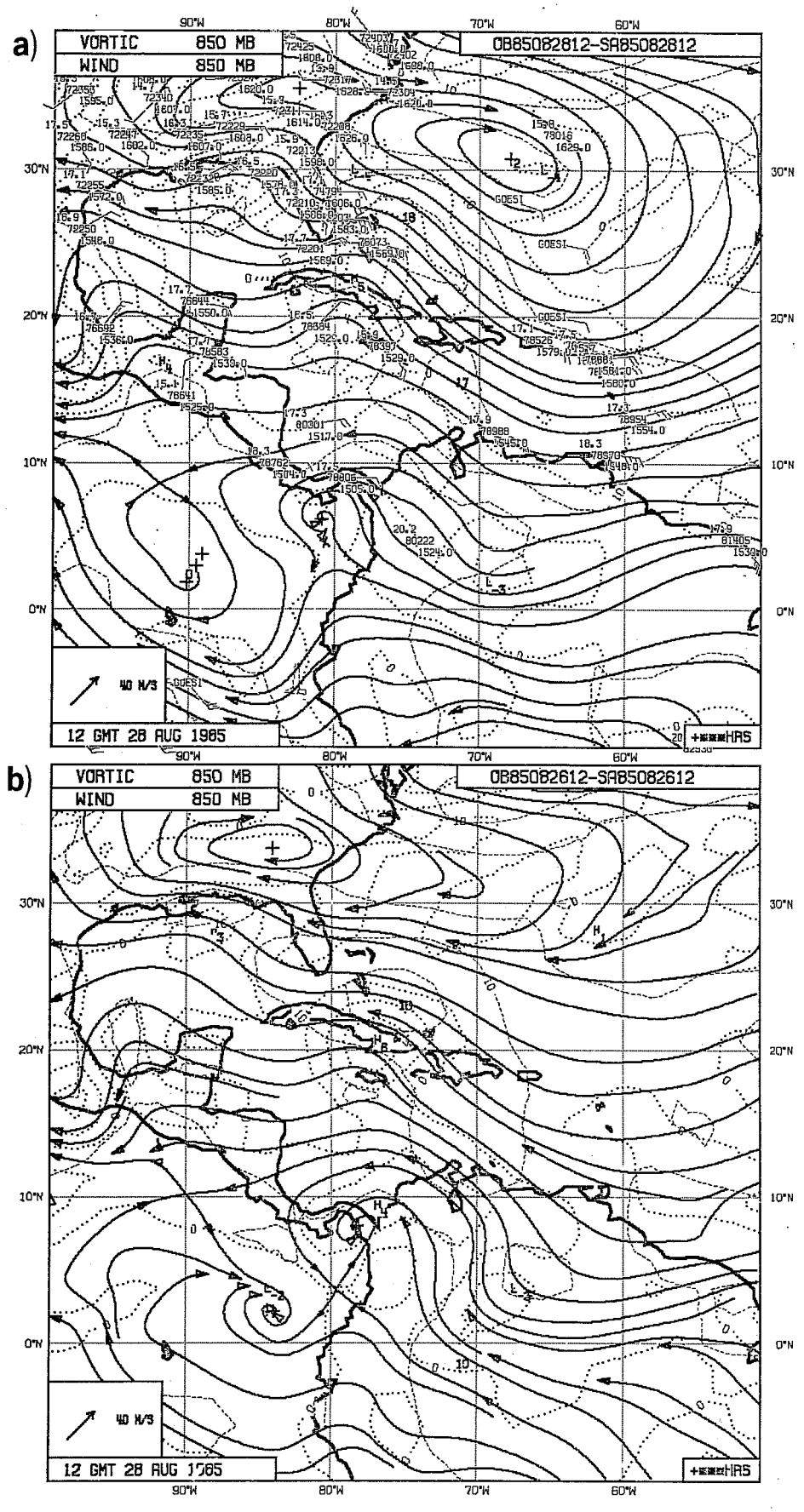

Fig. 20 Same as Fig. 19 for 28 August 1985.

seen that the errors in the forecast positions are very small: of the order of a degree or two in 22°-23° of travel. The forecasts for 23, 25 and 27 August (not shown) were equally good. Satellite imagery (Figs. 21 and 22) confirms the analysed positions, and the position on the 26th was also consistent with wind reports from downstream islands. Data coverage over the ocean, though sparse, was average or slightly better than average during this period. The coverage at 12 GMT 24 August was somewhat better than for the period as a whole, and that at 12 GMT 26 August was somewhat worse.

Elena reached hurricane strength on 29 August, soon after entering the Gulf of Mexico. After following a fairly steady course towards Louisiana, its movement became erratic. It eventually made landfall as a severe hurricane in Mississippi on 2 September. The rapid intensification of the system and the later erratic path were poorly forecast. Heckley et al., (1986) show the forecasts in this latter state to be extremely sensitive to the form of parameterisation of deep cumulus convection.

Example 3) Tropical Storm Fabian (11-17 September)

Between 9 and 10 September the cloud pattern along the ITCZ associated with wave "L" thickened and assumed a vortical shape. At 12 GMT 11 September the analysis (Fig. 23) still depicted only a weak wave in the wind field (near 15N, 60W) and failed to show a pronounced vorticity maximum. Two days later (Fig. 24a) a definite strengthening of the wave, now at 72°W was evident in the analysis; the forecast (Fig. 24b) showed the enhanced vorticity in nearly the correct position but underestimated the northerly flow component ahead of the wave axis. During the following two days the wave progressed only slightly westward and sharpened along its northern portion between 20-25°N (Fig. 25a). This behaviour was well handled by the forecast (Fig. 25b). A strengthening and east-northeastward movement of the disturbance, or vorticity

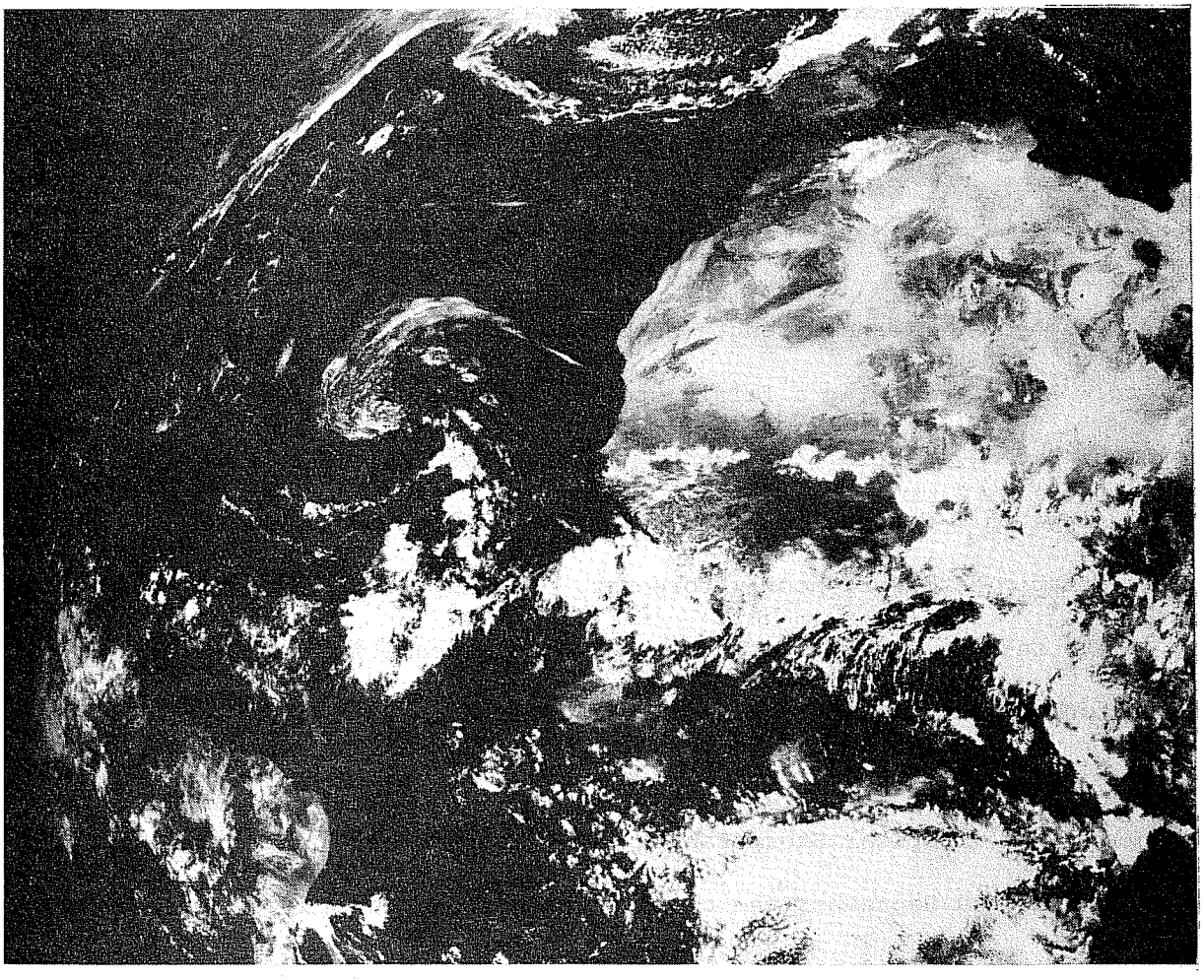

Fig. 21 Meteosat visible image for 1155 24 August 1985

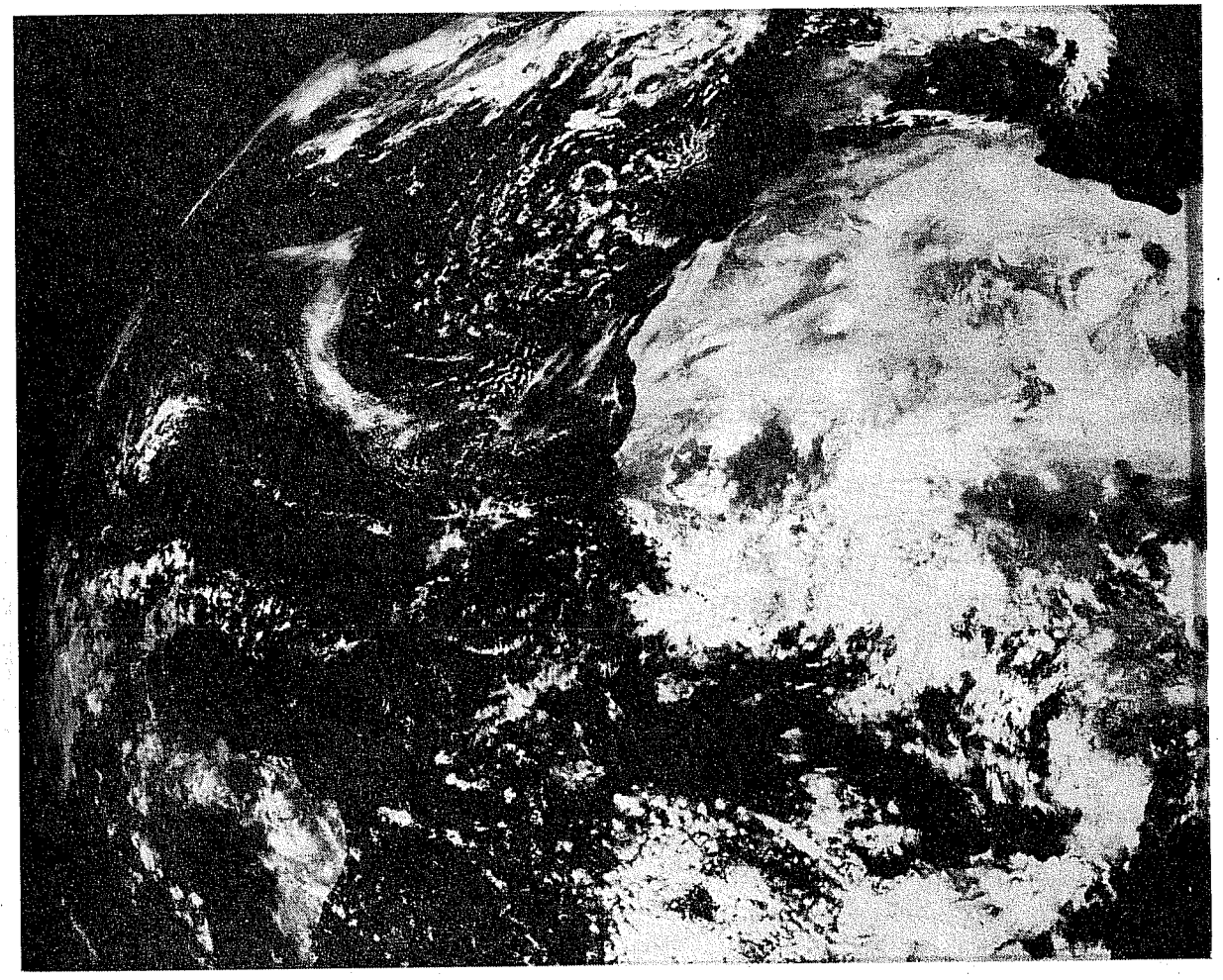

Fig. 22 Same as Fig. 21 for 26 August 1985.

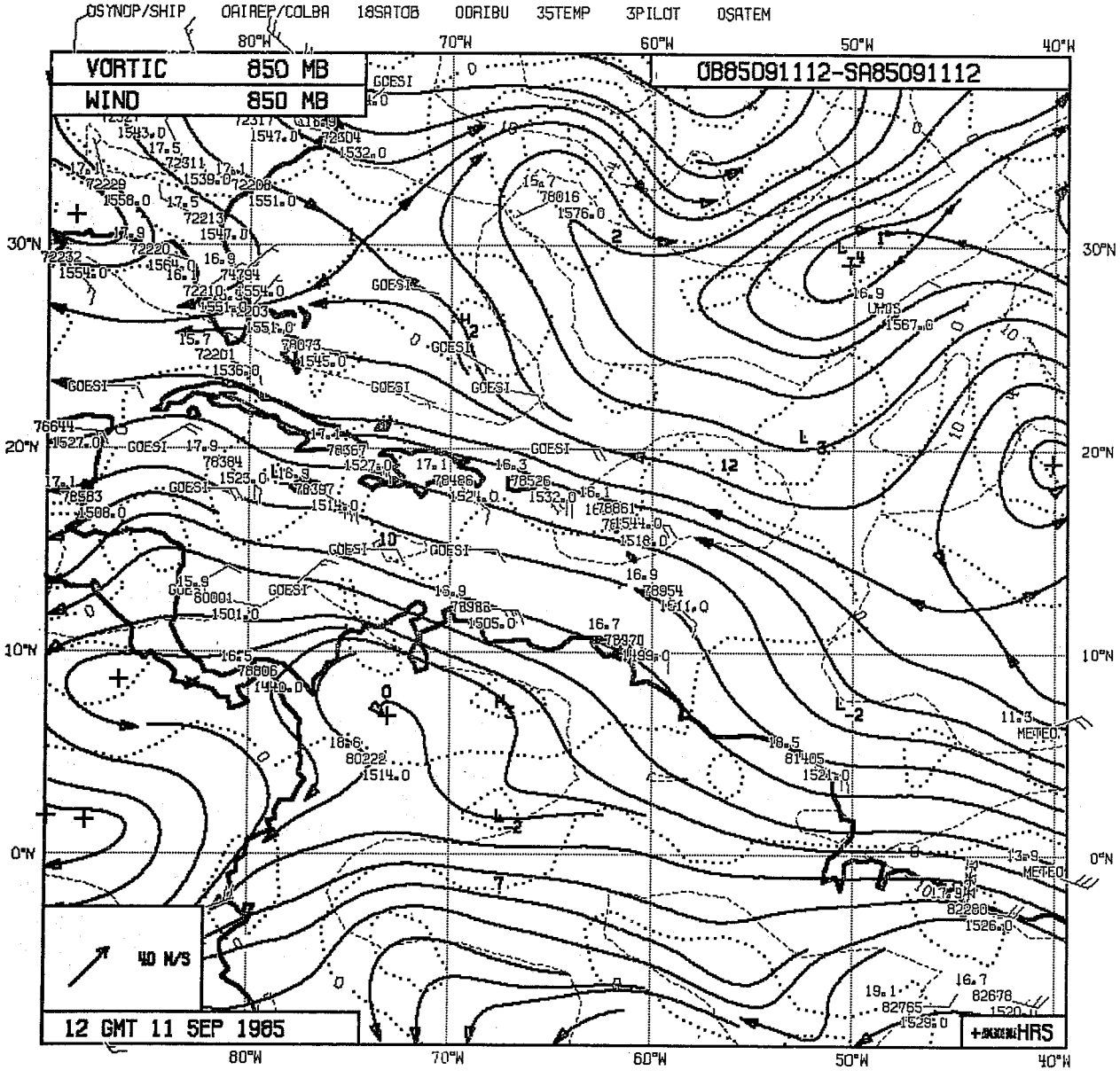

Fig. 23 850 mb analysis for 11 September, 1985. See Fig. 2a for further explanation.

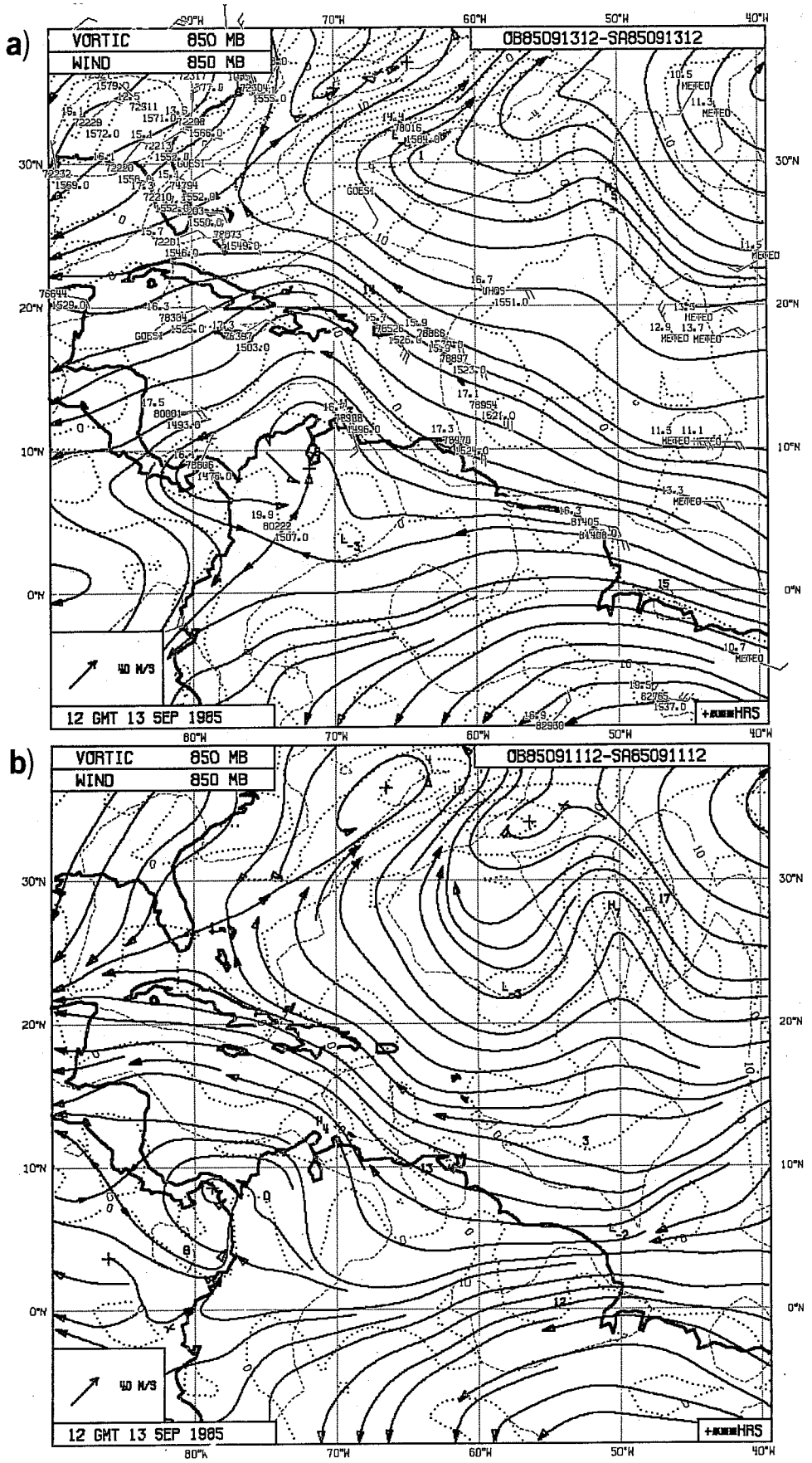

Fig. 24 (a) 850 mb analysis for 13 September, 1985. (b) 48 h forecast verifying at that hour. See Fig. 2a for further explanation.

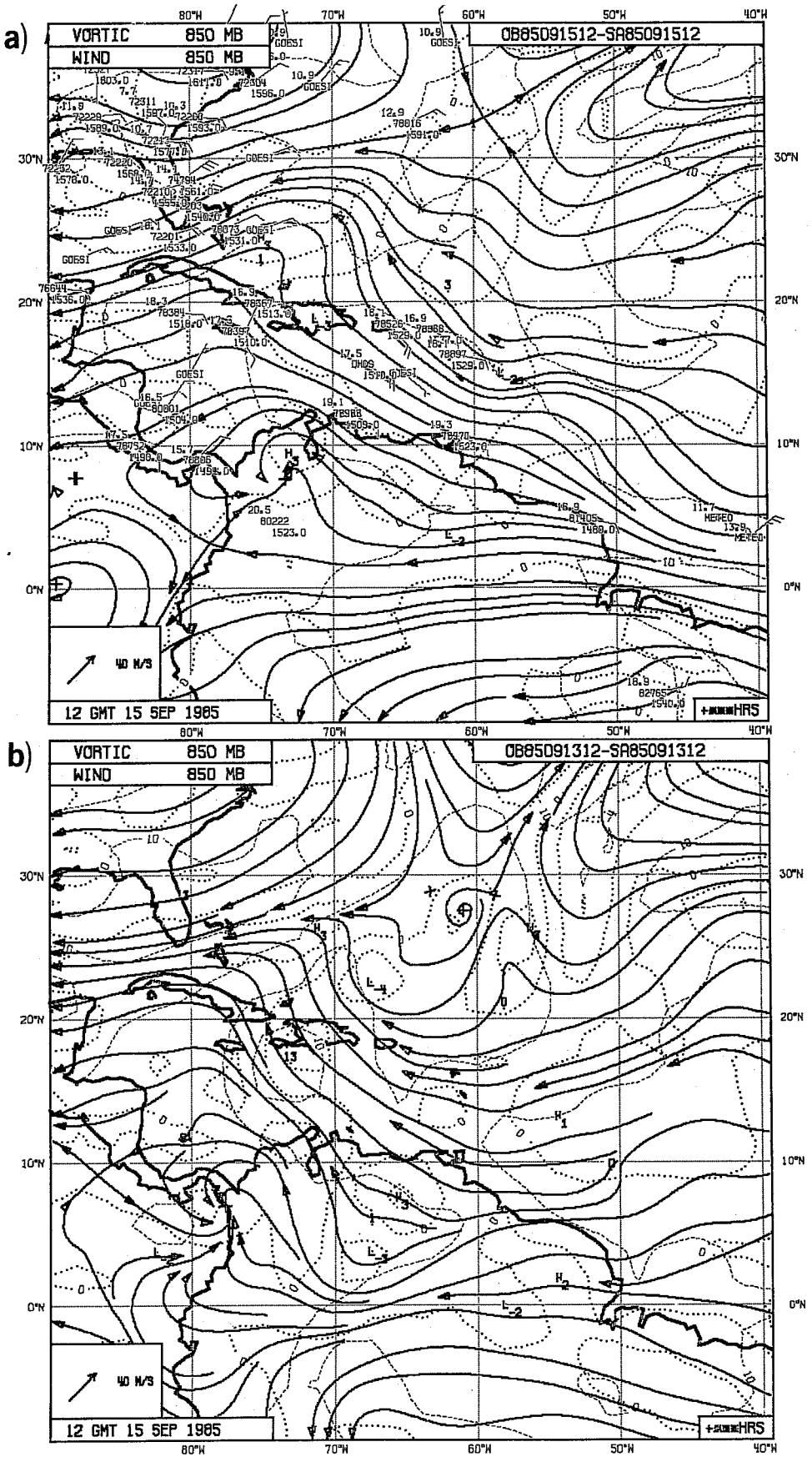

Fig. 25 Same as Fig. 24 for 15 September, 1985.

centre, to a position near 27N, 64W was predicted for the period 15-17 September (Fig. 26b). The forecast centre was located about 100-200 km southwest of the analysed centre (Fig. 26a). Although the actual disturbance was much stronger than the forecast (and analysed) disturbance, having attained tropical storm intensity on 17 September, the forecast gave a useful indication of the motion of the storm and of the tendency for intensification. Again because of insufficient resolution of the T106 forecast system, the analysis only succeeded in depicting the outer circulation of the storm.

Fabian subsequently moved rapidly into the Atlantic and remained a tropical storm only until 19 September.

Example 4) Hurricane Gloria (15 - 23 September)

This storm began as wave "0" over West Africa on 12 September or 8 September, depending upon which of two vorticity centres is regarded as its earliest manifestation. It reached the offshore waters of the U.S. on 25 September as an intense hurricane (sustained winds 67 m s^{-1}; gusts 77 m s^{-1}).

The beginning map in the series for 12 GMT 15 September 1985 (Fig. 5) depicts the disturbance located just off the African coast (vorticity maximum at 11N, 19W). Successive maps (Figs. 6-10) show its later history, as given by the analyses. These maps have already been discussed in Section 3 where it was remarked that the disturbance was maintained as an unusually strong system over the Atlantic despite a near absence of oceanic data.

The 48 h forecast for 12 GMT 17 September (Fig. 6b) shows a pronounced wave in the mid-Atlantic near 40°W that is located somewhat to the west of the analysed wave (Fig. 6a). However, as discussed in Section 3.2, the analysed

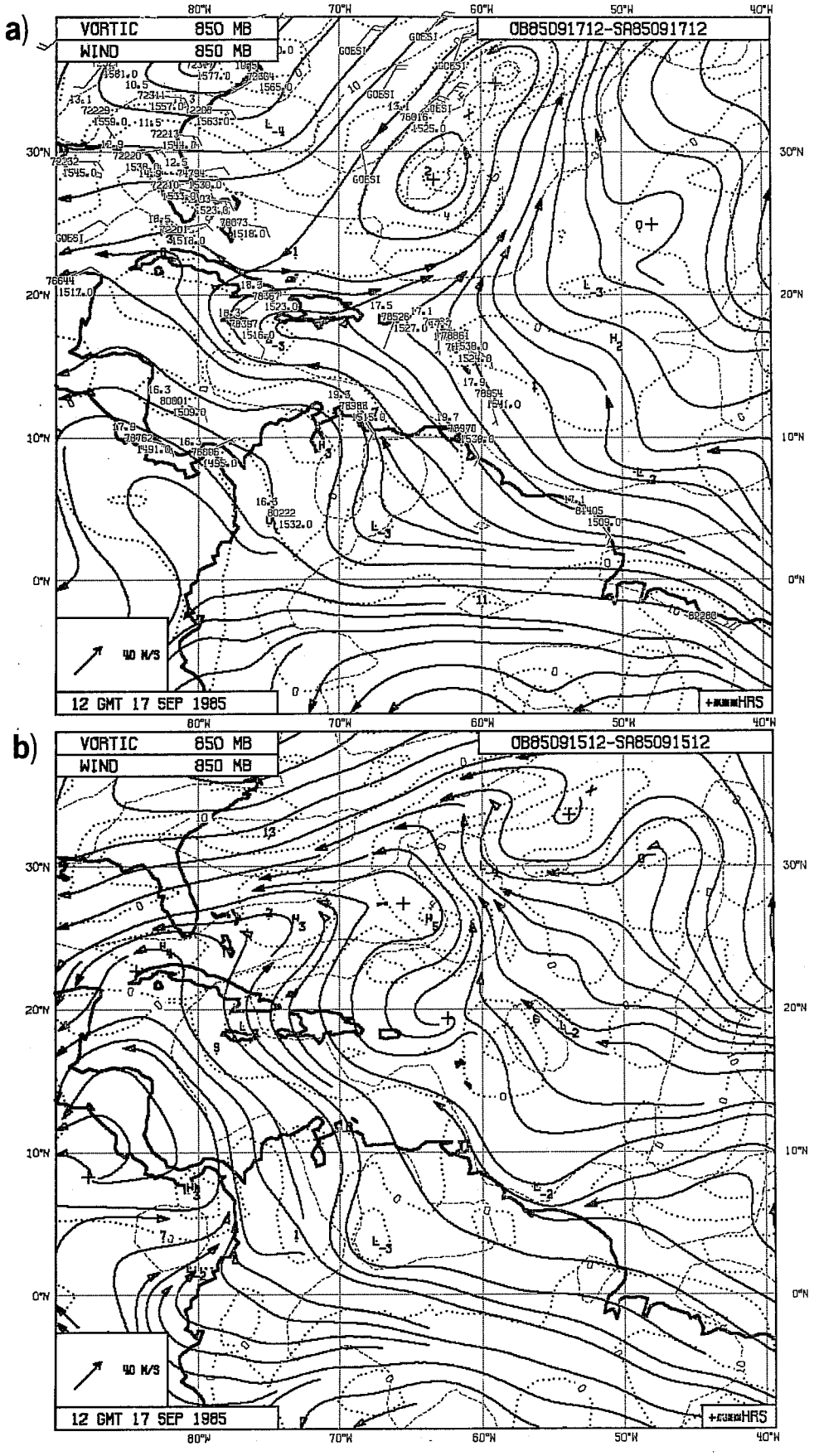

Fig. 26 Same as Fig. 24 for 17 September, 1985.

position of the primary vorticity maximum at 13N, 38W differs considerably from the position inferred from satellite imagery (large dot at 15°N, 29°W) in such a sense as to increase the error of the forecast. Analysed and forecast positions (17°N, 46°W and 19°N, 46°W, respectively, on Figs. 7a, 7b) are in reasonably good agreement at 12 GMT on the 19th, the forecast position being about 2 deg north of the analysed. Both positions are well to the west of the satellite derived position at 17°N, 41°W (large dot on Fig. 7a), but the discrepancies are not as large as they were earlier. At 12 GMT on 21 September the forecast centre (Fig. 8b) is at the same longitude (55°W) as the observed centre and 2 deg further south in latitude. The analysed position is now in good agreement with the position given by aircraft reconnaissance. The forecast position is not quite as satisfactory but is still remarkably good given the uncertainty of the initial analysis. The forecast called for the vorticity to maintain the same strength, whereas the strength increased considerably.

The forecast position (20°N, 64°W) at 12 GMT 23 September Fig. 9b is virtually identical with the analysed position and both positions agree well with the observed position as given by air reconnaissance, being located only about one degree too far to the west. The vorticity maximum was forecast to strengthen slightly. Its value was less than the analysed value and in view of the intensification of the storm to hurricane force, much less than the actual value. Another shortcoming of the forecast was the considerable displacement of the vorticity maximum from the circulation centre. In this case the vorticity maximum gave by far the better storm position.

Later forecasts displayed considerable skill in predicting the further movement of the storm. The 48h forecast verifying at 12GMT 24 September had a position error of about 400 km. This figure was reduced to 300 km for the

forecast verifying at 12 GMT on 25 September (Fig. 10) and to 200 km for the forecast verifying at 12 GMT on 26 September.

The predicted vorticity maximum at the latter time was 15 x 10^{-5} s^{-1} and the strongest predicted wind was 23 m s^{-1} at a position about 400 km to the northeast of the centre. Thus on the synoptic scale the T106 model was quite successful in forecasting the intensity of the storm as it approached the mainland. As with its predecessors the model lacked the resolution required for representing the tight inner core of the storm.

We close this discussion of Hurricane Gloria by returning to the forecast for 17 September in which the predicted vorticity maximum (Fig. 6b) was located more than 1000 km to the southwest of the satellite-derived storm centre. Earlier we described the evolution of the incorrectly placed vorticity maximum on the analysis. Here we note that the even more incorrectly placed maximum on the forecast chart had a different history than the analysed maximum. The 24h forecast for 16 September (not shown) reveals that the centre on the 48h forecast for 17 September (Fig. 6b) was associated with the secondary centre seen near 7°N, 29°W on the chart for 15 September (Fig. 5) or else with the vorticity lobe extending northwestward from it. Again there is evidence that some feature of the model, presumably its treatment of convection, causes the sudden enhancement or development of small areas of relatively strong positive vorticity.

Example 5) A subtropical system (13 - 15 September)

The 850 mb analysis for 12 GMT 13 September (Fig. 27) exhibits a weak vorticity maximum at 30°N, 30°W within the northeasterly flow around the Azores High. This vorticity maximum is forecast to move west-southwestward to

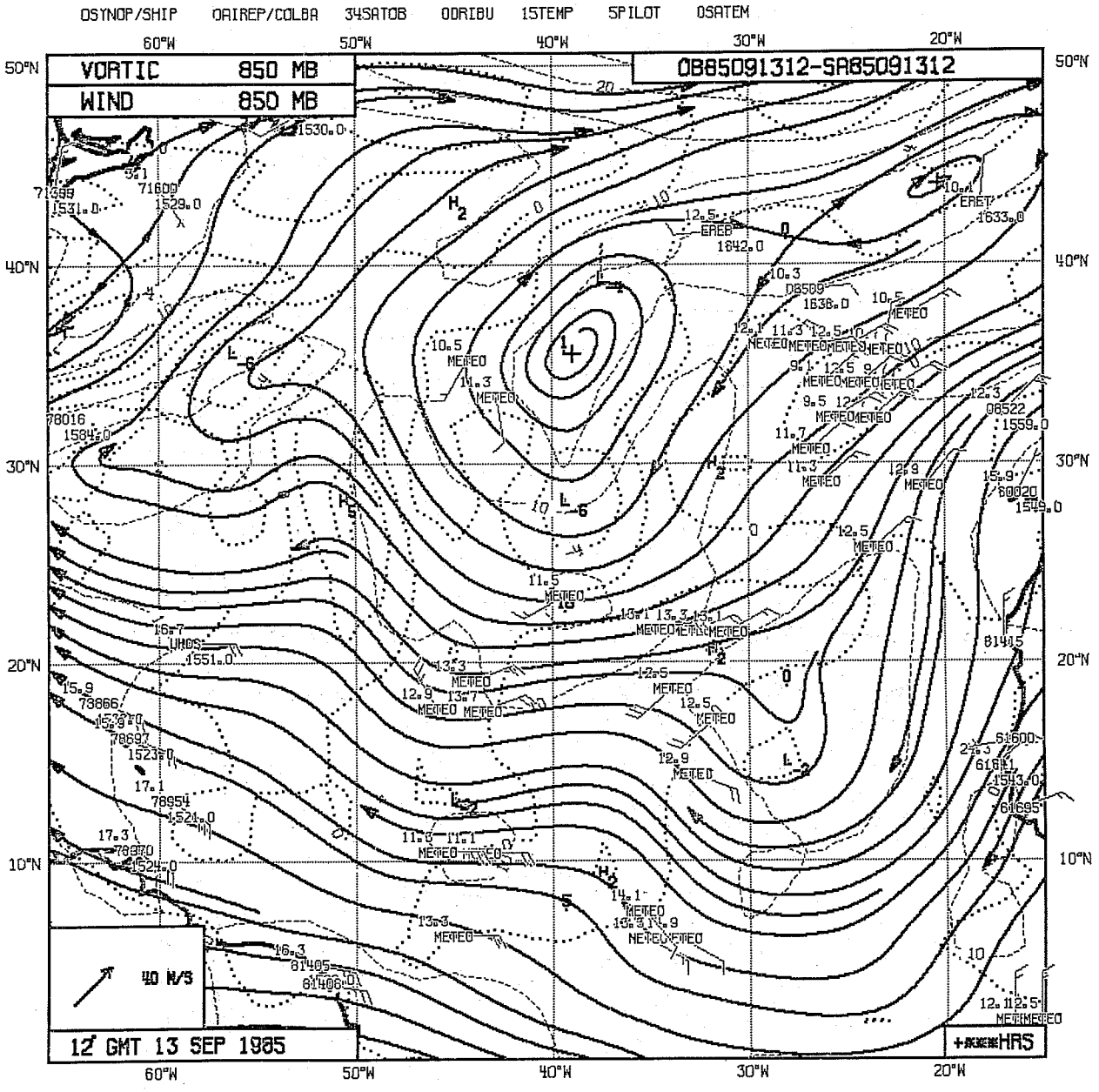

Fig. 27 850 mb analysis for 13 September, 1985. See Fig. 2a for further explanation.

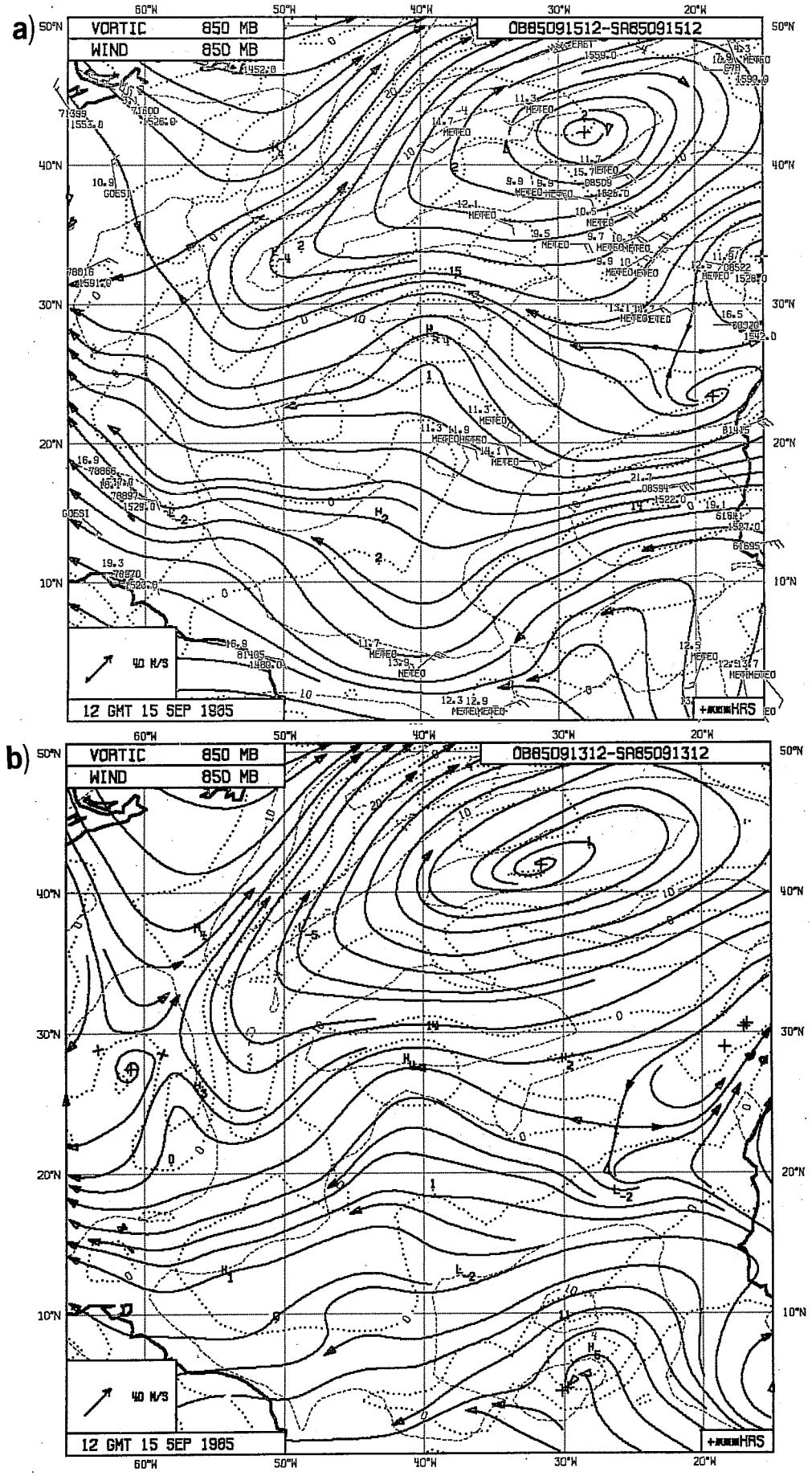

Fig. 28 (a) 850 mb analysis for 15 September, 1985 and (b) 48 h forecast verifying at that time. See Fig. 2a for further explanation.

28°N, 41°W and intensify during the subsequent 48h (Fig. 28b). The analysed position at 28°N, 39°W, admittedly based on very little data, supports the predicted movement and intensification. Fortunately, the METEOSAT observations for 12 GMT on 13 and 15 September provide strong confirmation of the predicted development. Visible images (Figs. 29a,b) for these hours show the sudden appearance of a swirling cloud mass in mid ocean. Water vapour imagery (Figs. 30a,b) reveals that the development is connected with the amplification of the middle of three upper-tropospheric waves or vortices in the mid-ocean trough and that the associated cloud field contains deep convective elements. The 200 mb analyses for the 13th and 15th are displayed in Fig. 31a and b. The chart for the 13th shows an elongated trough or cyclonic shear zone near 35°N, 30°W that digs southwestward and transforms into a well defined cut-off low by the 15th.

Clearly, the model was successful in predicting the upper-level development and its extension to lower levels. This ability to handle well developments within the upper-troposphere trough is a prerequisite for successful prediction of easterly wave behaviour in the western Atlantic, since the equatorward portion of the trough frequently extends into this part of the ocean and interacts with the westward moving waves.

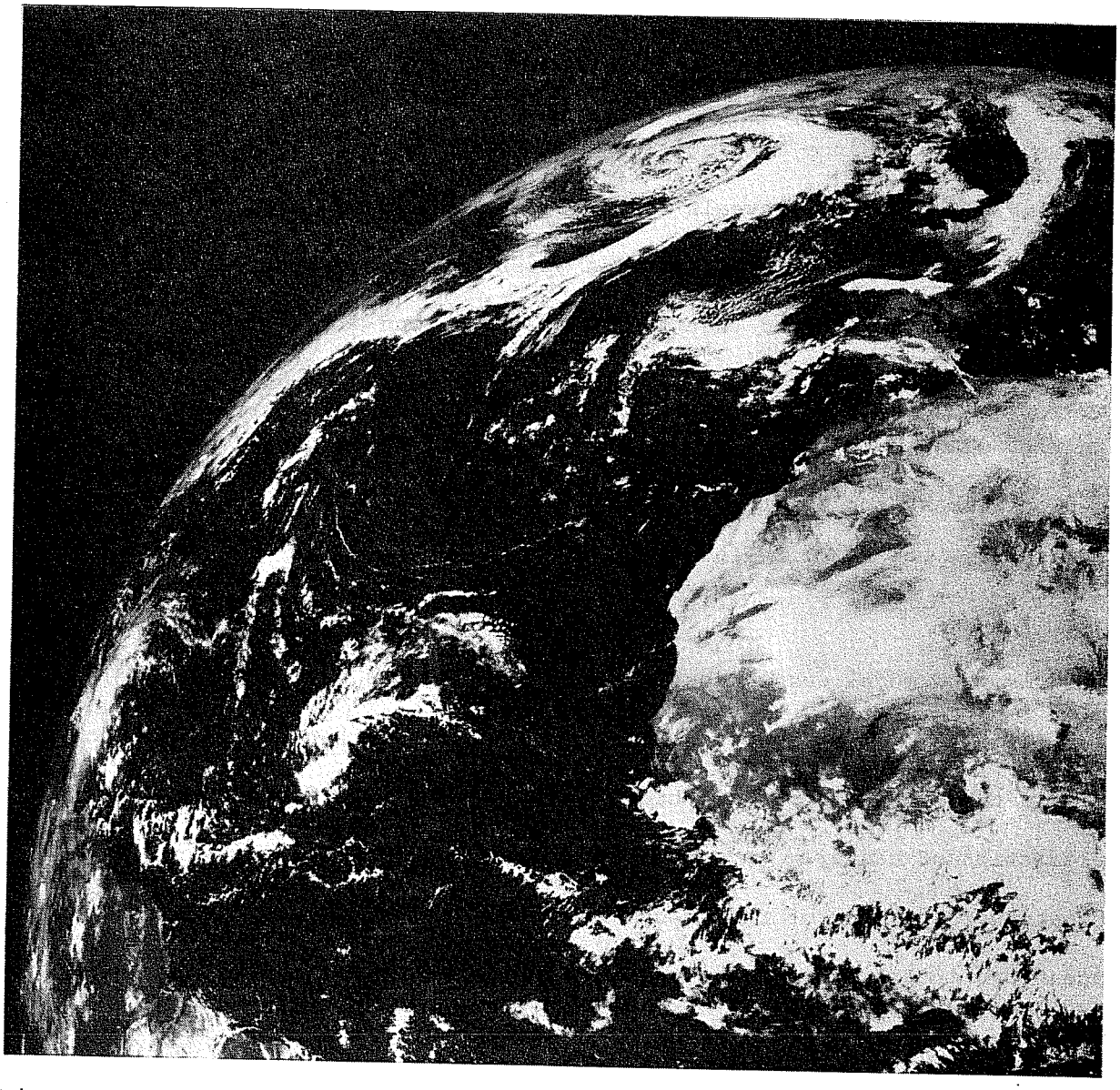

Fig. 29 Meteosat visible image for (a) 13 September 1985.

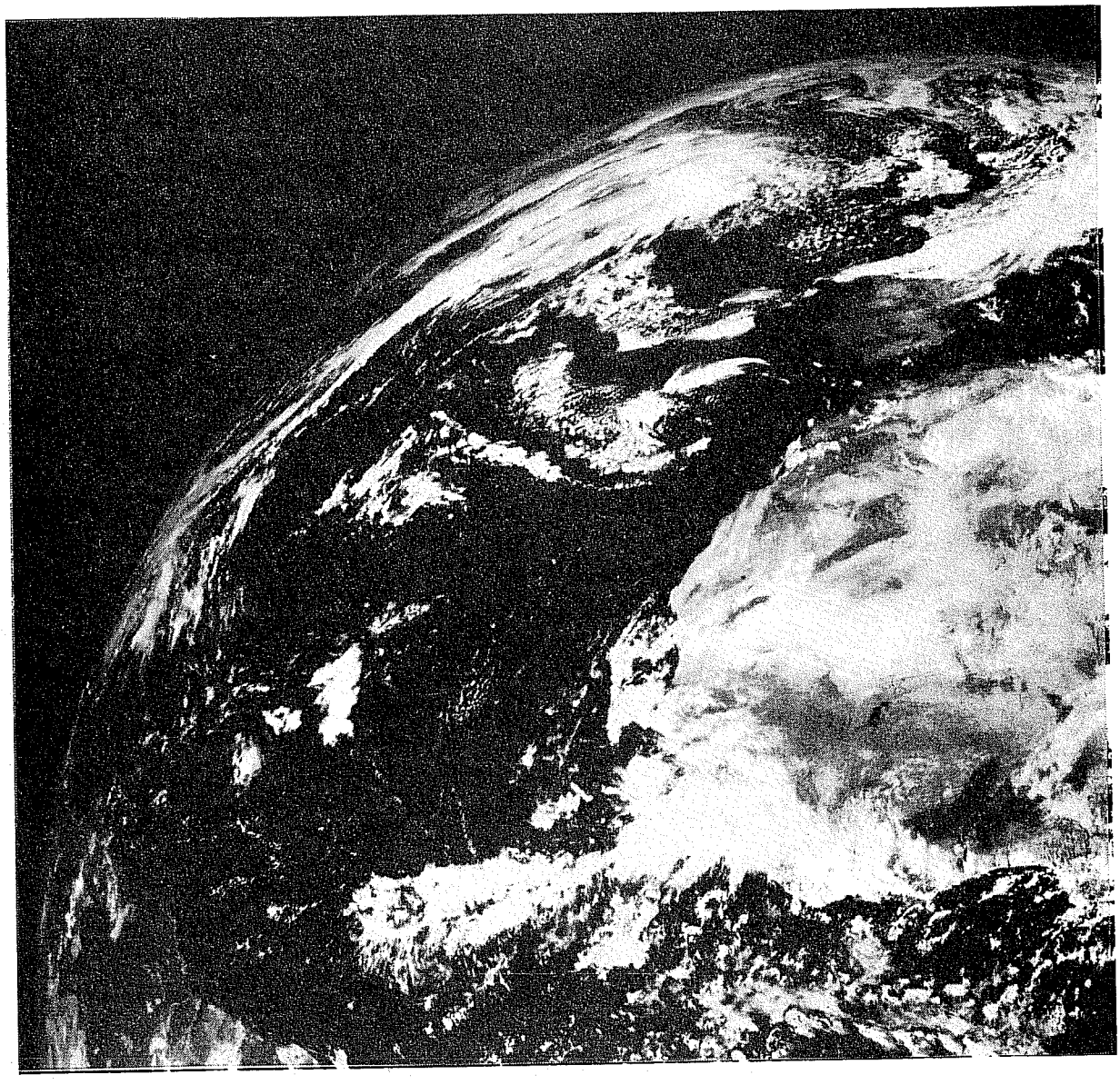

Fig. 29 Meteosat visible image for (b) 15 September 1985

Fig. 30 Meteosat wave vapour image for (a) 13 September 1985.
Arrow points to subtropical disturbance.

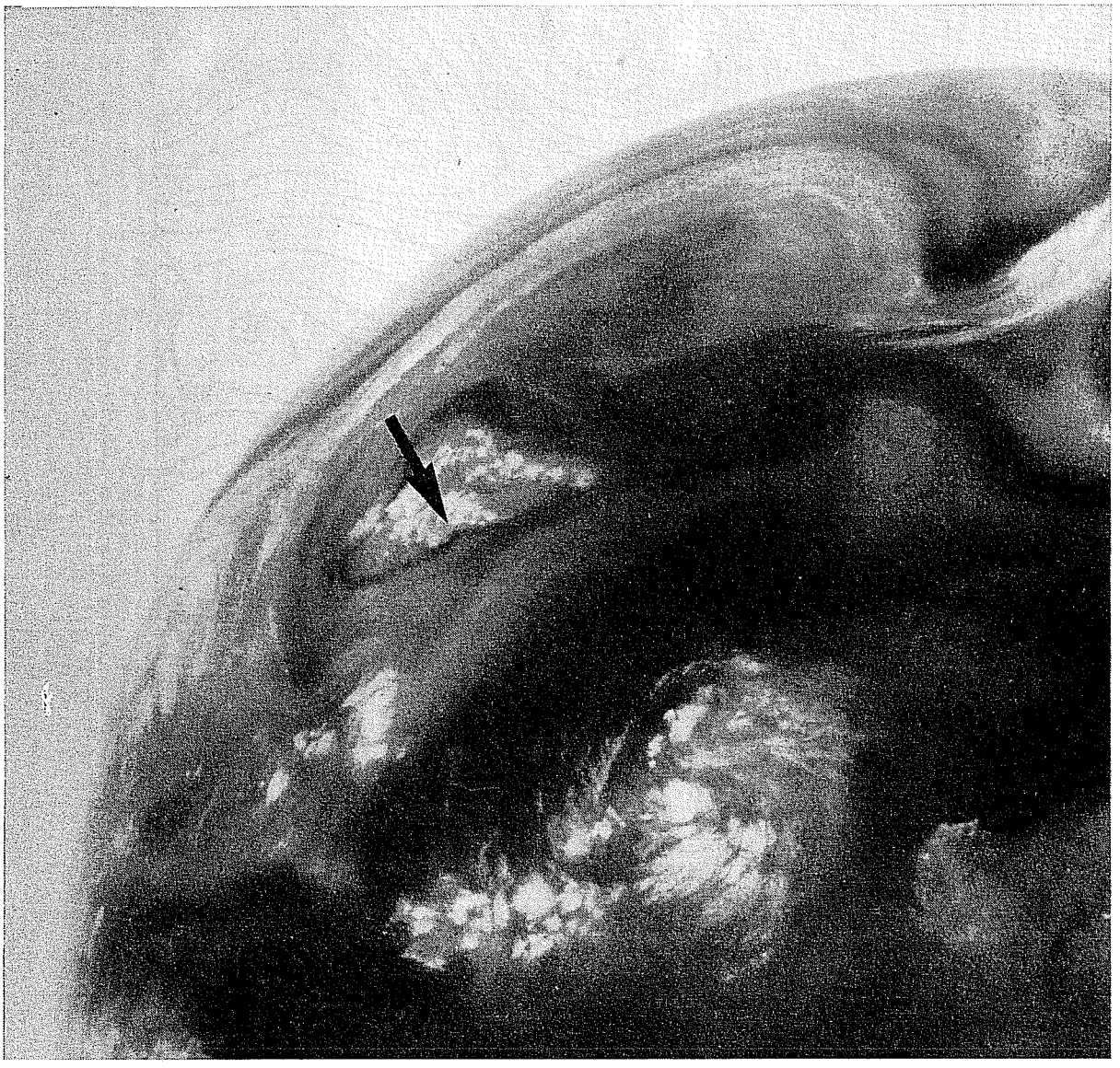

Fig. 30 Meteosat wave vapour image for (b) 15 September 1985. Arrow points to subtropical disturbance

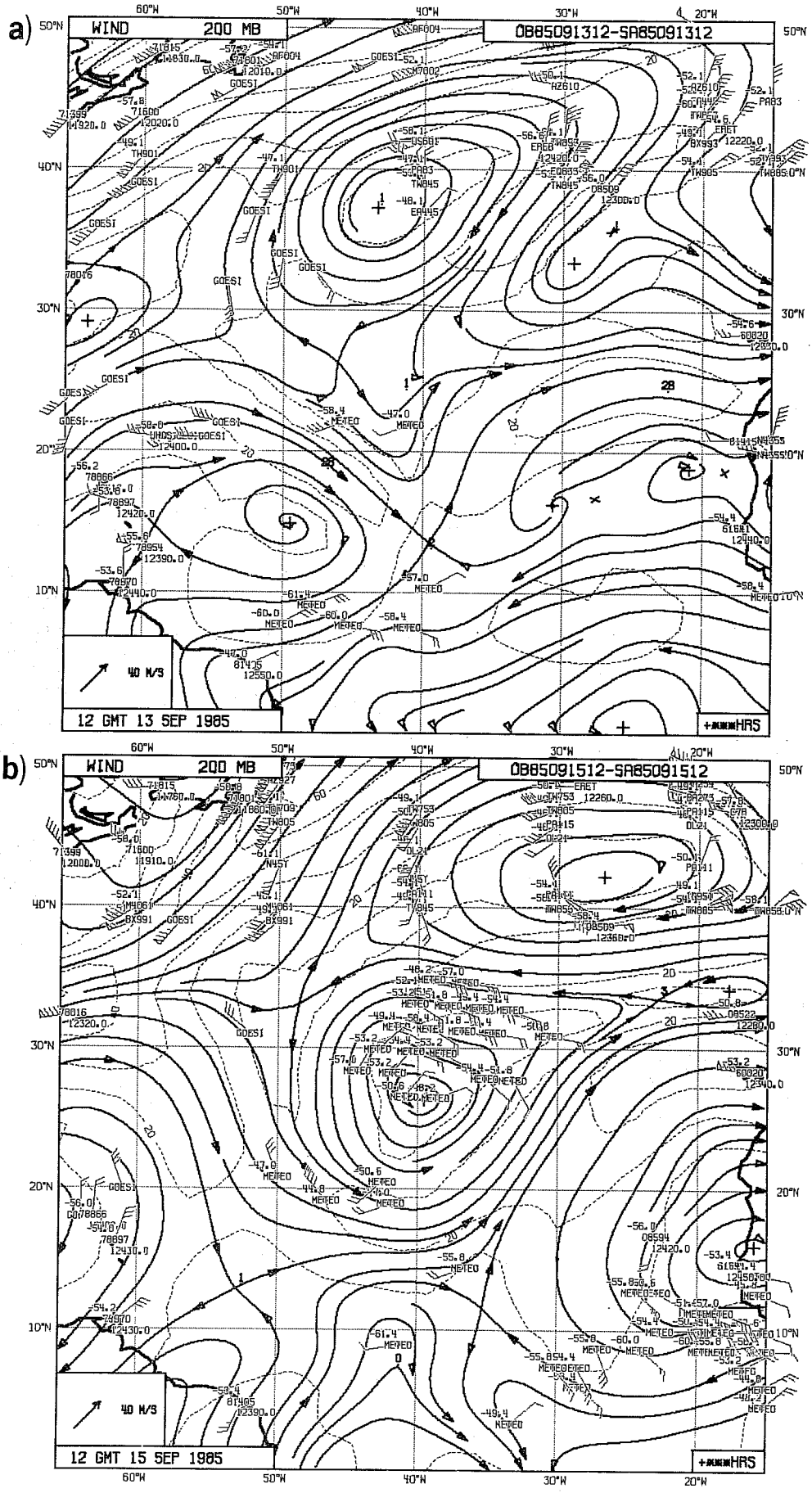

Fig. 31 200 mb charts for (a) 13 September and (b) 15 September 1985. Solid lines, streamlines. Dashed lines, isotachs (m^{-1}).

5. SUMMARY AND CONCLUSIONS

This study examines the ability of the current ECMWF operational system to analyse and predict African or easterly waves and the tropical storms and hurricanes that grow out of them. The study covers the two month period August-September 1985, during which 20 waves were identified and tracked. The identification was based on 850 mb vorticity maxima, 700 mb tough axes and satellite cloud patterns. Most of the waves originated over West Africa. There was some evidence of two main source regions, one in the desert region of northern Mali, southern Algeria and eastern Mauritania, downwind of the Hoggar mountains, and a second in the rain belt to the south, stretching from Lake Chad across Nigeria to northern Ghana. The existence of two source regions or two regions of primary development may be connected with the tendency noted by Carlson (1969), Burpee (1975) and Reed et al., (1977) for African waves to possess two circulation centres at low levels, a relatively cloud-free one in the sub-Saharan trough zone and one associated with the deep convection in the rain belt to the south.

Wave characteristics were similar to those reported in earlier studies. Wave lengths were typically in the 2000-3000 km range, periods in the 3-5 day range and phase speeds in the 6°-7° long d^{-1} range. Three of the waves developed into hurricanes.

The 850 mb vorticity maximum provided a useful tool for tracking the waves. It allowed a latitudinal as well as a longitudinal position to be assigned to a wave disturbance and in cases where closed circulations existed it generally gave a more uniform and credible path than the circulation centre.

For the purpose of evaluating the quality of the analyses, charts of the surface, 850 mb, 700 mb and 200 mb fields, with all data plotted on them, were produced at 6 hourly intervals for the entire two month period. Examination of the maps revealed the existence throughout the period of a huge data gap at lower levels covering much of central and eastern Africa. Since the waves were believed (though not proved) to have formed in the data network to the west of this region, the data void, regrettable though it was, did not seriously affect the early identification of them.

A smaller region with a deficiency of data was found over parts of the Sahara, including the region near the Hoggar shown by the analyses to be a major source region of the waves. The strong vorticity maxima often noted in this area cannot therefore be said to be fully verified, though they are believed to be real features. Another region with a deficiency of data was the central Atlantic where only low and middle-level cloud-track winds provided useful information for analysing the waves. Unfortunately, such winds were in short supply during the period of study. Surface ship observations and high-level cloud-track winds were relatively plentiful but were of little help in defining the waves. Low-level temperature soundings from polar-orbiting satellite were of no value. METEOSAT visible, IR and water vapour images were available for viewing cloud and moisture patterns over the ocean and were thus useful for identifying and tracking the waves. If higher yields of cloud track winds cannot be achieved, it would be desirable to develop objective pattern recognition schemes for detecting and categorizing wave signatures. If the latter could be related to the fields of the basic variables - admittedly a task of enormous difficulty - greatly improved oceanic analyses could no doubt be achieved. Hurricane Gloria is an example of a system that could be located with almost pin point accuracy from the cloud pictures for

which few cloud track winds were available, causing the disturbance to be badly misplaced at one stage in the analysis in mid-Atlantic.

In the relatively data-rich area of West Africa the analyses as a rule conformed well to the wind data, at least in the representation of the larger-scale features. Smaller-scale features, however, were not drawn to as faithfully as in higher latitudes. In many cases this was clearly advantageous, since 850 mb wind patterns over Africa have a much noisier appearance than in extratropical latitudes, possibly because of observational or transmission errors or possibly because of unrepresentative local winds connected with convective activity or topographical influences. In other cases, one of which was illustrated, the small-scale strongly convergent features omitted from the analyses are unquestionably real, being well supported by observations. It would seem desirable to retain such features in the analyses, though we have no evidence that their omission harmed the forecasts of the large scale systems. Small-scale features were not ignored in all cases. A further example was presented illustrating how well the analysis system portrayed the narrow, sharply-defined and mainly rotational trough that characterised Hurricane Elena during its early wave stage over West Africa.

The varied performance of the analysis system is discussed in terms of the ability of the utilized structure functions to represent small synoptic features and in terms of the effects on the analyses of the relative weights given to first guess fields and actual data. It is concluded that these aspects of the analyses need further attention.

Two examples are given of the performance of the analysis system in data sparse regions in situations where features appeared on satellite images that allowed independent verification of the analyses. One example dealt with the the disturbance which later became Hurricane Gloria as it passed through a data void in the central Atlantic. The second dealt with wave "K" which developed along the northern border of a large area of central and western Africa from which observations were missing for several days due to a transmission failure. In the latter case the analyses showed the wave to form along the border of the data sparse area and to grow into a strong vortex as it crossed the data void. A remarkable spiral-shaped dust cloud seen in METEOSAT IR imagery confirmed the existence of the vortex. The success of the analyses in portraying the development of this system is attributed to the fact that at least a small amount of data existed in the upstream region and to the ability of the model to capture the instability mechanism responsible for the wave growth. Since the disturbance first appeared in close proximity to the Hoggar mountains, it is possible that orography had an important influence on its development. In view of the high frequency with which the waves formed downstream of these mountains, further investigations of the role of orography is desirable.

In the case of the embryonic Hurricane Gloria the analyses maintained the disturbance with undiminished strength during its passage over the data-sparse region but, according to the cloud pattern seen by METEOSAT, the analysed position was in error by as much as 1000 km. With the help of the 6h time continuity it was found that the strong 850 mb vorticity centre that gave the incorrect position was one of a number of centres analysed within the general wave trough of Gloria. This vorticity maximum formed with great rapidity well downstream or west of an earlier centre and caused the disturbance to appear to jump forward.

This behaviour connected with Gloria, and other examples of sudden development of small areas of relatively large vorticity, especially in the ITCZ, require further investigation. We suspect that the vorticity areas, because of their rapidity of development and seemingly random positions relative to waves, are associated with convective events within the model (and perhaps in some cases in the atmosphere). In order to keep the present study within tractable limits, we have not examined vertical motion or precipitation patterns. Certainly this must be done if the origin of the smaller features of the vorticity patterns are to be understood.

The forecast performance of the model has been evaluated both statistically and by looking at individual cases. In the statistical evaluation, means and standard deviations were found for the errors in 48 h prediction of the positions and intensities of the primary 850 mb vorticity maximum within the wave troughs. Only those cases were verified in which sufficient data existed at the verification time to assure that the analysis was not dominated by the first guess field and therefore merely repeating the forecast.

Over West Africa and the Eastern Atlantic forecast displacements of the vorticity maximum were in error by less than one degree in both latitude and longitude. Forecast positions were in the mean too far to the north and east, and the differences in position were significant at the 10% level. Forecast vorticity intensities were correct in the mean in the coastal region but were somewhat too weak in the interior. In the western Atlantic and Caribbean forecast positions were significantly too far to the north in the mean. The forecast vorticity was about 30% too small on the average, and the discrepancy was highly significant statistically.

Numerous cases of successful forecasts existed for the West African region, including an impressive forecast of a strong disturbance (wave "M") that retained its strength during an unusual northwestward course in the Atlantic. We have, however, in choosing cases for illustration not attempted to show cases that were especially good or bad but rather to show cases that were of special interest. Thus the chosen cases were waves "A", "H", "O" and "L" which transformed in their later stages into hurricanes Danny, Elena and Gloria and Tropical Storm Fabian. In addition, to illustrate the versatility of the model, we have chosen a case of the successful prediction of a low-level subtropical disturbance in the middle Atlantic. The low-level system was evidently the outgrowth of upper-tropospheric events in the mid-ocean trough.

The 48 h forecasts of the three hurricanes and one tropical storm all had successful elements, but there were shortcomings as well. Generally, forecast positions were within a few hundred kilometres of the analysed positions for displacements that were typically in excess of 1000 km. The most serious positioning errors occurred with respect to Hurricane Elena which looped erratically in the Gulf of Mexico. (Further discussion of the Elena forecasts may be found in Heckley et al., 1986).

Predictions of intensity were less satisfactory in all cases. In three of the four cases the model forecast some strengthening of the vorticity as the disturbance approached the tropical storm or hurricane stage, but in all cases the predicted (and analysed) vorticities were much less than the vorticities to be expected in well developed storms. Because of the limited resolution of the T106 forecast system, it would be unreasonable to expect it to predict the intense inner circulations of the storms. At best it can be expected to depict the outer circulations, and this it did with some success.

The results of this study of a two month period during the summer of 1985, the first summer in which the T106 model with revised physics was used operationally, indicate that the model has an impressive capability for forecasting tropical wave disturbances and other synoptic-scale circulation features. The day in, day out accuracy of forecasts would no doubt be much improved if some of the identified data deficiencies over central Africa and the Atlantic could be remedied. Also a still higher resolution model might lead to improved forecasts. This is particularly true with respect to tropical storms and hurricanes whose true intensities were only hinted at by the T106 system. Finally, some evidence has been presented regarding the development of spurious areas of abnormally large vorticity over the ocean. It seems likely that these developments, which are sudden and erratic, were connected with convective events in the model. They require further study, first to determine whether they were indeed of convective origin and second, if they were associated with convection, to determine whether they were caused by some shortcoming of the model physics. The second objective can only be achieved with the help of a special data set. The data set acquired during the GARP Atlantic Tropical Experiment (GATE) is probably the only currently available set that is suitable for the purpose.

References

Albignat, J.P. and R.J. Reed, 1980: The origin of African wave disturbances during Phase III of GATE. Mon.Wea.Rev., 108, 1827-1839.

Anderson, R.K., J.P. Ashman, G.R. Farr, E.W. Ferguson, G.N. Isayeva, V.J. Oliver, F.C. Parmenter, T.P. Popava, R.W. Skidmore, A.H. Smith and N.F. Veltishchev, 1973: The Use of Satellite Pictures in Weather Analysis and Forecasting. W.M.O. Technical Note No. 124, Geneva, 274 pp.

Bengtsson, L., H. Böttger and M. Kanamitsu, 1982: Simulation of hurricane type vortices in a general circulation model. Tellus, 34, 440-457.

Burpee, R.W., 1972: The origin and structure of easterly waves in the lower troposphere of North Africa. J.Atmos.,Sci., 29, 77-90.

Burpee, R.W., 1974: Characteristics of North African easterly waves during the summers of 1968 and 1969. J.Atmos.Sci., 31, 1556-1570.

Burpee, R.W., 1975: Some features of synoptic-scale waves based on compositing analysis of GATE data. Mon.Wea.Rev., 103, 921-925.

Burpee, R.W. and R.J. Reed, 1982: Synoptic-scale Motions. In: The GARP Atlantic Tropical Experiment (GATE) Monograph. GARP Publications Series No. 25. WMO/ICSU, Geneva, 61-120.

Carlson, T.N., 1969: Some remarks on African disturbances and their progress over the tropical Atlantic. Mon.Wea.Rev., 97, 716-726.

Daley, R., 1985: The analysis of synoptic scale divergence by a statistical interpolation procedure. Mon.Wea.Rev., 113, 1066-1079.

European Space Agency, 1985: Meteosat Image Bulletin. August 1985 and September 1985. Issued by MEP/Data Service European Space Operation Centre. Robert-Bosch-Str. 5 6100 Darmstadt, Germany.

Gilchrist, A., P.R. Rowntree, D.B. Shaw, 1982: Large Scale Numerical Modelling in the GARP Atlantic Tropical Experiment (GATE). In: The GARP Atlantic Tropical Experiment (GATE) Monograph. GARP Pubications Series No. 25, WMO/ICSU, Geneva, 183-218.

Heckley, W.A., 1985: Systematic errors of the ECMWF operational forecasting model in tropical regions. Quart.J.Roy.Meteor.Soc., 111, 709-738.

Heckley, W.A., M.J. Miller and A.K. Betts; 1987: An example of hurricane tracking and forecasting with a global analysis/forecasting system. Bull.Amer.Met.Soc. (To be published)

Hollingsworth, A., D.B. Shaw, P. Lönnberg, L. Illari, K. Arpe and A.J. Simmons, 1986: Monitoring of observation quality by a data assimilation system. Mon.Wea.Rev., 114, 861-879.

Jarraud, M., A.J. Simmons and M. Kanamitsu, 1985: Development of the high resolution model. ECMWF Tech. Memo. 107. Reading, UK, 61 pp.

Kanamitsu, M., 1985: A study of the predictability of the ECMWF operational forecast model in the Tropics, J.Meteor.Soc.Japan, 63, 779-804.

Krishnamurti, T.N., 1985: Numerical Weather Prediction Studies. Advances in Geophysics, 28B, Series ed. B. Saltzman, Vol. ed. S. Manabe, Ac.Press, 283-332.

Lorenc, A.C., 1981: A global three-dimensional multivariate statistical interpolation scheme. Mon.Wea.Rev., 109, 701-721.

Nitta, T. and Y. Takayabu, 1985: Global analysis of the lower tropospheric disturbances in the tropics during the northern summer of the FGGE year. Part II: Regional characteristics of the disturbances. Pure and Appl. Geophys., 123, 272-292.

Reed, R.J., D.C. Norquist and E.E. Recker, 1977: The structure and properties of African wave disturbances as observed during Phase III of GATE. Mon.Wea.Rev., 103, 317-333.

Riehl, H., 1954: Tropical Meteorology. McGraw-Hill, New York, N.Y., 392 pp.

Rowntree, P.R., H. Cattle (eds) 1983: The meteorological Office GATE Modelling Experiment. U.K. Meteorological Office, Sci. Pap. 40, HMSO, London, 76 pp.

Sadler, J.C. and L.K. Oda, 1978: The synoptic (A) scale circulations during the third phase of GATE, 20 August - 23 September 1974. Dept. of Meteor., University of Hawaii, Honolulu, 41 pp.

—— and —— 1979: The synoptic (A) scale circulations during the second phase of GATE, 17 July - 19 August 1974. Dept. of Meteor., University of Hawaii, Honolulu, 36 pp.

—— and —— 1980: GATE Analyses. I. The Synoptic (A) Scale Circulations during Phase I, 26 June - 16 July 1974. II. Means for Phases I, II and III. Dept. of Meteor., University of Hawaii, Honolulu, 32 pp.

Shaw, D., P. Lönnberg and A. Hollingsworth, 1984: The 1984 revision of the ECMWF analysis system. ECMWF Research Department Tech. Memo. No. 92, ECMWF, Reading, UK, 69 pp.

Simpson, R.H., N. Frank, D. Shideler and H.M. Johnson, 1968: Atlantic tropical disturbances, 1967. Mon.Wea.Rev., 96, 251-259

Thompson, B.W., 1965: Climate of Africa. Oxford University Press, London, 132 pp.

Tiedtke, M., W.A. Heckley, J. Slingo, A. Simmons, M. Jarraud, G. Sommeria, 1987: Tropical forecasts at ECWMF: Impact of revised physics and increased horizontal resolution. To be submitted.

Wergen, W., 1986: Diabatic non-linear normal mode initialisation for a spectral model. (In preparation)

APPENDIX

A.1 Wave Histories

The derivation of the wave histories is described in the text. Table A.1 gives the details of the history of each wave. The construction of the table is most easily explained by an example: Wave D was identifiable from August 8 to August 20. Its position at 1200 GMT on its first day (August 8) was 3°W, 24°N, its position on its second day (August 9) was 9°W, 21°N, and so on.

The waves which reached tropical storm or hurricane strength during the period of the study were "A" (Hurricane Danny), "H" (Hurricane Elena), "L" (Tropical Storm Fabian) and "O" (Hurricane Gloria).

A.2 Data Coverage

Figure A.1 shows data coverage maps for the African and Atlantic area at 0000GMT during September 1985. The plots show the number of wind reports received at ECMWF for each 5°x5° box for selected observation types and levels. Panel A.1a shows the number of aircraft reports above 300mb, Panel A.1b shows the number of 250mb wind reports per box from rawinsonde or pilot reports, while Panel A.1c shows the corresponding counts for 850mb reports. Figs. A.2 and A.3 show the counts for 0600GMT and 12000GMT in September, while Fig. A.4 shows the counts at 1800GMT for August; the counts at 1800 GMT for September were unavailable for technical reasons.

There is regular coverage at 850mb at all four synoptic hours to the northwest of a line running from 0°N,0°E to 30°N,30°E, except for the major gap in the Western Sahara. To the southeast of this line there is a major data void. Rawinsonde or pilot reports are much sparser at 250mb than at 850mb. With few exceptions soundings only reach this level at 1200 GMT. The

850mb data volumes in West Africa at 1800 GMT in August are lower than might be expected because of the outage of telecommunications between August 24 and August 30.

Aircraft reports are most plentiful at 0000GMT and 0600GMT. They provide important coverage over the Atlantic. Very few aircraft reports are available over Africa, where they could be valuable.

Fig A.5 shows the data counts for Meteosat data at 0000GMT for three layers: at and above 300mb, between 850 and 300 mb, and at or below 850mb. Fig A.6 gives similar results for 1200GMT, the only other time for which reports are available. The paucity of low level reports along the main storm track for the waves is evident. No low level data is generated over land because the clouds may not be tracers for the motion there.

A.3 Regional Verifications of 48-hour Forecasts

All forecasts for the position and intensity of the vorticity maximum of a wave were verified when there was sufficient data coverage to have confidence in the verifying analysis. No account was taken of the data coverage in the starting analysis for the forecast. The verification results are tabulated by region: Table A2 - Central Africa (east of 0°E), Table A3 - West Africa (0°-14°W), Table A4 - Eastern Atlantic (15°W-29°W), Table A5 - Central Atlantic (30°W-54°W), Table A6 - Western Atlantic (west of 54°W). The tables show the observed (O) and forecast (F) latitude, longitude, and vorticity intensity, together with the corresponding forecast errors. The units for vorticity are $10^{-5}, s^{-1}$. The mean and standard deviation of the errors for each region are given at the end of each table, and are summarised in Table 2. Cases are marked unverifiable if the position of the forecast vorticity maximum is uncertain.

Table A1 - Daily Wave Positions (long/lat) at 1200 GMT

Wave	Date	Age (days) 1		2		3		4		5		6		7		8		9		10		11		12		13		14		15		16		17	
A	8/1-16	26W	13N	32W	12N	37W	12N	42W	12N	46W	13N	49W	13N	54W	12N	64W	12N	73W	14N	76W	15N	79W	17N	83W	20N	87W	22N	92W	24N	94W	29N				
B	8/4-13	9W	19N	15W	19N	20W	16N	27W	15N	35W	13N	43W	13N	50W	15N	57W	15N	64W	15N	72W	16N														
C	8/5-18	0	25N	4W	26N	7W	25N	13W	22N	20W	21N	27W	15N	36W	15N	45W	14N	53W	16N	62W	17N	70W	21N	76W	22N	81W	23N	86W	23N						
						2W	9N	9W	9N	17W	10N	23W	10N																						
D	8/8-20	3W	24N	9W	21N	11W	22N	17W	19N	25W	19N	33W	16N	42W	15N	51W	14N	60W	14N	67W	17N	73W	18N	78W	19N	83W	21N								
E	8/10-21	2E	18N	4W	21N	7W	22N	11W	16N	18W	17N	24W	12N	31W	12N	38W	13N																		
F	8/14-20	7W	24N	12W	24N	22W	24N	29W	24N	37W	23N	48W	24N	57W	25N	45W	14N	52W	15N	58W	17N														
G	8/16-29	5E	10N	2W	11N	9W	13N	17W	14N	21W	17N	28W	16N	35W	14N	44W	15N	56W	16N	66W	17N	72W	22N	81W	27N	87W	29N								
H	8/20-9/2	0	21N	8W	21N	13W	21N	21W	19N	32W	16N	43W	16N	55W	17N	67W	19N	78W	22N	86W	24N	89W	28N	86W	28N	85W	28N								
I	8/23-31	0	19N	6W	20N	11W	20N	20W	17N	33W	13N	43W	15N	53W	16N	64W	16N	75W	19N																
J	8/28-9/4	20W	17N	25W	15N	33W	15N	44W	15N	55W	11N	67W	15N	75W	21N	79W	23N																		
K	8/28-9/13	4W	19N	9W	19N	15W	16N	22W	15N	27W	14N	34W	13N	40W	12N	46W	12N	52W	12N	57W	13N	66W	14N	76W	20N	82W	20N	85W	16N	90W	17N	93W	17N		
L	9/3-18	16W	23N	24W	24N	31W	24N	38W	18N	44W	22N	49W	17N	53W	17N	57W	13N	61W	13N	66W	13N	71W	13N	74W	21N	73W	24N	69W	27N	64W	28N				
M	9/1-14	10E	15N	6E	11N	1E	10N	9W	10N	14W	12N	19W	14N	24W	17N	29W	20N	34W	21N	38W	20N	41W	22N	46W	27N	51W	28N	55W	24N						
N	9/5-20	10E	13N	4E	13N	2W	12N	7W	13N	12W	14N	18W	14N	24W	13N	30W	13N	37W	14N	44W	14N	48W	15N	49W	15N	51W	15N	53W	16N	57W	17N	62W	21N		
O	9/12-27	3E	11N	2W	10N	12W	12N	18W	13N	23W	14N	29W	15N	35W	16N	41W	17N	47W	18N	54W	18N	58W	18N	63W	20N	68W	22N	72W	26N	75W	30N				
P	9/14-30	14E	15N	8E	15N	0	16N	8W	15N	14W	18N	18W	15N	23W	16N	25W	16N	28W	17N	32W	19N	40W	20N	43W	18N	50W	17N	54W	18N	62W	20N	69W	22N	73W	22N
Q	9/17-25	11E	18N	8E	18N	5E	18N	2W	18N	8W	18N	12W	17N	19W	15N	28W	17N	31W	19N																
R	9/25-30	9W	19N	17W	19N	25W	16N	32W	15N	37W	15N	45W	18N																						
S	9/25-29	8E	12N	0	9N	11W	10N	19W	11N	27W	16N																								
T	9/28-30	7W	22N	13W	22N	18W	22N																												

Table A2 - Forecast Performance

Central Africa (east of 0°)

Wave	Date	Latitude Error (degrees) O	F	F-O	Longitude Error (degrees) O	F	F-O	Intensity Error ($10^{-5}s^{-1}$) O	F	F-O
G	16 Aug	Not verifiable								
M	2 Sept	11N	14N	+3	7E	5E	+2	3	5	+2
N	6 Sept	13N	17N	+4	4E	4W	+8	7	4	-3
O	10 Sept	17N	17N	0	0E	2E	-2	6	7	+1
Q	19 Sept	Not verifiable								
		Mean	2.3			2.7				0
		S.D.	2.1			5.0				2.6

Table A3 - Forecast Performance

West Africa (0° - 14°W)

Wave	Date	Latitude Error (degrees)			Longitude Error (degrees)			Intensity Error (10^{-5} s^{-1})		
		O	F	F-O	O	F	F-O	O	F	F-O
B	4 Aug	19N	26N	+7	9W	4W	-5	7	6	-1
D	7 Aug	24N	22N	-2	17W	16W	-1	8	5	-3
F	12 Aug	21N	21N	0	17W	17N	0	9	6	-3
G	18 Aug	13N	13N	0	13W	9W	-4	8	6	-2
H	21 Aug	21N	20N	-1	8W	7W	-1	8	5	-3
H	22 Aug	20N	21N	+1	13W	16W	+3	7	5	-2
M	3 Sept	10N	12N	+2	2W	6W	+4	3	3	0
M	4 Sept	9N	8N	-1	9W	11W	+2	11	4	-7
M	5 Sept	11N	11N	0	13W	13W	0	9	13	+4
N	8 Sept	17N	13N	-4	9W	9W	0	6	3	-3
O	12 Sept	17N	19N	+2	9W	9W	0	7	3	-4
O	13 Sept	15N	17N	+2	14W	14W	0	3	5	+2
O	13 Sept	10N	12N	+2	2W	3E	-6	2	4	+2
P	17 Sept	16N	17N	+1	7W	4W	-3	3	4	+1
Q	20 Sept	18N	22N	+4	3W	3W	0	3	3	0
Q	21 Sept	19N	19N	0	8W	10W	+2	5	2	-3
Q	22 Sept	17N	18N	+1	13W	15N	+2	5	3	-2
R	24 Sept	19N	20N	+1	7W	6W	-1	6	2	-4
R	25 Sept	Not verifiable								
R	26 Sept	19N	20N	+1	19W	17W	-2	3	3	0
S	27 Sept	19N	17N	-2	13W	7W	-6	4	5	+1
T	29 Sept	Not verifiable								
		Mean	0.7			-0.8			-1.4	
		S.D.	2.3			2.8			2.6	

Table A4 - Forecast Performance

Eastern Atlantic (15°W - 29°W)

Wave	Date	Latitude Error (degrees)			Longitude Error (degrees)			Intensity Error ($10^{-5}s^{-1}$)		
		O	F	F-O	O	F	F-O	O	F	F-O
B	6 Aug	17N	17N	0	20W	18W	-2	4	3	-1
B	7 Aug	17N	16N	-1	25W	25W	0	4	4	0
F	14 Aug	17N	21N	+4	20W	17W	-3	3	4	+1
F	15 Aug	13N	17N	+4	26W	20W	-6	4	3	-1
F	16 Aug	11N	11N	0	30W	32W	+2	6	5	-1
G	21 Aug	16N	17N	+1	28W	28W	0	4	3	-1
H	23 Aug	19N	21N	+2	22W	22W	0	5	5	0
K	31 Aug	15N	16N	+1	19W	19W	0	4	6	+2
M	6 Sept	13N	17N	+4	19W	18W	-1	5	10	+5
N	10 Sept	14N	15N	+1	19W	19W	0	5	5	0
O	14 Sept	11N	14N	+3	9W	9W	0	2	3	+1
P	18 Sept	19N	19N	0	15W	16W	-1	6	3	-3
P	19 Sept	6N	8N	+2	28W	28W	0	3	5	+2
P	21 Sept	24N	26N	+2	26W	26W	0	4	2	-2
P	22 Sept	24N	27N	+3	27W	28W	+1	2	1	-1
Q	23 Sept	15N	17N	+2	19W	19W	0	4	2	-2
			Mean	1.8			-0.6			-0.1
			S.D.	1.6			1.8			1.9

Table A5 - Forecast Performance

Central Atlantic (30°W - 54°W)

Wave	Date	Latitude Error (degrees)			Longitude Error (degrees)			Intensity Error ($10^{-5}s^{-1}$)		
		O	F	F-O	O	F	F-O	O	F	F-O
B	8 Aug	13N	14N	+1	32W	26W	-6	3	2	-1
G	22 Aug	14N	13N	-1	35W	34W	-1	3	2	-1
H	24 Aug	17N	19N	+2	32W	34W	+2	3	3	0
P_s	20 Sept	5N	6N	+1	32W	30W	-2	3	4	+1
P	23 Sept	22N	28N	+6	30W	28W	-2	2	2	0
S	26 Sept	8N	8N	0	0	0	0	3	7	+4
			Mean	1.5			-1.5			0.5
			S.D.	2.4			2.7			1.9

Table A6 - Forecast Performance

Western Atlantic (west of 54°W)

Wave	Date	Latitude Error (degrees)			Longitude Error (degrees)			Intensity Error ($10^{-5}s^{-1}$)		
		O	F	F-O	O	F	F-O	O	F	F-O
A	9 Aug	Not verifiable								
A	10 Aug	13N	13N	0	71W	73W	+2	4	3	-1
A	11 Aug	17N	13N	-4	79W	82W	+3	5	2	-3
A	12 Aug	21N	22N	+1	83W	83W	0	5	2	-3
A	13 Aug	22N	24N	+2	86W	86W	0	5	5	0
A	14 Aug	26N	28N	+2	92W	90W	-2	7	5	-2
A	15 Aug	29N	31N	+2	94W	94W	0	9	3	-6
D	16 Aug	22N	22N	0	75W	75W	0	2	2	0
D	17 Aug	23N	24N	+1	81W	81W	0	1	1	0
D	18 Aug	23N	25N	+2	85W	85W	0	1	1	0
G	27 Aug	26N	24N	-2	81W	86W	+5	3	2	-1
G	28 Aug	28N	28N	0	87W	88W	+1	4	3	-1
H	26 Aug	17N	18N	+2	56W	56W	0	5	6	+1
H	27 Aug	18N	18N	0	67W	66W	-1	4	6	-2
H	28 Aug	22N	21N	-1	78W	77W	-1	5	6	+1
H	29 Aug	24N	24N	0	86W	84W	-2	8	5	-3
H	30 Aug	28N	28N	0	88W	88W	0	11	3	-8
H	31 Aug	28N	30N	+2	86W	88W	+2	15	4	-11
H	1 Sept	28N	28N	0	85W	88W	+3	18	7	-11
H	2 Sept	20N	28N	-2	88W	92W	+4	18	15	-3
I	30 Aug	26N	25N	-1	64W	58W	-6	1	2	+1
I	31 Aug	24N	24N	0	66W	67W	+1	2	1	-1

Table A6 - Forecast Performance

Western Atlantic (west of 54°W) continued

Wave	Date	Latitude Error (degrees) O	F	F-O	Longitude Error (degrees) O	F	F-O	Intensity Error ($10^{-5}s^{-1}$) O	F	F-O
J	1 Sept	22N	26N	+4	56W	53W	-3	3	2	-1
J	2 Sept	Not verifiable								
J	3 Sept	21N	21N	0	75W	76W	+1	2	1	-1
K	9 Sept	Not verifiable								
K	10 Sept	Not verifiable								
K	11 Sept	16N	16N	0	85W	84W	-1	1	1	0
L	12 Sept	Not verifiable								
L	13 Sept	13N	13N	0	69W	71W	+2	3	4	+1
L	14 Sept	22N	23N	+1	74W	74W	0	2	1	-1
L	15 Sept	24N	26N	+2	75W	72W	-3	3	3	0
L	16 Sept	28N	28N	0	87W	88W	+1	4	3	-1
L	17 Sept	28N	26W	-2	63W	69W	+1	6	5	-1
O	22 Sept	19N	23N	+4	58W	60W	+2	7	4	-3
O	23 Sept	20N	21N	+1	64W	64W	0	8	6	-2
O	24 Sept	22N	24N	+2	68W	71W	+3	10	6	-4
O	25 Sept	28N	28N	0	71W	73W	+2	15	11	-4
O	26 Sept	30N	30N	0	77W	74W	-3	15	15	0
P	30 Sept	Not verifiable								
		Mean		0.5			0.4			-2.1
		S.D.		1.7			2.3			3.0

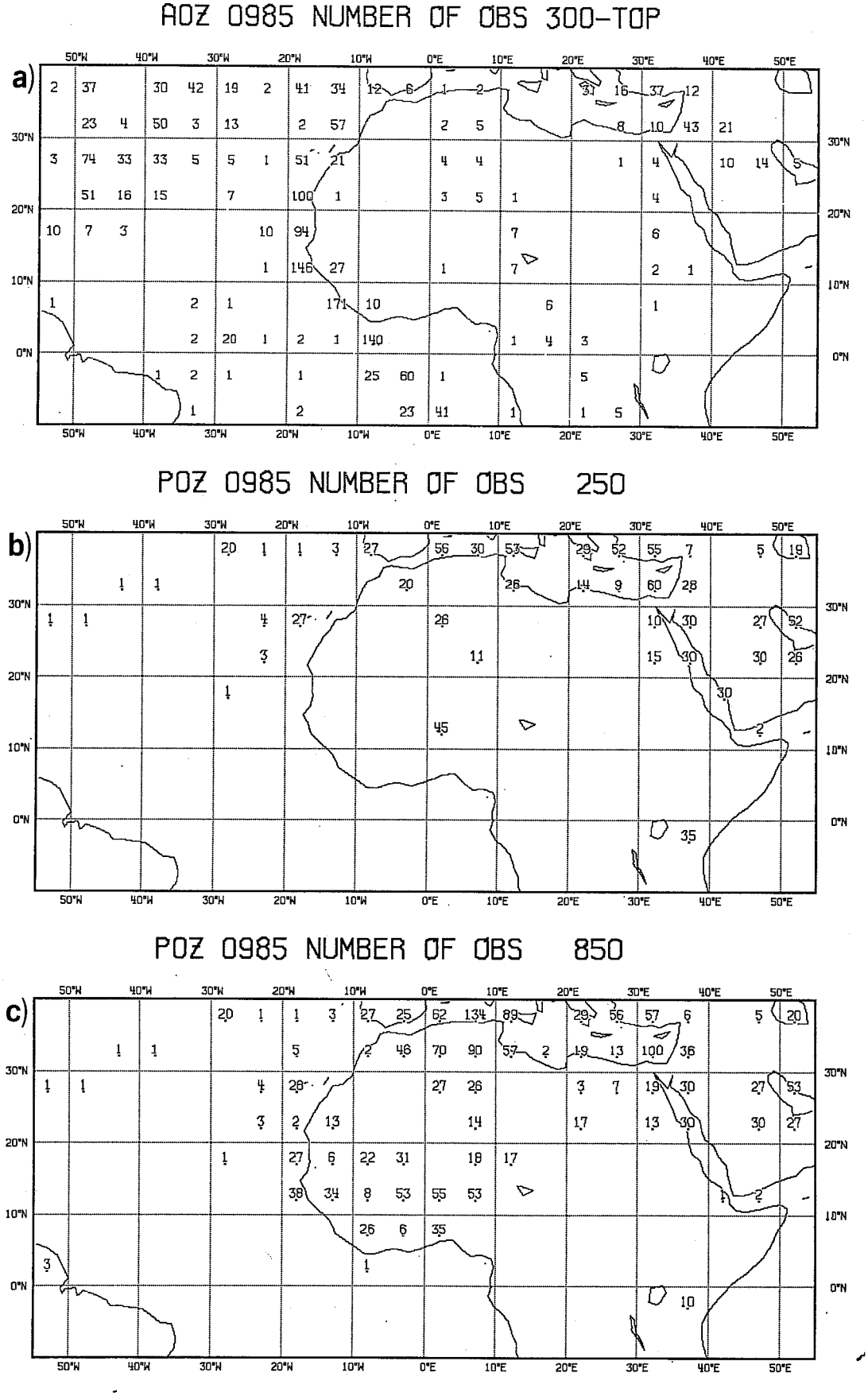

Fig. A1 Data coverage maps for wind reports from a) Aircraft at or above 300mb, b) Balloons (Temp or Pilot) at 250mb, c) Balloons (Temp or Pilot) at 850 mb, for 0000 GMT in September 1985. The plots give the numbers of reports received at ECMWF during the month for each 5°x5° box.

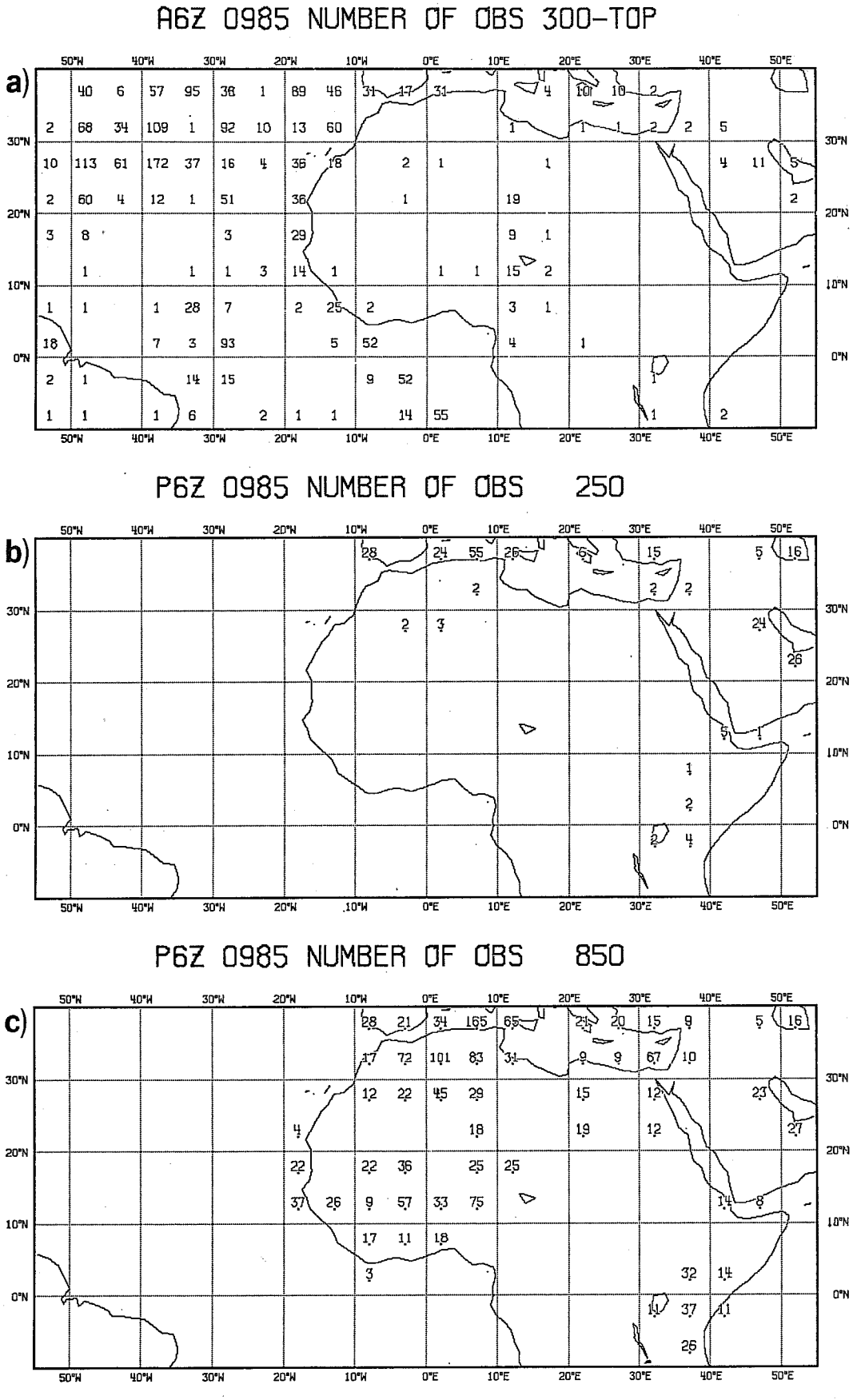

Fig. A2 Same as Fig. A1 for 0600 GMT in September 1985

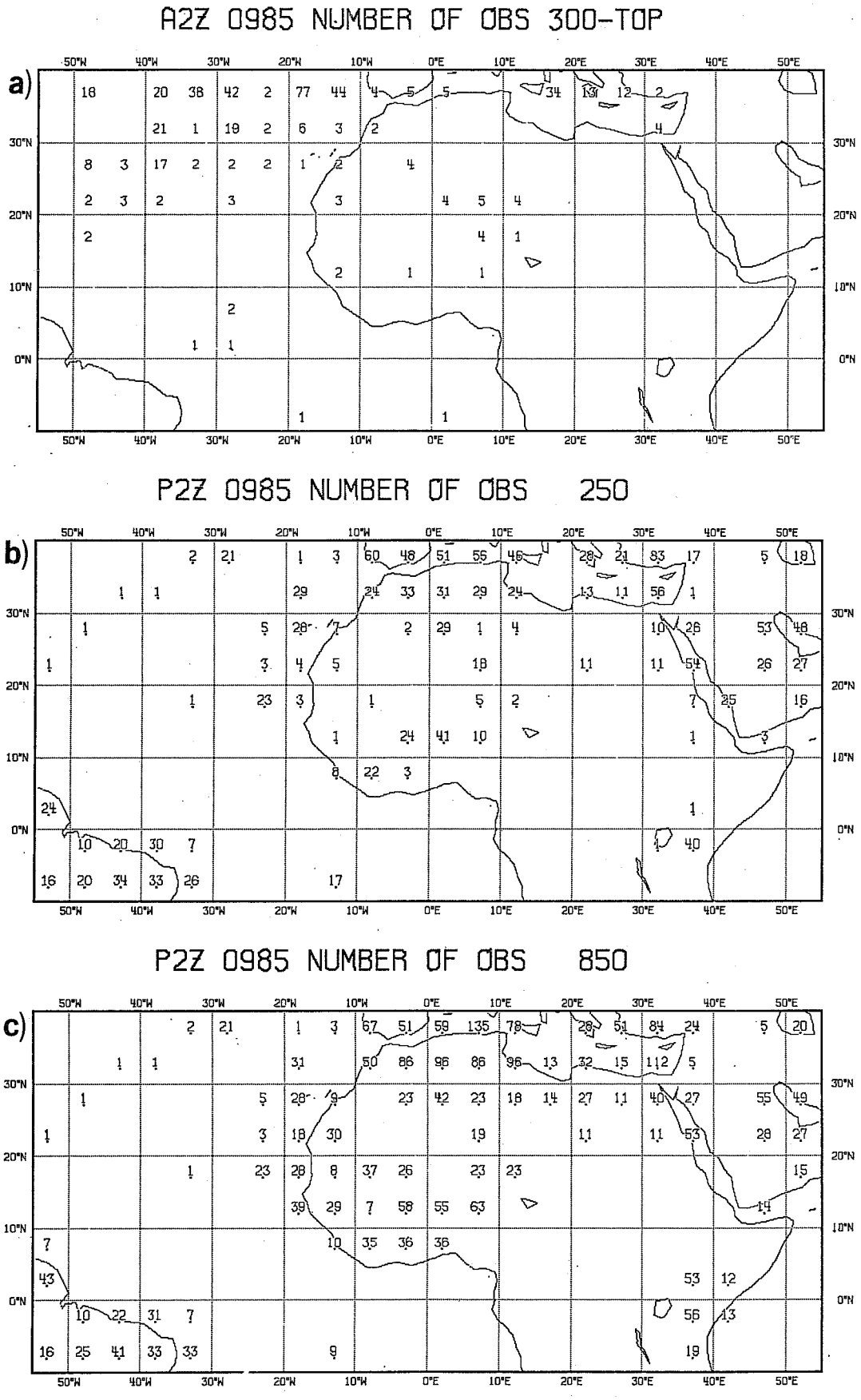

Fig. A3 Same as Fig. A1 for 1200 GMT in September 1985

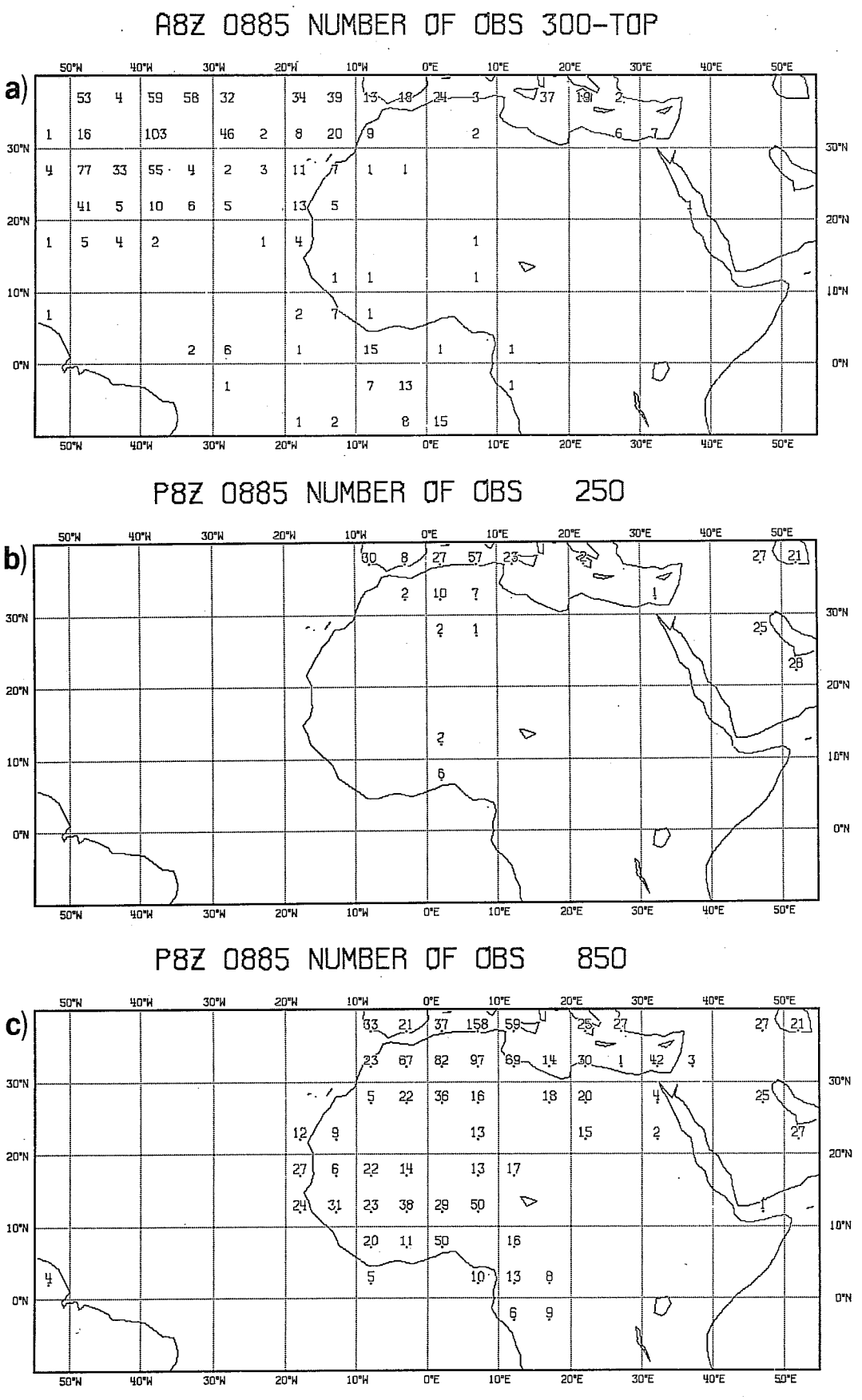

Fig. A4 Same as Fig. A1 for 1800 GMT in August 1985

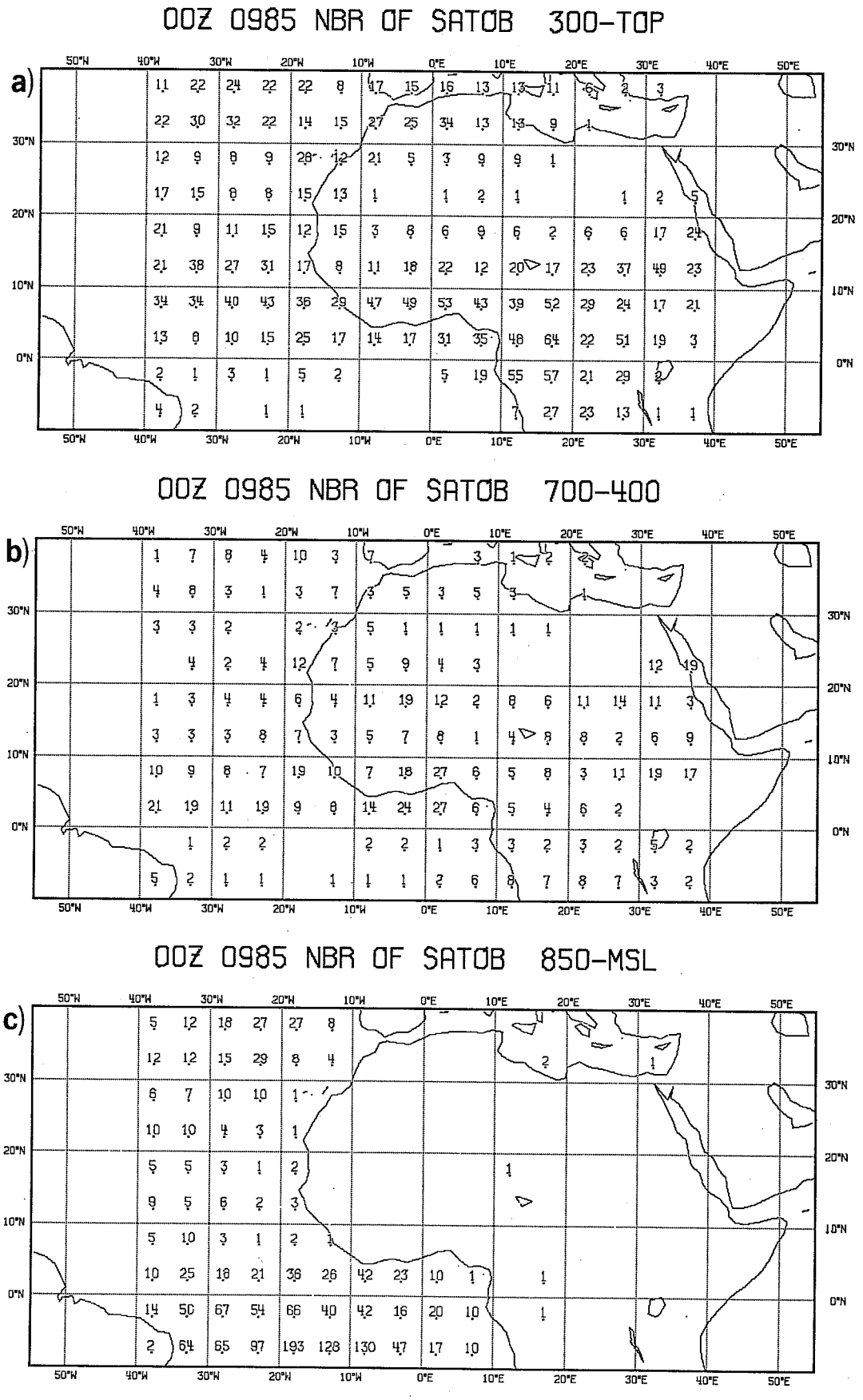

Fig. A5 Data coverage maps for Meteosat wind reports a) at or above 300mb, b) above 850mb and below 300mb, c) at or below 850mb, for 0000 GMT in September 1985. The plots give the numbers of reports received at ECMWF during the month for each 5°x5° box.

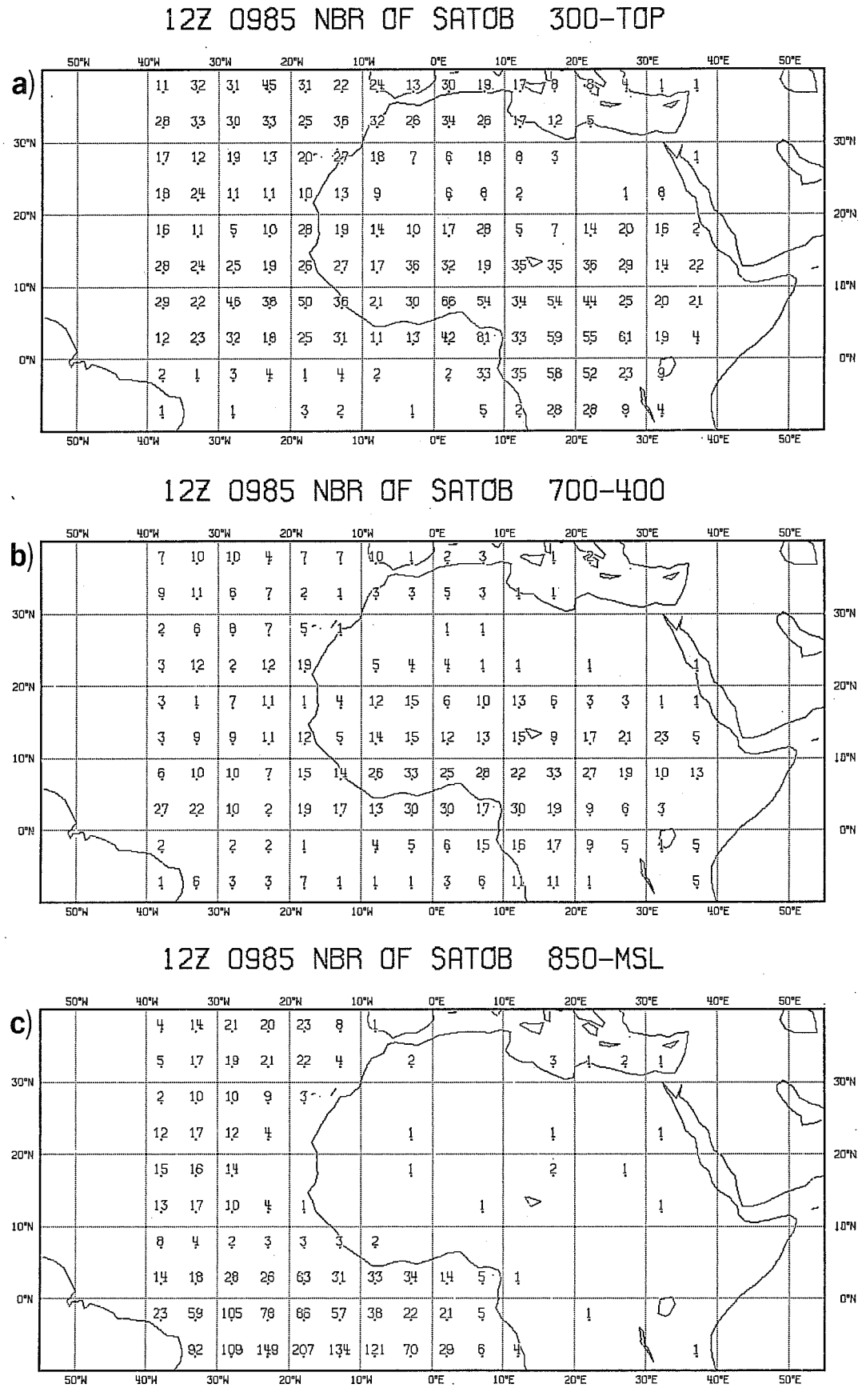

Fig. A6 Same as Fig. A5 for 1200 GMT in September 1985

ECMWF PUBLISHED TECHNICAL REPORTS

No.1 A Case Study of a Ten Day Prediction

No.2 The Effect of Arithmetic Precisions on some Meteorological Integrations

No.3 Mixed-Radix Fast Fourier Transforms without Reordering

No.4 A Model for Medium-Range Weather Forecasting - Adiabatic Formulation

No.5 A Study of some Parameterizations of Sub-Grid Processes in a Baroclinic Wave in a Two-Dimensional Model

No.6 The ECMWF Analysis and Data Assimilation Scheme - Analysis of Mass and Wind Fields

No.7 A Ten Day High Resolution Non-Adiabatic Spectral Integration: A Comparative Study

No.8 On the Asymptotic Behaviour of Simple Stochastic-Dynamic Systems

No.9 On Balance Requirements as Initial Conditions

No.10 ECMWF Model - Parameterizationb of Sub-Grid Processes

No.11 Normal Mode Initialization for a Multi-Level Gridpoint Model

No.12 Data Assimilation Experiments

No.13 Comparisons of Medium Range Forecasts made with two Parameterization Schemes

No.14 On Initial Conditions for Non-Hydrostatic Models

NO.15 Adiabatic Formulation and Organization of ECMWF's Spectral Model

No.16 Model Studies of a Developing Boundary Layer over the Ocean

No.17 The Response of a Global Barotropic Model to Forcing by Large-Scale Orography

No.18 Confidence Limits for Verification and Energetic Studies

No.19 A Low Order Barotropic Model on the Sphere with the Orographic and Newtonian Forcing

No.20 A Review of the Normal Mode Initialization Method

No.21 The Adjoint Equation Technique Applied to Meteorological Problems

No.22 The Use of Empirical Methods for Mesoscale Pressure Forecasts

No.23 Comparison of Medium Range Forecasts made with Models using Spectral or Finite Difference Techniques in the Horizontal

No.24 On the Average Errors of an Ensemble of Forecasts

ECMWF PUBLISHED TECHNICAL REPORTS

No.25 On the Atmospheric Factors Affecting the Levantine Sea

No.26 Tropical Influences on Stationary Wave Motion in Middle and High Latitudes

No.27 The Energy Budgets in North America, North Atlantic and Europe Based on ECMWF Analyses and Forecasts

No.28 An Energy and Angular-Momentum Conserving Vertical Finite-Difference Scheme, Hybrid Coordinates, and Medium-Range Weather Prediction

No.29 Orographic Influences on Mediterranean Lee Cyclogenesis and European Blocking in a Global Numerical Model

No.30 Review and Re-assessment of ECNET - a Private Network with Open Architecture

No.31 An Investigation of the Impact at Middle and High Latitudes of Tropical Forecast Errors

No.32 Short and Medium Range Forecast Differences between a Spectral and Grid Point Model. An Extensive Quasi-Operational Comparison

No.33 Numerical Simulations of a Case of Blocking: the Effects of Orography and Land-Sea Contrast

No.34 The Impact of Cloud Track Wind Data on Global Analyses and Medium Range Forecasts

No.35 Energy Budget Calculations at ECMWF: Part I: Analyses

No.36 Operational Verification of ECMWF Forecast Fields and Results for 1980-1981

No.37 High Resolution Experiments with the ECMWF Model: a Case Study

No.38 The Response of the ECMWF Global Model to the El-Nino Anomaly in Extended Range Prediction Experiments

No.39 On the Parameterization of Vertical Diffusion in Large-Scale Atmospheric Models

No.40 Spectral characteristics of the ECMWF Objective Analysis System

No.41 Systematic Errors in the Baroclinic Waves of the ECMWF Model

No.42 On Long Stationary and Transient Atmospheric Waves

No.43 A New Convective Adjustment Scheme

No.44 Numerical Experiments on the Simulation of the 1979 Asian Summer Monsoon

No.45 The Effect of Mechanical Forcing on the Formation of a Mesoscale Vortex

ECMWF PUBLISHED TECHNICAL REPORTS

No.46 Cloud Prediction in the ECMWF Model

No.47 Impact of Aircraft Wind Data on ECMWF Analyses and Forecasts during the FGGE Period, 8-19 November 1979 (not on WP, text provided by Baede)

No.48 A Numerical Case Study of East Asian Coastal Cyclogenesis

No.49 A Study of the Predictability of the ECMWF Operational Forecast Model in the Tropics

No.50 On the Development of Orographic Cyclones

No.51 Climatology and Systematic Error of Rainfall Forecasts at ECMWF

No.52 Impact of Modified Physical Processes on the Tropical Simulation in the ECMWF Model

No.53 On the Performance and Systematic Errors of the ECMWF Tropical Forecasts (1982-1984)

No.54 Finite Element Schemes for the Vertical Discretization of the ECMWF Forecast Model Using Linear Elements

No.55 Finite Element Schemes for the Vertical Discretization of the ECMWF Forecast Model using Quadratic and Cubic Elements

No.56 Sensitivity of medium-range weather forecasts to the use of an envelope orography (Jarraud, Simmons and Kanamitsu)

No.57 Zonal diagnostics of the ECMWF 1984-85 operational analyses and forecasts (Brankovic)

No.58 An evaluation of the performance of the ECMWF operational forecasting system in analysing and forecasting tropical easterly wave disturbances Part 1: Synoptic investigation (Reed, Hollingsworth, Heckley & Delsol)